ISSN 1039-3218

Hydrodynamic Models of Port Phillip Bay

S. J. Walker
CSIRO Marine Research
Castray Esplanade, Hobart, Tasmania, Australia

GPO Box 1538, Hobart 7001 Australia

Technical Report No. 38

Port Phillip Bay Environmental Study
CSIRO Environmental Projects Office
Building 9, Forestry Site, Banks Street
Yarralumla, ACT, Australia

PO Box 225, Dickson, ACT 2602 Australia

February 1997

Contents

1 Introduction

This report describes the development, calibration, validation and application of hydrodynamic models of Port Phillip Bay. These models were developed as part of the Port Phillip Bay Environmental Study P8 task. The main purpose of developing these models was to provide detailed information on the movement of water around the Bay. This information was fed into the Transport and Ecological models of the Bay to form the so-called Integrated model (Technical Reports 39 and 44 - Walker and Sherwood 1997 and Murray and Parslow 1997) - a model of the Bay which was developed to describe the physics and ecology of the Bay at a wide range of time and space scales.

A prime requirement was a hydrodynamic model which realistically represented the longer term (predominantly wind driven) circulations within the Bay, as well as representing the slow exchange between the Bay and Bass strait. In order to be able to provide climatologically realistic simulations, it was also necessary that the model was capable of performing very long model runs (simulations of the order of five to ten years) in a realistic time frame. As well, the model output needed to be in a form suitable for use by the Transport model.

A number of hydrodynamic models of the Bay were implemented during the course of the study. The models were fully three-dimensional, non-linear and included density effects. Horizontal model resolutions ranged from 500m to 3000m. Vertical resolution was generally set to 2m. Most simulations were performed using a model with 1000m horizontal resolution, and this report concentrates on that model. The model was calibrated against data obtained during the May 1994 field program, and was validated against data obtained during the September 1994 field program. This report describes the models used to provide the long term hydrodynamic simulation data for the Bay. At the time of writing this report, runs had been performed to simulate the period 1 July 1990 to 30 June 1995. Some other model development, calibration and validation is also described in Lawson and Treloar Pty Ltd (1995).

The hydrodynamic models provided three-dimensional distributions of velocity, temperature and salinity, given input fluxes of water, salt, heat and and forcing by winds, atmospheric pressure gradients and sea-level variations. As well, the models included a large number of 'particles' which were tracked in a Lagrangian manner to provide the exchange inputs required by the Transport model.

The model code used in this study is a three dimensional, non-linear, variable density, hydrodynamic model developed by CSIRO in Hobart. It provides three dimensional distributions of velocity, temperature and salinity as well as concentrations of passive tracers given input fluxes of water, salt, heat and passive tracers, and forcing by winds, atmospheric pressure gradients and tides. The equations forming the basis of the model are similar to those described in Blumberg and Herring (1987) , except that the model uses so-called 'z' coordinates in the vertical to better represent stratified flows. The equations are solved using finite-difference techniques on a C-type grid (see for example Mesinger and Arakawa, 1976) . The model is described in more detail in Walker and Fandry (1993).

2 Model Inputs

2.1 Bathymetry

The model covers the entire Bay, plus a region of Bass Strait just outside the Bay which was included to allow a reasonable representation of exchange between the Bay and Bass Strait. Figure 1 shows the 1000m resolution model grid and the locations of sites at which various field data were obtained.

Bathymetric data was obtained in digital form from the Royal Australian Navy Hydrographic Office. These data were obtained from survey data relating to charts AUS 143, 154, 155, 157 and 158. Depths were obtained at 3419 locations, covering the Bay and a narrow strip of northern Bass Strait adjacent to the Bay. Data were adjusted so that all depths were referenced to mean sea level rather than chart datum.

These data were averaged within each model cell. Depths for cells with no data were set by interpolating, using a weighted nearest neighbour technique, from surrounding cells. It was necessary to modify some of the model bathymetry in the Rip and the Sands area manually, in order to adequately represent the rather narrow and deep channels in those areas. The model was quite sensitive to these changes, particularly with regard to tidal elevations and tidal currents. A number of runs were done to determine the bathymetry which allowed the most accurate representation of tides in the Bay.

For the 1000m resolution grid, there were 3 cells across the Rip, so that the very complex bathymetry there was not well represented. Model bathymetry was set there to maintain the cross-sectional area of the Rip (about 38000m^2, from Black and Mourtikas (1992) - Technical Report 3). Some smoothing of the bathymetry in Bass Strait immediately outside the Rip was done, in order to improve the stability of the model. Tidal currents reach several metres per second in this area, causing large vertical velocities which constrain the model time step, regardless of horizontal resolution.

Vertically, the model grids had 25 layers, with uniform resolution of 2m in each layer. The maximum depth in the models was 50 metres. This slightly truncated the actual bathymetry in Bass Strait near the south-western boundary, but had negligible effects on model results (some preliminary runs were done without truncated bathymetry).

2.2 Sea-level

The open boundary of the model was forced by specifying elevations from observed sea level data at Lorne, about 60 km along the Victorian coast to the south-west of the Bay. Sea-level data for Lorne were obtained by the study from the National Tidal Facility (NTF), covering the period 1993 to

1995.

In order to provide forcing data prior to 1993 (when Lorne observations were not available) sea-levels were synthesised by combining tidal levels calculated from the M2, S2, K1 and O1 harmonic constituents for Lorne (calculated by the NTF) with residual (low-pass filtered) sea-levels observed at Point Lonsdale. Point Lonsdale data was obtained from the NTF, for the period 1985 to 1995. Although not entirely accurate, this procedure does capture the main characteristics of the tidal signal, and reproduces low frequency changes in sea-level well. Raw Point Lonsdale sea-level data is not suitable for forcing the model, as it comes from an area where there are very rapid spatial changes in tidal amplitudes, and where the observed signal is strongly affected by the dynamics of the energetic tidal currents through the Rip.

In preliminary runs, the models were forced with hourly data, linearly interpolated in time. This was observed to give a noisy model response in the Bass Strait part of the model. This effect is probably due to an artificial seiche between the coast and the model boundary, with a period near to 1 hour and hence excited by the hourly sampling frequency of the data. This effect was completely eliminated by re-sampling the tidal data to 15 minute resolution, using a smooth spline technique.

A depth-averaged 4km resolution model of Bass Strait (previously developed at CSIRO Oceanography) was used to estimate the phase speed of the tidal signal along the model boundary in Bass Strait. Tidal elevations along the boundary were then specified as those at Lorne, delayed by a time which depended on the distance from a specified point. This attempted to correct both for the fact that Lorne is located some distance to the southwest of the model, and for the propagation of the tidal signal along the boundary.

As well as the sea-levels and phase correction described above, a slope was imposed on the south-eastern open boundary (the more 'cross-shore' boundary in Bass Strait). This imposed slope was proportional to the net flow through that boundary times the Coriolis parameter.

2.3 Freshwater

Freshwater forcing for the models consisted of data describing rainfall, evaporation, and flow data for the major rivers, creeks and drains. These data were obtained primarily from the Bureau of Meteorology, the Victorian EPA and Melbourne Water.

All freshwater inputs (rain and flows from rivers, creeks and drains) were assumed to have zero salinity, and a temperature variation corresponding to the seasonal air temperature observed over the Bay (between about 9.5 and 18.5 degrees C). The inputs from rivers, creeks and drains were located in the model grid at the cells nearest their actual locations around the Bay. Rainfall and evaporation were applied over the surface of the Bay according to their observed distributions.

The various freshwater inputs are described in more detail in the following sections.

2.3.1 Rainfall

Rainfall data were obtained from a number of sources during the study. For the purposes of modelling, rainfall data were required on a uniform grid covering the Bay. Due to the lack of data from gauges located on the Bay (only Hovell Pile, 1994-1995), rainfall data were interpolated from sites on land surrounding the Bay. Such data were obtained from both the Victorian EPA, and the Bureau of Meteorology. These two data sets were very similar, with small differences probably due to slight differences in choice of sites and interpolation techniques.

In all, 14 sites were used to provide rainfall coverage over the Bay. An inverse distance weighted interpolation scheme was used to calculate rainfall on a uniform 10km resolution grid covering the Bay, for the period 1985 to 1995. This data was used as model input. As an example of this data, Figure 2 shows total annual rainfall over the Bay for 1994, together with the sites for which data was obtained. Figure **??** shows a time-series of (spatial mean) rainfall over the Bay for the period 1990 to 1995.

2.3.2 Evaporation

Evaporation is only recorded at two stations in the Melbourne area, both on land and to the north of the Bay (Hunter 1992). For input to the physical models, data describing hourly evaporation from the Bay surface was obtained from the Victorian EPA, covering the years 1985 to 1994, and the first half of 1995. The data was located on a 10km resolution grid, calculated from wind speed, air and water temperature and relative humidity, using a method described in World Meteorological Organisation Technical Note No. 83 - 'Measurement and estimation of evaporation and evapotranspiration'.

When used by both the hydrodynamic models and transport models (see Technical Report 39 - Walker and Sherwood 1997), these calculated evaporation rates led to predictions of salinity in the Bay which were higher than observed values. A problem with the evaporation calculation is that it is highly sensitive to the humidity value used. Unattended measurement of humidity for extended periods is a difficult task, particularly over water, and so the humidity (and hence evaporation) values obtained by the study need to be treated with some caution. Better comparisons between observed and modelled salinities was obtained when the evaporation values were reduced by about 30% (or rainfall increased by about 60%, which is almost equivalent as far as the models are concerned - an important difference being that rainfall and evaporation appear to exhibit different spatial patterns over the Bay). A somewhat arbitrary experiment was done to reduce the evaporation values by re-doing the calculation with a slightly higher, constant, humidity of 80%. By comparison, average humidity at Laverton, calculated from an 11 year record of wet and dry bulb temperatures, was 74% (Section 2.7.4). This recalculation led to significantly better agreement between modelled and measured salinities. Further investigation of the fresh-water budget of the Bay is warranted, but is considered beyond the scope of this report.

2.3.3 Yarra River

Flow data for the Yarra River and some of its tributaries were obtained as part of the catchment modelling work done for the PPBES by the Victorian Institute of Marine Science (VIMS). Data were obtained for the sites and periods shown in Table 1.

Site	Period
Yarra River (Chandler Highway)	1975-1995
Maribyrnong River (Keilor)	1980-1995
Gardiners Creek	1980-1995
Merri Creek	1980-1995
Moonee Ponds Creek	1990-1995

Table 1: Flow data for the Yarra river and its tributaries.

The long term mean flow at the Yarra mouth for the period January 1980 to October 1995 is about $21m^3/s$. There is substantial variability, both seasonal and from year to year. Figure 4 shows flows at the mouth of the Yarra over the period 1990 to 1995. Note the large ‘seasonal’ events, particularly towards the ends of 1992 and 1993, and the lack of any such event in 1994.

2.3.4 Eastern rivers, creeks and drains

Flow data for rivers, creeks and drains on the eastern side of the Bay were obtained as shown in Table 2.

Data for the Patterson River/Mordialloc creek system were obtained as part of the catchment modelling work undertaken by VIMS. These data incorporate the effects of a simple algorithm which takes into account the flow diversion which occurs in this system. Dandenong and Eumemmerring creeks were not directly used in the modelling of the Bay, as their flows are included in data for the Patterson River/Mordialloc creek system

Site	Period
Dandenong creek	1994
Eumemmerring creek	1994
Mordialloc creek	1988 - 1994
Patterson river	1988 - 1994
Elsternwick MD	1990 - Feb 1994

Table 2: Flow data for the main eastern inputs to the Bay

For modelling purposes, data was required for the entire period covering 1985 to 1995. Where data was not available, it was synthesised as follows:

- Mordialloc creek: Mean flow of 2.24m^3/s was used.
- Patterson River: Correlation against total Yarra flow was used. The relationship found was Patterson = 0.1663 Yarra + 0.406, with an r squared value of 0.42. The correlation is not good, and mainly arises from seasonal variations in the flows. Correlations with various Yarra tributaries and with rainfall were also explored, but all fitted more poorly than that shown above.
- Elwood Canal (Elsternwick): Mean flow of 0.18 m^3/s was used.

Mean flows and correlations quoted above were calculated over the entire period where data was available.

Figure A shows flow in the Patterson River for the period 1990 to 1995. Note the change in nature of the data in 1995, where correlation with the Yarra river was used. Data for this year has recently become available, and should be used for any future model runs.

2.3.5 Western Treatment Plant

Inputs of fresh water enter the Bay from the Western Treatment Plant via four outlets (15E, 145W, Lake Borrie and Murtcaim). These outlets are located over about 10km of coastline on the western side of the Bay. Flow data for these outlets were obtained from Melbourne Water for the period 1980 - 1995. Data was also obtained for a fifth outlet (Little River), which ceased operation in 1989. All five outlets were included as model inputs, distributed in the model grid according to their locations along the coast.

Figure **??** shows total flow from the Western Treatment Plant for the period 1990-1995. A clear seasonal signal is present, but on an annual basis, flow rates have remained fairly constant in the past 6 years. The distribution of flows has changed, however, with increased flow from the 15E outlet, and decreased flows from other outlets. Note that changes in the flow data sampling frequency are also apparent in Figure **??**.

2.3.6 Western rivers, creeks and drains

Data for two further sources of fresh water were obtained by the study, as shown in Table 3.

Site	Period
Werribee river	1993 - May 1995
Kororoit creek	1993 - Feb 1994

Table 3: Flow data for western rivers and creeks.

Neither of these inputs showed significant flows apart from a single event in September 1993, when flows peaked at over $300m^3/s$ in the Werribee river, and over $60m^3/s$ in Kororoit creek. At most other times flows in both of these systems was less than $0.5m^3/s$. This makes it essentially impossible to extend these data sets to cover the period 1985 to 1995 in a realistic way. No correlation with rainfall was found. In the end, to fill periods where data was not available, flows were set to the low values of $0.25m^3/s$ for the Werribee river, and $0.20m^3/s$ for Kororoit creek. The model thus does not show effects of flood events which may have occurred in these systems prior to 1993.

2.4 Wind

Wind data over the Bay were provided by the Victorian EPA, interpolated from observations at 3 sites within the Bay (Hovell Pile, Point Wilson and Fawkner Beacon) and one site on land (Point Cook - a well exposed site with a long record of observations).

Correlations between points on the Bay and Point Cook were calculated for periods when all sites were available, and these correlations were used to calculate Bay-wide winds when only Point Cook data were available. The end results of this process were continuous hourly wind data on a 10km resolution grid covering the entire Bay for the period 1985 to 1995.

Potential problems with this data set are that there is no source of wind data from any point near the main (central) body of the Bay, and that for much of the period the data is from a single site. There will undoubtedly be times when the wind varies strongly from place to place on the Bay (during local storms, and the passage of fronts, for example). During such times, the winds used to force the model are unlikely to be realistic, and so the ability of the model to reproduce circulation patterns in the Bay will be compromised.

In order to calculate the stress exerted by the wind on the water surface in the models, the formulation of Large and Pond (1981) was used.

2.5 Atmospheric pressure

Atmospheric pressure affects sea-level (the inverse barometer effect). However, the Bay is much smaller than the typical length scales associated with atmospheric pressure gradients, and differences across the Bay are likely to be very small. The effect on sea-level is incorporated in the observed sea-level values prescribed at the model open boundary in Bass Strait. As a result, it was not necessary to include spatial or temporal variations in atmospheric pressure as an explicit model input.

2.6 Salinity

As stated above, the salinity of all freshwater inputs was assumed to be zero. As well, salinity needs to be specified at the model open boundary in Bass Strait. In the absence of measurements in Bass Strait during the study, data extracted from surveys conducted by VFRI were used to set Bass Strait boundary conditions for the model. These data were obtained from a site near the Rip (the N1F site), where measurements were made during the flood tide to minimise the influence of Bay waters. Examination of these data showed that the salinity varied little from a value of 35.4, and so that value was used as the Bass Strait boundary salinity for all model runs.

Initial salinity fields for model runs were obtained by interpolating (in both space and time) the underway salinity observations collected by VFRI roughly monthly throughout the study. The water column was assumed to have uniform salinity with depth, except in Hobsons Bay, where the profile from VFRI site 9 was used to guide the model initialisation. For model runs simulating periods which started prior to the study (before about mid-1993), initial salinities were interpolated from the VFRI fortnightly stations known as sites 1, 4, 6, 9, 11 and 13 (see Technical Report 24 - Longmore *et al.*, 1996). A dummy site reproducing the properties of site 11 was also added near Point Cook, to limit the area of influence of site 9 (which is situated in Hobsons Bay, and so strongly affected by the Yarra).

2.7 Heat

In order to model changes in water temperature in the Bay, bulk formulae were used to calculate surface heat fluxes (see Gill (1982) for example). These formulae required the data sets described below.

2.7.1 Solar radiation

Hourly total solar radiation (TSR) data was obtained from the Victorian EPA for sites at Brighton (1994-1995) and Dandenong (1995). Half-hourly TSR data was also obtained from the Bureau of Meteorology for a site at Laverton, covering the period January 1985 to February 1994. These data sets were combined to give hourly coverage of the period 1985 to 1995, using mostly Laverton data, and Brighton data to cover the last part of the period. Small gaps (less than about 4 hours) were filled by linear interpolation. There were some larger gaps, which were filled with calculated clear sky TSR values (using a maximum solar input at normal incidence of 1200 W/m^2, a value chosen to give a good match between calculated and observed values).

When applying the TSR data in the model, the albedo of the water surface was set to 0.2, and the attenuation coefficient of light with depth was set to $0.2m^{-1}$. These values were chosen to best match the observed Bay water temperature during 1994 (see Section 5 and Figure 97).

2.7.2 Wind

Wind data, as described previously, were used in the calculation of sensible heat flux, according to Gill (1982).

2.7.3 Air temperature

Air temperature is also needed in the calculation of sensible heat flux. Data were obtained from Victorian EPA sites at Frankston and Point Wilson, and from measurements at Hovell Pile. Data were also obtained from the Bureau of Meteorology for sites at Melbourne, Moorabbin and Laverton for the period 1985 - 1995. For the purposes of driving the hydrodynamic model, air temperature observed over the Bay waters is most desirable.

However, data from Hovell Pile were only available for a period of 1 year, with significant gaps. Much longer records were available at the land-based Bureau of Meteorology sites (Laverton, Melbourne and Moorabbin). These sites showed a larger diurnal cycle than that observed at Hovell Pile. Apart from this obvious difference, however, these sites, particularly Laverton and Moorabbin, show similar behaviour to the records from Hovell Pile. As a result, data from Laverton and Moorabbin were lightly low-pass filtered to reduce the amplitude of the diurnal cycle to that seen at Hovell Pile. The data from the two sites was then averaged to provide the long term air temperature time series used to drive the model.

2.7.4 Humidity

For the purposes of the surface heat flux (and assuming evaporation is already known) humidity is needed in the radiative heat flux terms. Humidity data were obtained from Victorian EPA sites at Frankston and Point Wilson, and from measurements at Hovell Pile. The Hovell Pile data contained many gaps, and was not considered to be reliable. The EPAV data spanned 1990 to 1993, and also contained numerous gaps. As a result, humidity values used by the model were calculated from dry and wet-bulb temperature records from Bureau of Meteorology sites at Laverton. Over the eleven year period 1985 to 1995, the calculated humidity at Laverton had a mean value of 74.0% and a standard deviation of 16.4%.

2.7.5 Evaporation

Heat loss due to evaporation was calculated using the evaporation data described in Section 2.3.2.

2.7.6 Cloud cover

Cloud cover affects the radiative heat flux terms. Because observed TSR values were used, they were not further modulated by cloud cover values inside the model. However, the long-wave radiative heat flux term did include the effects of cloud cover. Three hourly cloud cover data were obtained from the Bureau of Meteorology for sites at Melbourne, Moorabbin and Laverton for the period 1985 - 1995. There were large gaps in the data for Moorabbin and Laverton, so that the Melbourne data was used as model input, applied uniformly across the Bay. This is obviously a fairly coarse approximation.

2.7.7 Bass Strait temperature

Again, in the absence of measurements in Bass Strait during the study, data extracted from surveys conducted by VFRI at the N1F site (the Rip, flood tide) were used to set Bass Strait temperature boundary conditions for the model. Temperatures show a clear seasonal fluctuation, ranging from about 12.5C to 18.0C (during the measurement period from March 1994 to March 1995). These data were used for all model runs, with the data repeated in an annual cycle to provide conditions for years where there were no measurements.

Note that historical data may exist which might allow better temperature boundary conditions to be set. For example, the CSIRO Division of Oceanography holds an extensive archive of AVHRR satellite imagery which could possibly be used to estimate surface temperature. Discussion of the annual cycle of the density field in Bass Strait can be found in Baines and Fandry (1983).

Initial temperature fields inside the Bay were obtained by interpolating monthly VFRI underway data in a way similar to that described for salinity in Section 2.6.

2.8 Bottom friction parameters

Quadratic bottom friction was used in the model, with a roughness length of 0.002m and minimum drag coefficient of 0.0025 (Blumberg and Herring 1987, equation 19). These parameters were constant in both time and space throughout the models.

The model was found to be relatively insensitive to these choices. decreasing roughness length to 0.001m increased tidal elevation and tidal current amplitudes inside the Bay by about 5%. Increasing roughness length to 0.01m reduced tidal elevation amplitudes inside the Bay (north of the Great Sands) by about 15%, but increased tidal elevation amplitudes at Queenscliff (south of the Great Sands) by about 10%.

2.9 Mixing parameters

The vertical momentum diffusion coefficient V_z and vertical tracer diffusion coefficient K_z were calculated in the models using a formulation along the lines described in Csanady (1982), equation 6.22b, with modification due to stratification as described by Bowden and Hamilton (1975):

$$V_z = V_{z0} + \alpha_V u_\star H (1 + 10R_i)^{-\frac{1}{2}} \quad (1)$$

$$K_z = K_{z0} + \alpha_K u_\star H (1 + 3.33R_i)^{-\frac{3}{2}} \quad (2)$$

where $u_\star$ is the maximum of the surface and bottom friction velocities (to account for both tidal and wind mixing), H is the depth of water, V_{z0}, K_{z0}, α_V and α_K are constants, and R_i is a Richardson number, dependent on the vertical stratification and vertical velocity shear. The background mixing constants V_{z0} and K_{z0} were both set to the value of $0.00001\text{m}^2\text{s}^{-1}$. The model sensitivity to the value of α_V was explored, with a value of 0.08 giving best results (in terms of comparisons with measured currents inside the Bay). This value is somewhat higher than the value of 1/16 (0.0625) quoted by Csanady (1982). The value of α_K was set to 0.04.

Horizontal diffusion of momentum was added, with a diffusion coefficient of $2m^2s^{-1}$. This value is consistent with observations of horizontal mixing in the Bay (Pattiaratchi *et al.* 1989). No exploration of the sensitivity of the model to this value was performed, and it may be that the model will remain stable with smaller values.

Horizontal diffusion of tracers (salinity and temperature) was not explicitly included in the model. The upwind scheme used by the model for advection of tracers yields a numerical diffusion of the order of $\frac{1}{2}u\Delta x$, where u is the local velocity and Δx is the grid resolution. For typical velocities of 0.1m/s inside the Bay, and a grid resolution of 1000m, this corresponds to a numerical diffusion coefficient of of 50 m^2/s, which is about an order of magnitude larger than observed (Pattiaratchi *et al.* 1989. Whether this is a problem or not is debatable. It certainly affects the fields of temperature and salinity, particularly where there are large velocities (the Rip and Sands area), or strong gradients (salinity in Hobsons Bay, for example). However, tracers used for ecological simulations of the Bay were included in the Transport Model (see Technical Report 39, Walker and Sherwood 1997), not the Hydrodynamic model, and transports used to drive that model were calculated from the hydrodynamic simulations using particle tracking - a technique which is not subject to this sort of numerical diffusion effect.

3 Model Calibration

Model calibration data consisted primarily of measured sea-levels and currents inside the Bay during the month of May 1994. A number of model runs were performed, adjusting mainly model bathymetry in the Rip and Sands, and vertical mixing parameter (α_V), to obtain good agreement between simulation and observation. The most important adjustment for tidal comparisons was the bathymetry in the Rip and Sands areas, with the model being particularly sensitive to the cross-sectional area of the Rip, the representation of the South channel, and the depth over the shallow areas of the Sands. For non-tidal (low-pass filtered) currents, the vertical mixing parameter (α_V) was the most significant adjustment.

Figure 7 shows the sea-level from Lorne used to force the model for the calibration period. As an example of the winds used to force the model, winds measured at Hovell Pile during May 1994 are shown in Figure 8. The latter half of this month was very windy, with strong north to north-westerly winds rarely dropping below speeds of 10 m/s. An unusual feature earlier in the month is a strong easterly wind, on the 8th and 9th of May.

Salinity and temperature were measured during two CTD surveys, one conducted on 3-4 May and the other over the period 12 - 16 May 1994. As well, underway surface salinity and temperature data were collected roughly monthly during the study as part of the nutrient surveys of the Bay (Technical Report 24 - Longmore *et al.*, 1996). As described above, the model initial salinity and temperature fields were derived from the underway data.

Given the long flushing time of the Bay (of the order of a year), only relatively minor changes occur in salinity (and temperature, which is mainly seasonal) over periods of the order of one month, except during infrequent events such as major floods. It is hence not very practical to attempt to adjust the salinity or temperature performance of the model using a one month (May 1994) calibration period. Instead, a coarser model (3000m resolution) was set up, and its tidal behaviour adjusted to match the 1000m model as much as possible. This allowed a large number of long (1 to 2 year) runs to be done, in order to examine longer term modelled time series of salinity and temperature. Salinity was calibrated primarily by varying the evaporation input (which is only known relatively poorly), and temperature was adjusted primarily by adjusting the albedo of the Bay (for solar radiation input).

3.1 Elevation

Figures 9 to 13 show plots of measured and modelled sea-level at 5 sites inside the Bay. Note that, as supplied, the Hovell Pile observations appeared to show a constant offset of 7cm below other gauges in the Bay. This offset can be seen in Figure 10. Apart from that offset, all sites show good agreement between modelled and observed values. This agreement was achieved after a number of minor adjustments to the model bathymetry in the Rip and Great Sands areas. The tidal response of the model is sensitive to the bathymetry in these areas.

The results of harmonic analysis of measured and modelled sea-levels are presented with the model validation results below (Section 4).

3.2 Velocities

The first current meter deployment covered the period from 21 April 1994 to 2 June 1994, with 5 moorings, located near Martha Point, the northern edge of the Great Sands, the Bay centre, Point Cook, and Red Bluff. There were 2 meters on each mooring, generally at about 4-5m below the water surface and about 4-5m above the bottom. Data were recovered from all meters during this period.

A comparison of raw measured and modelled currents for the month of May 1994 is shown in Figures **??** to **??**. These plots show both tidal and non-tidal currents. At most sites, the tidal part of the currents are reproduced well by the model. This is quantified by tidal analyses of the measured and modelled currents for the period, presented in Appendix A. At most sites, the agreement between modelled and observed tidal currents is very good, particularly for the dominant M2 component. There is a large phase error at the lower Great Sands meter during the May calibration period. This probably arises from a timing error in the observed data, as comparisons of time series of currents from the upper and lower meter at that site show a similar large difference in phase.

Of course, tidal currents are strongest in the southernmost parts of the Bay, where there were no current meter moorings. However, coastal radar (COSRAD) data was obtained in the Sands region for the period 5 - 12

May 1994 (Prytz and Heron 1994). Comparisons between measured COSRAD currents and modelled currents for this period were produced at 3 locations shown in Figure **??**. The measured and modelled current time-series at these sites are shown in Figures **??** to **??**. These figures all indicate that the model does a good job of representing the tidal flows in the southern part of the Bay.

Of more interest for the transport of substances around the Bay are the longer term non-tidal currents. Comparisons of low-pass filtered (24.8 hour period cutoff) measured and modelled currents are shown as both time series plots and as scatter plots in Figures **??** to **??**. As well, a comparison of the vector mean current at each meter over the entire May calibration period is shown in Figure **??**.

In summary, during the calibration period (May 1994) the model represents low-pass filtered currents very well at Point Cook, Red Bluff, and the lower meter at the Great Sands site. It performs reasonably well at the Central Bay site and at the lower meter at Martha Point, and performs poorly at the upper meters at the Martha Point and Great Sands sites. This poor agreement at the upper Martha Point meter can probably be explained by the proximity of this site to the bay-ward end of the South channel. The modelled currents at Martha Point were found to be very sensitive to the model bathymetry in this region. The poor agreement at the upper Great Sands meter is problematic, particularly given the very good agreement at the lower meter at this site. The upper meter there may be affected by flows over the Sands, or possibly through Symonds Channel.

The low-pass filtered current comparisons are discussed in more detail for each mooring site below:

3.2.1 Martha Point

The model does not reproduce low-pass filtered currents well at the upper meter. The east component shows some correlation ($r = 0.68$), but there is little correlation for the north component. The model underestimates speeds during some events, but overestimates during others. Directions show little or no agreement. The observed and modelled mean currents over the entire period (Figure **??**) disagree in direction, but the magnitude of both is quite small (less than about 0.02m/s).

The relationship between measurements and model is more obvious at the lower meter, particularly in the north component (correlation coefficient $r = 0.76$), but the agreement is poor for the east component ($r = -0.33$). Here the model tends to under-predict current speeds, particularly during the windy second half of the month. The mean modelled current also has smaller magnitude than the observed mean, but directional agreement is reasonably good, and much better than at the upper meter. The observed and modelled east components appear to be out of phase, due to the fact that currents at this meter are predominantly directed to the north, with the model slightly more westwards than the observations.

3.2.2 Great Sands

The correlation between observed and modelled currents is poor at the upper meter (east component $r = 0.09$, north component $r = -0.11$). Overall the model shows similar speeds to those observed, but at any given time there is little agreement in either speed or direction. An unusual feature in the measured currents at this meter is the steadily rising current speed (and north component) over the last week of May. Strong currents were not seen at any other meter in the Bay during that week, and the feature does not correlate with wind forcing. The cause of this feature is unknown, and no sign of it is seen in the model results.

In contrast, the model reproduces low-pass filtered currents very well at the lower meter. Speed and direction both show a good match throughout the month. The mean currents over the whole month agree well in direction, with the model slightly overestimating the magnitude of the mean current. The regression analysis indicates that the model tends to underestimate both east and north components by about 15%. However, the time series plots show that during the wind events later in the month the model tends to over-predict speeds to a moderate extent. The east and north components show correlation coefficients of $r = 0.88$ and $r = 0.80$ respectively.

3.2.3 Central Bay

At this site, the model represents the current north component reasonably well at both the upper and lower meters ($r = 0.75$ and $r = 0.80$ respectively). However, the east component is poorly represented ($r = -0.06$ at the top meter and $r = -0.16$ at the bottom meter). The time series plots show that speeds are well represented at both meters, but directions are not, particularly during the first half of the month, when low-pass filtered currents at this site are small (typically a few centimetres per second). Both meters show better agreement in direction during the windy second half of the month.

3.2.4 Point Cook

This site shows good agreement between the model and measured currents, apart from the north component at the lower meter, where there is little signal in either model or measurements. At the top meter, the east and north correlation coefficients are $r = 0.88$ and $r = 0.68$ respectively. Here, the model tends to overestimate current speed during strong wind events. It also shows a systematic direction offset of about 40 degrees anticlockwise with respect to the measurements. This offset could possibly be caused by bathymetric variations near the meters, although it is somewhat hard to understand why the upper meter would be affected more than the lower meter. At the bottom meter, the east and north correlation coefficients are $r = 0.89$ and $r = 0.00$ respectively. Here the model gives a good representation of both speed and direction.

The magnitude of the mean current is overestimated by the model at both the upper and lower meters at this site. The observed means are very small (about 0.005 m/s at the top meter and 0.008 m/s at the bottom meter). Mean directions agree well at the bottom meter, whereas the top meter shows the model offset about 40 degrees anticlockwise, as noted above.

3.2.5 Red Bluff

The top meter at this site shows the strongest currents measured during the May calibration periods. The model does a reasonably good job of reproducing them, with some significant departures during specific events, when the model overestimates speeds. The model overestimates the north component, and shows two predominant current directions - slightly east of south and slightly west of north (directions which are parallel to the coast in that part of the Bay). By contrast, the measured currents tend to be more variable in direction. At this meter the east components are poorly correlated ($r = 0.32$), with a somewhat better correlation for the north components ($r = 0.63$).

The model represents the measured currents well at the lower meter. The east and north correlation coefficients are $r = 0.78$ and $r = 0.86$ respectively. There is generally good agreement in both speed and direction. The model tends to underestimate speeds in the later part of the month, but gives a good representation of the south-easterly direction of flow during this period.

The mean current over the month is represented well at both meters, apart from an overestimate in speed of almost 40% at the top meter.

3.3 Salinity and Temperature

Figures **??** to **??** show measured and modelled surface salinities for the CTD surveys carried out on 3-4 May and 12-16 May 1994. The observed and modelled distributions are very similar on both occasions, with most of the Bay having a salinity near 34, and with lower salinity water associated with the Yarra plume extending along the north-east coast. The influence of the Western Treatment Plant can also be seen near its outfalls in the west of the Bay. Quantitative comparisons of these plots are somewhat problematic, as the observations are collected over a period of 2 - 4 days, whereas the model yields a plot at a single instant in time. A more rigorous comparison would be possible by sampling the model using the same schedule (the same times and places) as used for the observations. This somewhat time-consuming exercise has not been attempted for this report.

Figures **??** to **??** show measured and modelled surface temperatures for the same CTD surveys. The measured and modelled temperatures for the survey on 3-4 May are very similar - a not very surprising result, given that the model was initialised from observed underway temperatures (interpolated in time) four model days earlier. For the survey on the 12-16 May, the model shows the main body of the Bay to be about 0.5°C cooler than observed. The model also shows substantially more cooling than observed towards the Werribee coast and in the Geelong Arm, with modelled temperatures up to 2°C cooler than observations in those regions. The reasons for this discrepancy are probably related to the approximations made in the surface heat fluxes for the model, particularly evaporation, humidity and air temperature.

4 Model Validation

Model validation data consisted of measured sea-levels and currents inside the Bay during September and the first half of October 1994. As well, CTD surveys of the Bay were carried out on 14-15 September and 29 September to 3 October 1994. The validation period was simulated using the model parameters chosen during the calibration process. The model was initialised with salinity and temperature fields at 00:00, 31 August 1994 from the monthly VFRI underway data, interpolated in space and time. The results are described below.

4.1 Elevation

Figures ?? to ?? show comparisons of measured and modelled sea-level as both time series (for September 1994) and scatter plots (for the entire 1994 calendar year) at 5 sites inside the Bay. These plots indicate that the model does a very good job of representing sea-level inside the Bay. As well, a harmonic analysis was performed on modelled and observed sea-level data from 5 sites for the entire 1994 calendar year. The results are shown in Tables 4 (amplitudes) and 5 (phases).

Site		O1	K1	N2	M2	S2
Breakwater Pier	observed	0.068	0.098	0.039	0.236	0.054
	model	0.074	0.106	0.040	0.229	0.057
Geelong	observed	0.072	0.100	0.047	0.268	0.066
	model	0.078	0.112	0.045	0.267	0.069
Hovell Pile	observed	0.070	0.096	0.035	0.202	0.049
	model	0.072	0.102	0.033	0.189	0.046
Queenscliff	observed	0.085	0.111	0.052	0.259	0.073
	model	0.086	0.122	0.052	0.292	0.088
West Channel Pile	observed	0.067	0.096	0.036	0.205	0.046
	model	0.074	0.104	0.034	0.195	0.048

Table 4: Observed and modelled tidal constituent amplitudes (in metres) calculated for 1994.

It is clear from these tables that the model reproduces both the amplitude and phase of the major tidal constituents very well. The largest discrepancy occurs at Queenscliff, where the model overestimates the M2 amplitude by 3.3cm, and has an M2 phase error of 7 degrees. It should be noted that Queenscliff is near the entrance to the Bay - an area where tidal amplitudes and phases change rapidly with position. At other sites, amplitude errors are of the order of 1cm or less, and phase errors are of the order of a few degrees.

Site		O1	K1	N2	M2	S2
Breakwater Pier	observed	95.1	131.8	12.4	60.4	197.6
	model	94.8	129.8	14.7	62.7	193.4
Geelong	observed	96.1	133.3	17.4	61.3	198.1
	model	96.6	130.4	17.1	64.6	197.7
Hovell Pile	observed	96.0	133.4	14.1	60.4	199.9
	model	95.6	129.5	14.1	62.4	194.0
Queenscliff	observed	62.2	95.0	297.3	344.8	119.7
	model	49.2	80.7	290.4	337.7	103.1
West Channel Pile	observed	94.9	131.1	10.2	57.0	193.5
	model	92.6	126.3	8.1	56.5	187.4

Table 5: Observed and modelled tidal constituent phase (in degrees) calculated for 1994.

4.2 Velocities

During the validation period (late August to mid October 1994), current meter moorings were again made at 5 sites, with meters at two depths at each site. The sites used during this period were Martha Point, Schnapper Point, the Central Bay, Point Cook, and Red Bluff. No data was recovered from the lower meters at the Central Bay and Red Bluff moorings for this deployment.

A comparison of raw measured and modelled currents for the validation period is shown in Figures **??** to **??**. These plots show both tidal and non-tidal currents. As was found during the May calibration period, the tidal part of the currents are reproduced well by the model. This is again quantified by tidal analyses of the measured and modelled currents for the period, presented in Appendix A.

Comparisons of low-pass filtered (24.8 hour period cutoff) measured and modelled currents are shown as both time series plots and as scatter plots in Figures **??** to **??**. As well, a comparison of the vector mean current at each meter over the entire validation period is shown in Figure **??**.

In summary, the model reproduces low-pass filtered currents well in the northern part of the Bay (Point Cook and Red Bluff). Its performance is less good at the Schnapper point and Central Bay sites, but both measured and modelled currents at these sites are very weak throughout the validation period, so that, although the relative errors between modelled and measured currents are large, the absolute errors are quite small. Performance at the Martha Point site is improved at the upper meter (compared to the calibration period), but poorer at the lower meter, where the model significantly underestimates current speeds.

These comparisons are discussed in more detail for each mooring site below:

4.2.1 Martha Point

There is moderate agreement between the model and measurements at the upper meter, with the model overestimating speeds on some occasions and underestimating on others. The east component shows a better correlation ($r = 0.54$) than the north component ($r = 0.39$). Current directions tend to agree during periods when the current speed is higher (an unsurprising result, as directions become ill-defined as speeds approach zero). The mean current over the entire period is quite well represented by the model, apart from a directional offset of about 30 degrees clockwise.

At the lower meter, there is good agreement in the east component (correlation coefficient $r = 0.65$), but poor agreement in the north component ($r = 0.17$), with the model rarely showing a north component magnitude above a few centimetres per second. The model almost always underestimates speeds at this meter, a result consistent with the May calibration period. There is occasional agreement in direction, but the modelled currents are often weak and hence tend to show large variations in direction. The mean current over the entire period is badly underestimated by the model at this meter.

4.2.2 Schnapper Point

The model correlates well with the observed north component ($r = 0.76$) at the upper meter, but underestimates its amplitude. The east component is poorly represented at this meter ($r = 0.27$), and is underestimated during stronger events. Current speeds are well represented during the mid-September period (when they are very low), but are underestimated by the model at other times. There is some agreement in direction, particularly during mid-September. It should be noted that records accompanying the data from this meter state that the raw data were very noisy, were subjected to a significant amount of post-processing prior to delivery, and that caution is needed in their use, particularly for residual or mean currents.

At the lower meter, the model again represents speed reasonably well during mid-September, and underestimates speeds at other times. Modelled and measured speeds are both low (mostly less than 0.05m/s) at this meter. Directions tend to be variable, but with the measurements tending to favour a westerly direction, while the model appears to favours a northerly direction. The correlation coefficients for the east and north components are $r = 0.33$ and $r = 0.49$ respectively.

The mean currents over the entire period are weak at this site - about 0.02m/s directed to the south-east at the upper meter and about the same speed directed to the west at the lower meter. The modelled means are both directed roughly to the north, with somewhat smaller magnitude. Because speeds are so small, the absolute error in the means is small, but the relative error is large.

4.2.3 Central Bay

Both modelled and measured currents are small at the upper meter throughout the validation period. The east component shows a fair correlation ($r = 0.52$), but there is no correlation between model and observations for the north component ($r = 0.09$). The model overall shows a similar range of speeds to those observed, but there is only occasional agreement at various times in the period. The observed currents show a long term rotation in current direction, with 3 full clockwise rotations in direction between mid-September and mid-October. Interestingly, the model shows similar behaviour, but with the opposite sense of rotation. As a result, there is only occasional agreement in direction, mainly when the currents are flowing northward.

The mean measured current at the upper meter over the validation period is very small - about 0.005 m/s. The model shows a mean current of about 0.02m/s directed to the northeast over this period.

No data was obtained from the lower meter at this site during the validation period.

4.2.4 Point Cook

The model gives a very good representation of currents at both meters at this site. In general, speeds are slightly underestimated at both meters, with good agreement in direction. At the upper meter, both east and north component correlation coefficients have a value of $r = 0.82$. At the lower meter the values are $r = 0.66$ and $r = 0.70$ respectively. Here, the model underestimates speed during a couple of stronger events. The mean currents over the entire period are small (about 0.01 m/s) at both meters. The model reproduces these well, with a direction offset of about 45 degrees anticlockwise at the lower meter.

4.2.5 Red Bluff

As in the calibration period, the model tends to overestimate speed at the upper meter at this site. The east and north components show good correlation with measurements, with $r = 0.77$ and $r = 0.62$ respectively.

Both model and measurements show flow predominantly directed towards the south-east, with occasional reversals. The measured directions tend to be somewhat more variable than those shown by the model. The mean current over the period is directed to the south-east, with the model showing good agreement in direction, but overestimating magnitude by almost 50%. In general, the model does a good job of representing the nature of the currents at this site, but with speeds that are somewhat high.

No data was obtained from the lower meter at this site during the validation period.

4.3 Salinity and Temperature

Figures **??** to **??** show measured and modelled surface salinities for the CTD surveys carried out on 14-15 September and 29 September - 3 October 1994. As in the calibration period, the observed and modelled distributions are again very similar on both occasions, apart from the fact that in this (validation) period, the model tends to show the main body of the Bay having a salinity about 0.25 (psu) higher than the measurements. The Yarra plume can again be seen extending along the north-east coast, with a more significant influence in the late September distribution than that in mid September. The influence of the Western Treatment Plant can just be seen near its outfalls in the model output, but not in the measured distributions (perhaps due to the contour interval chosen for these plots).

Temperature plots (Figures **??** to **??**) show the main body of the Bay at around 11.5°C on the 14-15 September, and perhaps 0.25 to 0.5 degrees cooler at the 29 September to 3 October survey. The model appears to be cooling faster, showing the Bay at about 10.5° C on 15 September, and between 9.5°to 10° C on 1 October. The model again shows more pronounced cooling along the western coast, a feature which is not present in the observations. This again points to inadequacies in the data sets used to provide heat fluxes for the model and in possibly also in the model heat flux terms.

5 Long term simulations - Transport model inputs

In order to produce long-term forcing sets for the Transport model, hydrodynamic simulations were performed for the entire period from 1 July 1990 to 30 June 1995. Primarily for computing convenience, these runs were done in six month segments, with the model re-initialised just prior to the start of each six month period. As an example of the output of these runs, Figures **??** and 97 shows time series of modelled salinity and temperature at the Central Bay site plotted against monthly observations from the nearby VFRI site known as MW2. Salinity rises throughout 1994, due to the low rainfall over this period. The model reproduces these salinity changes well at this site (which is representative of the main body of the Bay). Temperature shows an obvious seasonal cycle, with the model tending to overshoot by 1 or 2 degrees C in both summer and particularly late winter and spring. These are not intended to be rigorous comparisons, as more detailed comparisons of observed and modelled salinity at a number of sites around the Bay are presented in Technical Report 39, where the Transport model was forced by the output of the long term runs described above.

In order to provide the exchanges of water required by the transport model, the hydrodynamic model included a particle tracking module. A very large number of particles (typically 200000) were seeded randomly into the model and tracked for 24 hours, after which time all particle positions were recorded, and the particles then re-seeded. The transport model interface used particle positions at the start and end of each 24 hour period to calculate daily exchanges of water between transport model cells. Both horizontal and vertical exchanges were represented in this way, as the particles were tracked in three dimensions in the hydrodynamic model, and their movement included a diffusive process (random walk) scaled by the diffusivities calculated in the hydrodynamic model.

Time series of daily particle positions have been generated for the period July 1990 to June 1995 (a data set requiring approximately 9Gb of storage). These are used to calculate exchanges for various Transport model geometries, and the resulting exchange files form the primary physical forcing data to the Transport Model (Technical Report 39).

6 Summary

A number of hydrodynamic models of Port Phillip Bay have been set up as part of this study. Most calibration and validation work has been performed on a 1000m resolution model of the Bay, a resolution chosen primarily with regard to the computing resources available to the study. Importantly, a very comprehensive data set has been assembled to provide forcing data for the model. This data set contains a vast amount of oceanographic and meteorological information, and allows model runs to be performed which simulate any period in the decade 1985 to 1995.

The model has been calibrated and validated against data sets obtained from field measurement programs conducted in May and September, 1994. The model reproduces changes in sea-level (both tidal and non-tidal) very well throughout the Bay. It also gives a good representation of tidal currents throughout the Bay. Its ability to represent low frequency currents is more mixed, with consistently good performance in the north of the Bay (Point Cook, Red Bluff), and more variable performance elsewhere.

For low-pass filtered currents, the performance of the model at the Martha Point site is not good during either the calibration or validation periods. Although the model shows currents which are of similar magnitudes to those observed, there are generally only fair to poor correlations between modelled and observed currents there. It seems clear that there are processes affecting the currents at this site which are not well represented in the model. Possible candidates are the formation of persistent jets or eddies in response to the energetic tidal flows through the Sands region (particularly the South channel). It is significant that the modelled currents at this site are quite sensitive to the model bathymetry in the area and in the South channel, and it may be that a 1000m resolution model is not sufficient to resolve the flows in this area. Although 750m and 500m resolution models were developed during the course of this task, both were abandoned as being too expensive (in terms of CPU time) to run on the computers available to the task at the time.

As well, the limitations of the data sets used to force the model should be remembered. Wind data was available from between 1 and 4 sites, all near the edges of the Bay. Given that the low frequency currents in the Bay are primarily wind forced, an improvement in the input wind field to the model is likely to result in an improvement in model performance. As well, the fresh-water budget of the Bay still contains significant uncertanites, particularly with regard to evaporation.

Long term hydrodynamic simulations of the Bay have been conducted for the period July 1990 to June 1995. These outputs have been processed to provide forcing data for the Transport model (Technical Report 39), so that long term ecological simulations of the Bay (Technical Report 44) can be developed with a realistic range of hydrodynamic and climatological forcing.

7 Acknowledgements

A great many people and organisations contributed to the development of the model and data sets described in this report. Data sets were obtained from the Victorian EPA, the Bureau of Meteorology, Melbourne Water, the Port Authorities, the National Tidal Facility, WNI Pty. Ltd. (formerly Oceanroutes) VFRI and VIMS (now MAFRI), James Cook University, the University of Western Australia, and Lawson and Treloar Pty. Ltd. Models were obtained from the Victorian EPA, Lawson and Treloar Pty. Ltd, and the (then) CSIRO Division of Oceanography. Special mention should be made of Barry Cook (formerly Vic. EPA) and Andy Longmore (MAFRI), who both fielded requests for historical data sets most helpfully. John Hunter (CSIRO) designed the physics tasks and over-saw much of the physical field work. Brian Newell, Colin Arrowsmith, Doug Hall and Rob Molloy provided valuable support and interfacing throughout the study.

Funding was provided by Melbourne Water through the Port Phillip Bay Environmental Study.

References

Baines, P. G., and C. B. Fandry, 1983: Annual cycle of the density field in Bass Strait, *Aust. J. Mar. Freshw. Res.*

Black, K. P., and S. Mourtikas, 1992: Literature review of the Physics of Port Phillip Bay, *Tech. Rep. 3*, CSIRO Port Phillip Bay Environmental Study.

Blumberg, A. F., and J. Herring, 1987: Circulation modelling using orthogonal curvilinear coordinates, in *Three-Dimensional Models of Marine and Estuarine Dynamics*, edited by Nihoul, and Jamart, Elsevier.

Bowden, K. F., and P. Hamilton, 1975: Some experiments with a numerical model of circulation and mixing in a tidal estuary, *Estuarine and Coastal Marine Science*, **3**, 281–301.

Csanady, G. T., 1982: *Circulation in the coastal ocean*, D. Reidel Publishing company.

Gill, A. E., 1982: *Atmosphere-ocean dynamics*, Academic press.

Hunter, J. R., 1992: Review of physical processes, in *Port Phillip Bay Environmental Study: Status review*, edited by D. N. Hall, Technical Report 9, CSIRO.

Large, W. G., and S. Pond, 1981: Open ocean momentum flux measurements in moderate to strong winds, *J. Phys. Oceanogr.*, **11**, 324–336.

Lawson & Treloar Pty Ltd, 1995: Port Phillip Bay Environmental Study hydrodynamic model, *Tech. Rep. J5007/R1598.*

Longmore, A. R., R. A. Cowdell and R. Flint, 1996: Nutrient status of the water in Port Phillip Bay, *Tech. rep.*, CSIRO Port Phillip Bay Environmental Study.

Mesinger, F., and A. Arakawa, 1976: Numerical methods used in atmospheric models, GARP Publ. Ser. No. 17 WMO-ICSU.

Murray, A. G., and J. P. Parslow, 1997: Port Phillip Bay integrated model: final report, *Tech. Rep. 44*, CSIRO Port Phillip Bay Environmental Study.

Pattiaratchi, C. B., T. Svenson and J. Imberger, 1989: Field study program off Werribee, Port Phillip Bay, *Tech. Rep. WP-288-CP*, University of Western Australia, CWR.

Prytz, A., and M. L. Heron, 1994: HF ocean surface radar surface currents: Final report, *Tech. rep.*, Port Phillip Bay Environmental Study.

Walker, S. J., and C. B. Fandry, 1993: Modelling effluent dispersion in Australian coastal waters – Devonport 1991–1992, hydrodynamic modelling, *Tech. Rep. OMR-59/40*, CSIRO Division of Oceanography.

Walker, S. J., and C. R. Sherwood, 1997: A transport model of Port Phillip Bay, *Tech. Rep. 39*, CSIRO Port Phillip Bay Environmental Study.

A Harmonic analyses of currents

This Appendix contains results of harmonic analyses of both measured and modelled currents from the May 1994 and September 1994 current meter deployment periods. Results are missing for observed currents in some of the tables, due to current meter failures or gaps in observed data.

Harmonic analysis for Martha Point, May 1994

Component		O1	K1	M2	S2
East	observed	0.007	0.015	0.056	0.019
	model	0.010	0.019	0.058	0.020
North	observed	0.017	0.031	0.063	0.031
	model	0.008	0.026	0.072	0.022

Table 6: Amplitudes (m/s), upper meter

Component		O1	K1	M2	S2
East	observed	252.4	358.5	337.3	106.3
	model	23.8	27.3	339.0	106.9
North	observed	41.7	64.2	8.5	148.0
	model	12.7	40.7	341.7	120.4

Table 7: Phase (degrees), upper meter

Component		O1	K1	M2	S2
East	observed	0.009	0.011	0.042	0.009
	model	0.009	0.011	0.048	0.012
North	observed	0.021	0.034	0.060	0.005
	model	0.011	0.013	0.062	0.018

Table 8: Amplitude (m/s), lower meter

Component		O1	K1	M2	S2
East	observed	314.4	53.5	330.8	90.1
	model	352.3	62.3	336.4	124.7
North	observed	60.5	110.3	7.4	163.4
	model	53.2	14.3	331.8	101.1

Table 9: Phase (degrees), lower meter

Harmonic analysis for Great Sands, May 1994

Component		O1	K1	M2	S2
East	observed				
	model	0.003	0.013	0.024	0.010
North	observed				
	model	0.009	0.031	0.085	0.026

Table 10: Amplitude (m/s), upper meter

Component		O1	K1	M2	S2
East	observed				
	model	53.1	349.0	321.7	62.5
North	observed				
	model	355.0	48.7	343.2	121.0

Table 11: Phase (degrees), upper meter

Component		O1	K1	M2	S2
East	observed	0.003	0.005	0.029	0.007
	model	0.007	0.006	0.015	0.003
North	observed	0.011	0.014	0.063	0.017
	model	0.016	0.014	0.079	0.022

Table 12: Amplitude (m/s), lower meter

Component		O1	K1	M2	S2
East	observed	298.8	333.5	205.0	344.0
	model	306.3	108.0	312.2	140.9
North	observed	318.2	346.5	223.9	357.8
	model	47.3	38.3	334.2	106.1

Table 13: Phase (degrees), lower meter

Harmonic analysis for Central Bay, May 1994

Component		O1	K1	M2	S2
East	observed	0.002	0.002	0.002	0.003
	model	0.005	0.006	0.001	0.002
North	observed	0.004	0.014	0.049	0.015
	model	0.005	0.022	0.063	0.017

Table 14: Amplitudes (m/s), upper meter

Component		O1	K1	M2	S2
East	observed	252.2	336.4	310.2	129.1
	model	119.1	338.6	286.9	338.5
North	observed	33.8	41.3	338.0	115.3
	model	1.0	50.7	343.1	117.2

Table 15: Phase (degrees), upper meter

Component		O1	K1	M2	S2
East	observed	0.003	0.003	0.001	0.004
	model	0.004	0.008	0.004	0.003
North	observed	0.008	0.014	0.051	0.014
	model	0.011	0.007	0.052	0.015

Table 16: Amplitude (m/s), lower meter

Component		O1	K1	M2	S2
East	observed	325.3	111.2	75.0	225.7
	model	301.7	142.9	114.2	248.7
North	observed	57.4	41.3	333.8	105.9
	model	48.0	25.8	329.7	99.7

Table 17: Phase (degrees), lower meter

Harmonic analysis for Point Cook, May 1994

Component		O1	K1	M2	S2
East	observed	0.006	0.003	0.008	0.004
	model	0.003	0.003	0.012	0.004
North	observed	0.006	0.006	0.015	0.007
	model	0.005	0.007	0.017	0.006

Table 18: Amplitudes (m/s), upper meter

Component		O1	K1	M2	S2
East	observed	322.9	25.6	147.7	318.1
	model	320.8	291.9	158.8	317.2
North	observed	357.1	32.2	334.2	103.0
	model	10.6	54.2	346.8	110.4

Table 19: Phase (degrees), upper meter

Component		O1	K1	M2	S2
East	observed	0.007	0.001	0.010	0.004
	model	0.001	0.003	0.011	0.002
North	observed	0.005	0.007	0.012	0.004
	model	0.005	0.004	0.016	0.005

Table 20: Amplitude (m/s), lower meter

Component		O1	K1	M2	S2
East	observed	228.4	64.5	149.2	297.9
	model	325.1	194.4	154.9	273.6
North	observed	18.0	36.2	334.7	97.4
	model	43.9	35.6	343.4	110.5

Table 21: Phase (degrees), lower meter

Harmonic analysis for Red Bluff, May 1994

Component		O1	K1	M2	S2
East	observed	0.007	0.004	0.008	0.002
	model	0.002	0.001	0.007	0.002
North	observed	0.008	0.008	0.020	0.011
	model	0.006	0.004	0.031	0.007

Table 22: Amplitudes (m/s), upper meter

Component		O1	K1	M2	S2
East	observed	95.2	38.5	142.9	97.5
	model	126.3	33.5	139.2	288.2
North	observed	346.8	63.1	323.5	101.1
	model	309.6	56.6	323.8	110.3

Table 23: Phase (degrees), upper meter

Component		O1	K1	M2	S2
East	observed	0.006	0.004	0.014	0.005
	model	0.002	0.002	0.011	0.002
North	observed	0.006	0.006	0.024	0.004
	model	0.002	0.001	0.018	0.003

Table 24: Amplitude (m/s), lower meter

Component		O1	K1	M2	S2
East	observed	108.0	153.0	128.1	273.3
	model	110.0	154.4	127.1	249.6
North	observed	227.6	263.3	314.0	103.5
	model	321.3	281.2	313.4	89.6

Table 25: Phase (degrees), lower meter

Harmonic analysis for Martha Point, September 1994

Component		O1	K1	M2	S2
East	observed	0.007	0.014	0.043	0.014
	model	0.013	0.022	0.057	0.018
North	observed	0.020	0.022	0.068	0.020
	model	0.017	0.016	0.073	0.020

Table 26: Amplitudes (m/s), upper meter

Component		O1	K1	M2	S2
East	observed	320.6	54.9	333.3	86.6
	model	337.1	52.1	332.2	101.7
North	observed	23.4	114.3	358.1	148.7
	model	355.9	80.0	337.6	114.9

Table 27: Phase (degrees), upper meter

Component		O1	K1	M2	S2
East	observed	0.014	0.013	0.037	0.010
	model	0.010	0.006	0.049	0.012
North	observed	0.018	0.034	0.057	0.017
	model	0.007	0.035	0.062	0.018

Table 28: Amplitude (m/s), lower meter

Component		O1	K1	M2	S2
East	observed	346.9	345.9	321.9	94.0
	model	19.5	351.6	336.8	104.8
North	observed	62.5	49.5	338.0	109.0
	model	309.4	17.4	326.8	93.5

Table 29: Phase (degrees), lower meter

Harmonic analysis for Schnapper Point, September 1994

Component		O1	K1	M2	S2
East	observed	0.010	0.019	0.029	0.009
	model	0.005	0.016	0.026	0.009
North	observed	0.016	0.009	0.045	0.011
	model	0.011	0.010	0.057	0.017

Table 30: Amplitudes (m/s), upper meter

Component		O1	K1	M2	S2
East	observed	310.0	62.1	322.5	124.5
	model	325.6	69.7	327.3	87.8
North	observed	26.4	119.6	329.2	127.9
	model	353.6	78.3	333.7	106.7

Table 31: Phase (degrees), upper meter

Component		O1	K1	M2	S2
East	observed	0.005	0.008	0.025	0.003
	model	0.006	0.010	0.023	0.006
North	observed	0.001	0.024	0.050	0.016
	model	0.006	0.019	0.052	0.014

Table 32: Amplitude (m/s), lower meter

Component		O1	K1	M2	S2
East	observed	41.3	245.9	345.3	121.0
	model	28.9	291.3	333.9	116.3
North	observed	64.5	4.0	355.8	108.6
	model	348.4	16.5	328.0	96.4

Table 33: Phase (degrees), lower meter

Harmonic analysis for Central Bay, September 1994

Component		O1	K1	M2	S2
East	observed	0.011	0.020	0.004	0.005
	model	0.004	0.015	0.003	0.001
North	observed	0.017	0.022	0.049	0.012
	model	0.013	0.020	0.064	0.017

Table 34: Amplitude (m/s), upper meter

Component		O1	K1	M2	S2
East	observed	324.4	48.1	298.6	91.8
	model	301.7	47.7	293.1	92.7
North	observed	6.9	108.9	332.9	117.8
	model	1.3	92.6	340.9	108.8

Table 35: Phase (degrees), upper meter

Component		O1	K1	M2	S2
East	observed				
	model	0.006	0.014	0.007	0.003
North	observed				
	model	0.003	0.025	0.052	0.013

Table 36: Amplitude (m/s), lower meter

Component		O1	K1	M2	S2
East	observed				
	model	121.5	220.0	95.8	252.5
North	observed				
	model	350.7	16.6	325.7	95.4

Table 37: Phase (degrees), lower meter

Harmonic analysis for Point Cook, September 1994

Component		O1	K1	M2	S2
East	observed	0.004	0.018	0.008	0.001
	model	0.002	0.010	0.013	0.004
North	observed	0.005	0.009	0.014	0.005
	model	0.007	0.005	0.018	0.005

Table 38: Amplitudes (m/s), upper meter

Component		O1	K1	M2	S2
East	observed	90.1	206.0	167.7	348.0
	model	320.4	228.4	174.5	315.3
North	observed	32.9	171.6	331.8	96.1
	model	18.6	193.5	334.3	90.7

Table 39: Phase (degrees), upper meter

Component		O1	K1	M2	S2
East	observed				
	model	0.001	0.018	0.010	0.003
North	observed				
	model	0.003	0.007	0.017	0.003

Table 40: Amplitude (m/s), lower meter

Component		O1	K1	M2	S2
East	observed				
	model	184.3	223.6	164.3	295.5
North	observed				
	model	332.8	14.0	332.5	108.1

Table 41: Phase (degrees), lower meter

Harmonic analysis for Red Bluff, September 1994

Component		O1	K1	M2	S2
East	observed	0.005	0.012	0.007	0.005
	model	0.003	0.009	0.006	0.003
North	observed	0.004	0.009	0.023	0.006
	model	0.005	0.014	0.032	0.009

Table 42: Amplitudes (m/s), upper meter

Component		O1	K1	M2	S2
East	observed	305.5	161.7	159.2	261.6
	model	335.4	87.8	160.2	299.8
North	observed	5.2	357.7	325.1	120.3
	model	30.0	265.7	328.7	101.4

Table 43: Phase (degrees), upper meter

Component		O1	K1	M2	S2
East	observed				
	model	0.004	0.007	0.011	0.002
North	observed				
	model	0.003	0.014	0.016	0.004

Table 44: Amplitude (m/s), lower meter

Component		O1	K1	M2	S2
East	observed				
	model	157.7	165.7	117.7	245.0
North	observed				
	model	350.9	325.5	312.8	87.3

Table 45: Phase (degrees), lower meter

List of Figures

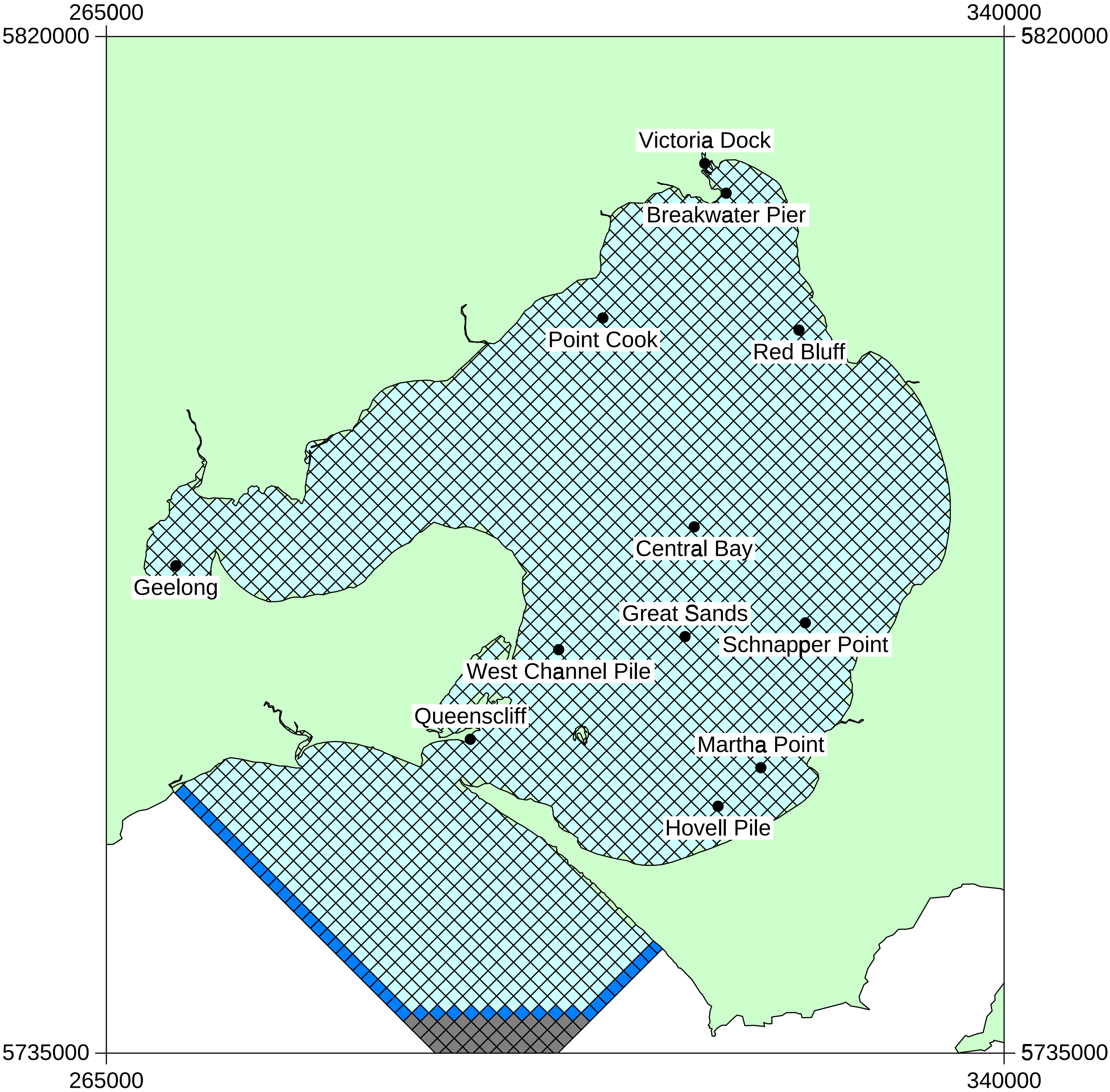

Figure 1: Location diagram for the Port Phillip Bay model grid and field measurement sites. Coordinates shown on the edge of this plot and other plots are in metres (Australian Map Grid, Zone 55)

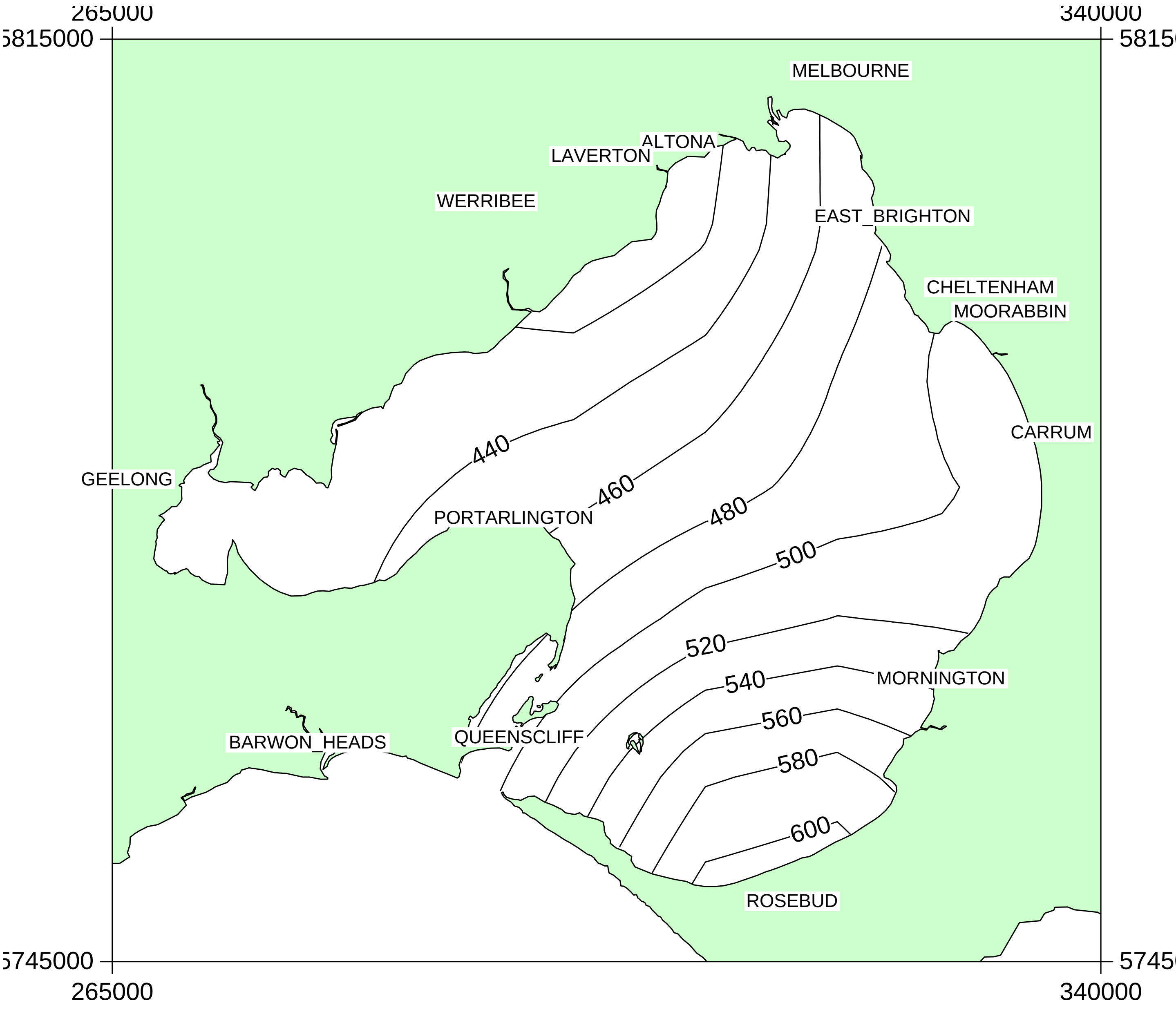

Figure 2: Contours of total annual rainfall (mm) for 1994, calculated from interpolated rainfall data, observed at the stations shown.

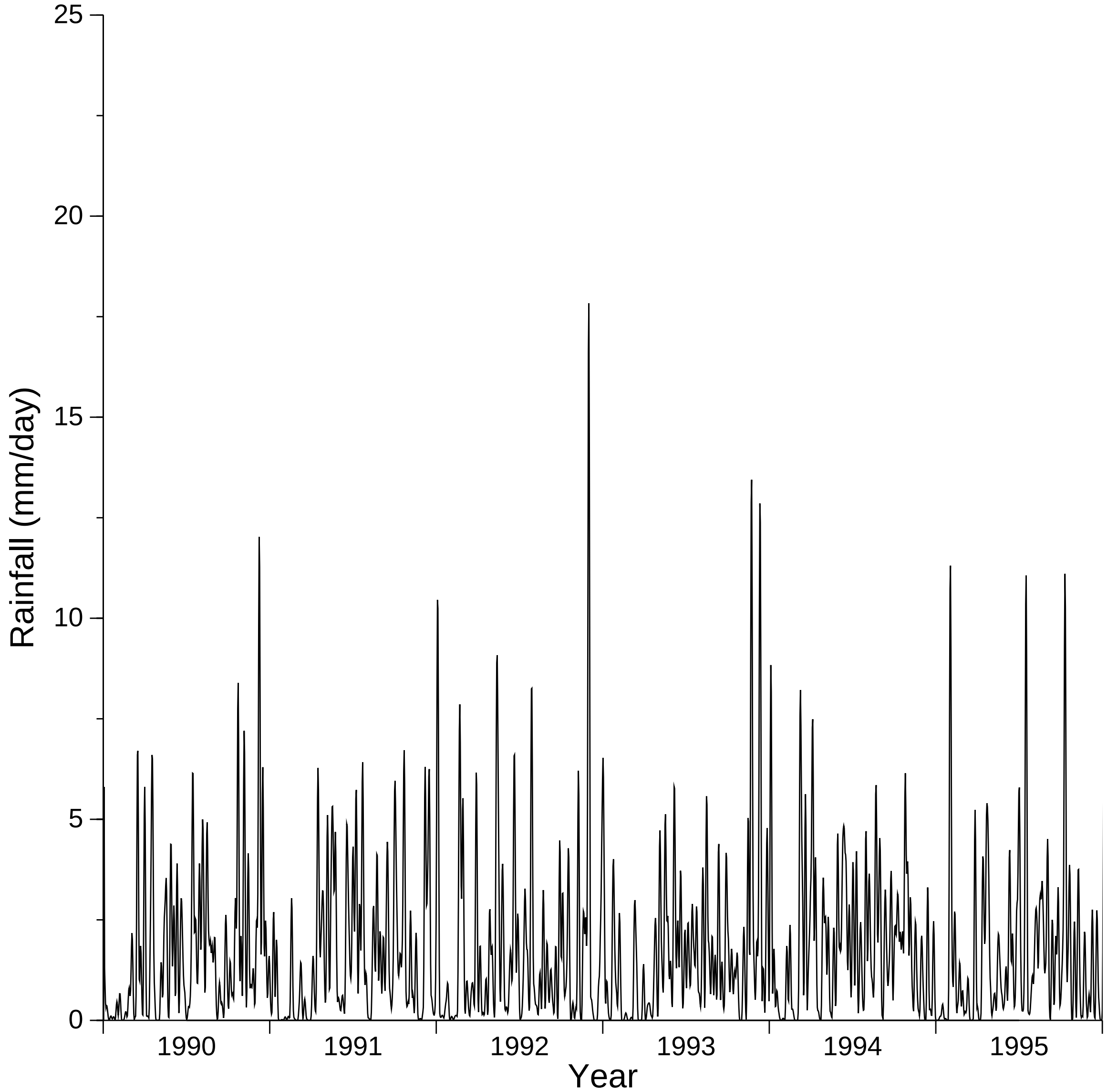

Figure 3: Bay-wide (spatial mean) rainfall (mm/day), 1990 - 1995

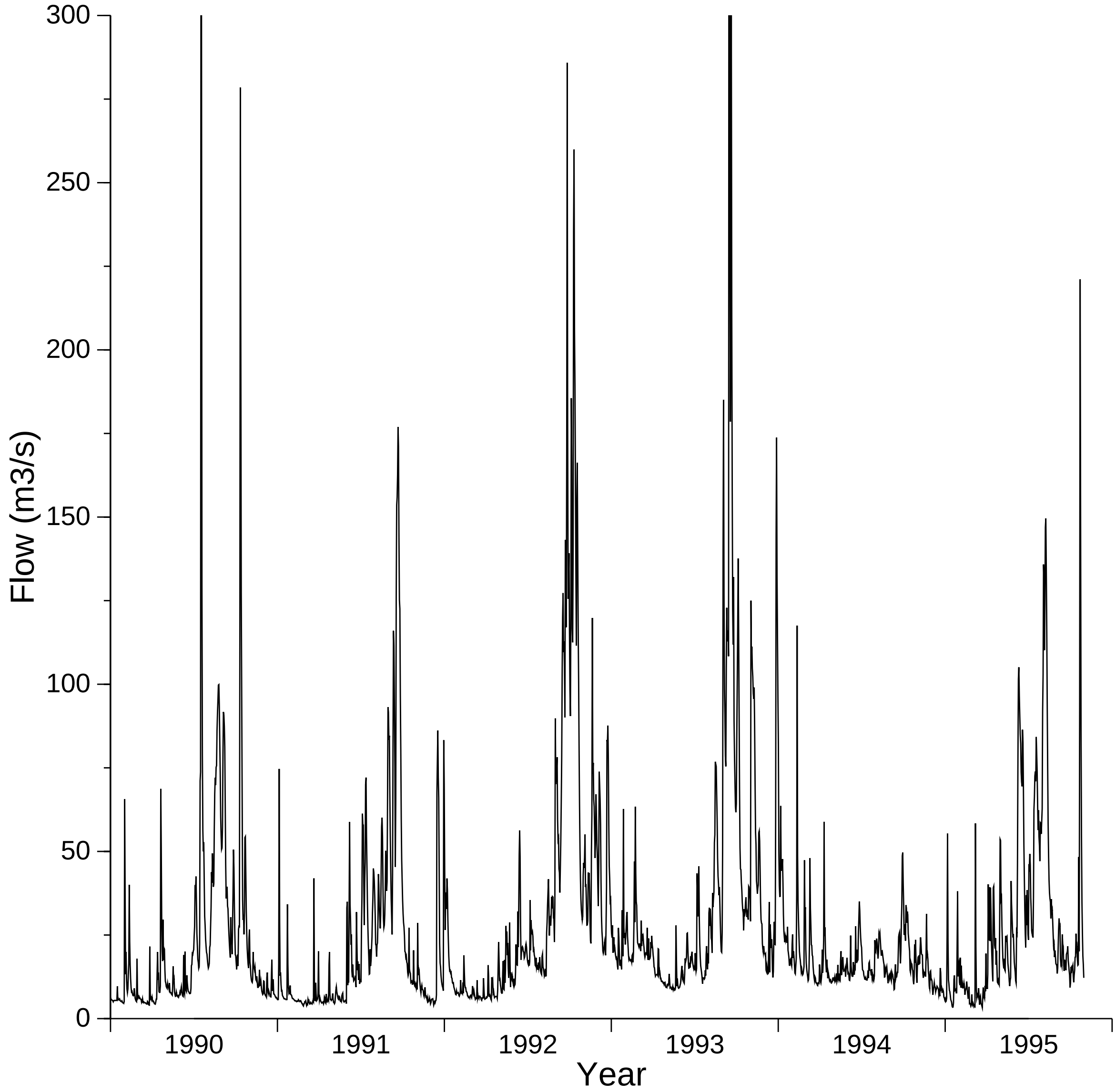

Figure 4: Total flow (m^3/s) at the mouth of the Yarra river, 1990 to 1995

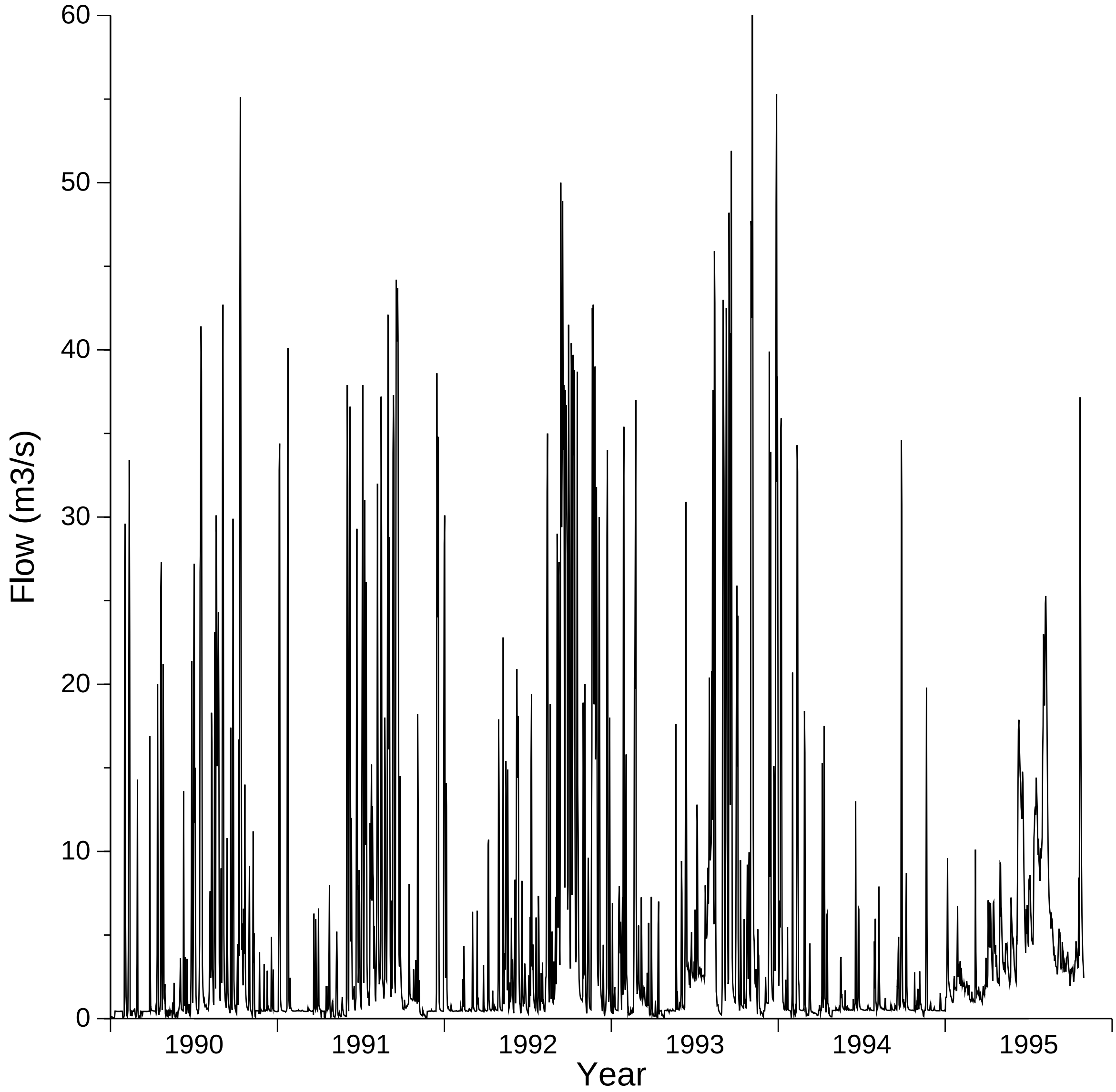

Figure 5: Patterson river flow (m^3/s), 1990 to 1995

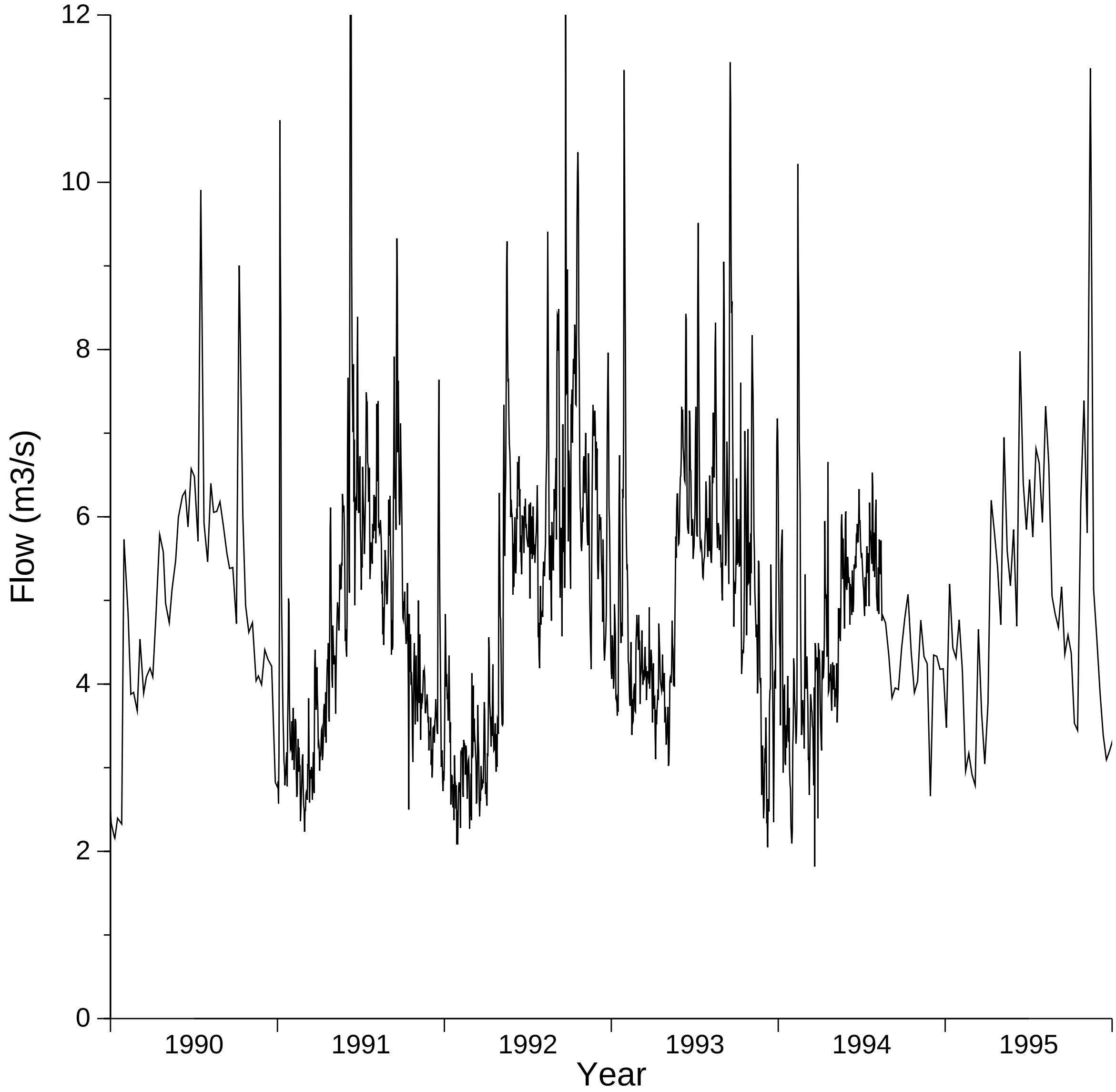

Figure 6: Western Treatment Plant outlets, total flow to the Bay (m^3/s), 1990 to 1995

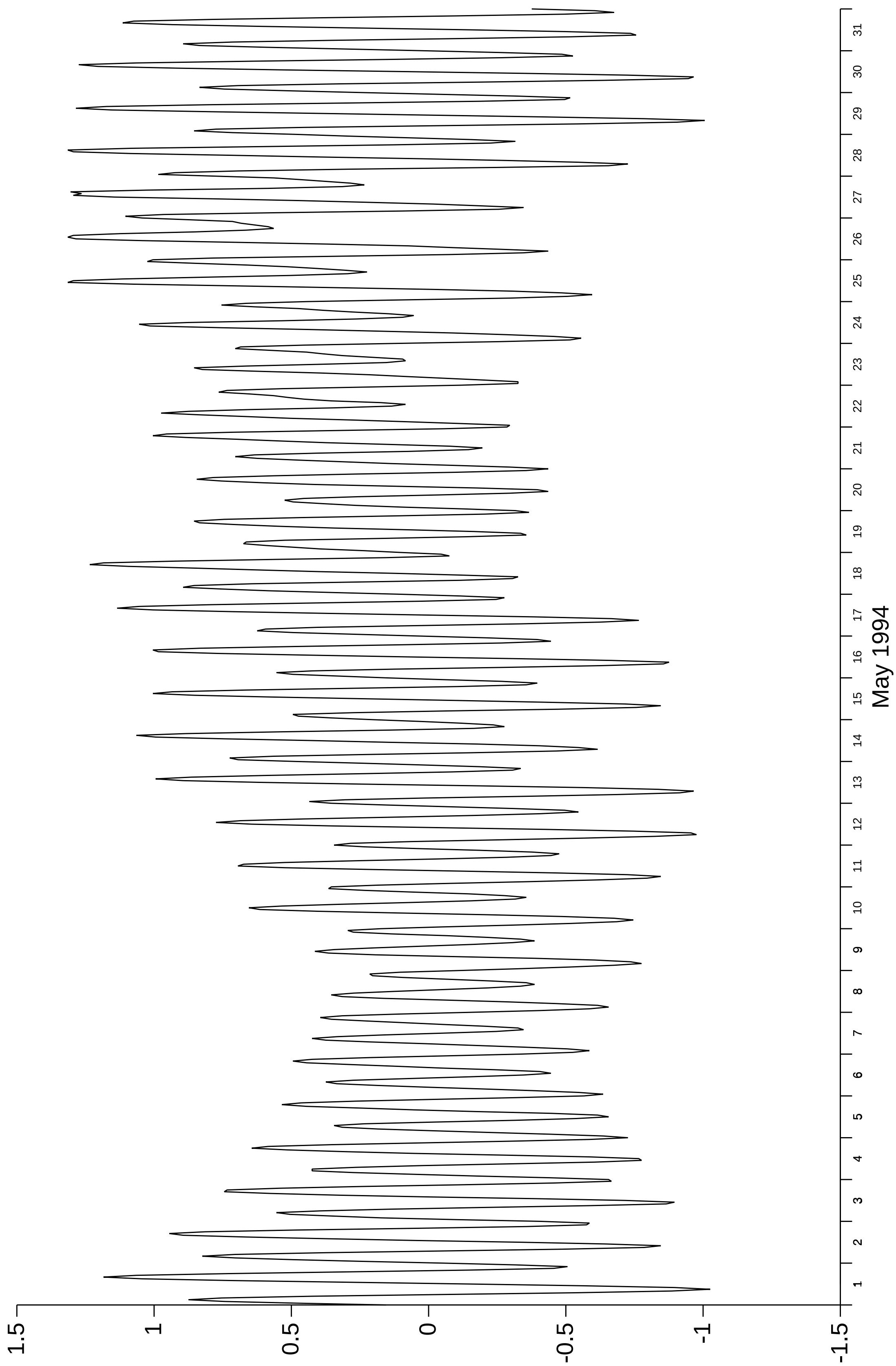

Figure 7: Sea-level data from Lorne, used to drive the model open boundary for May 1994.

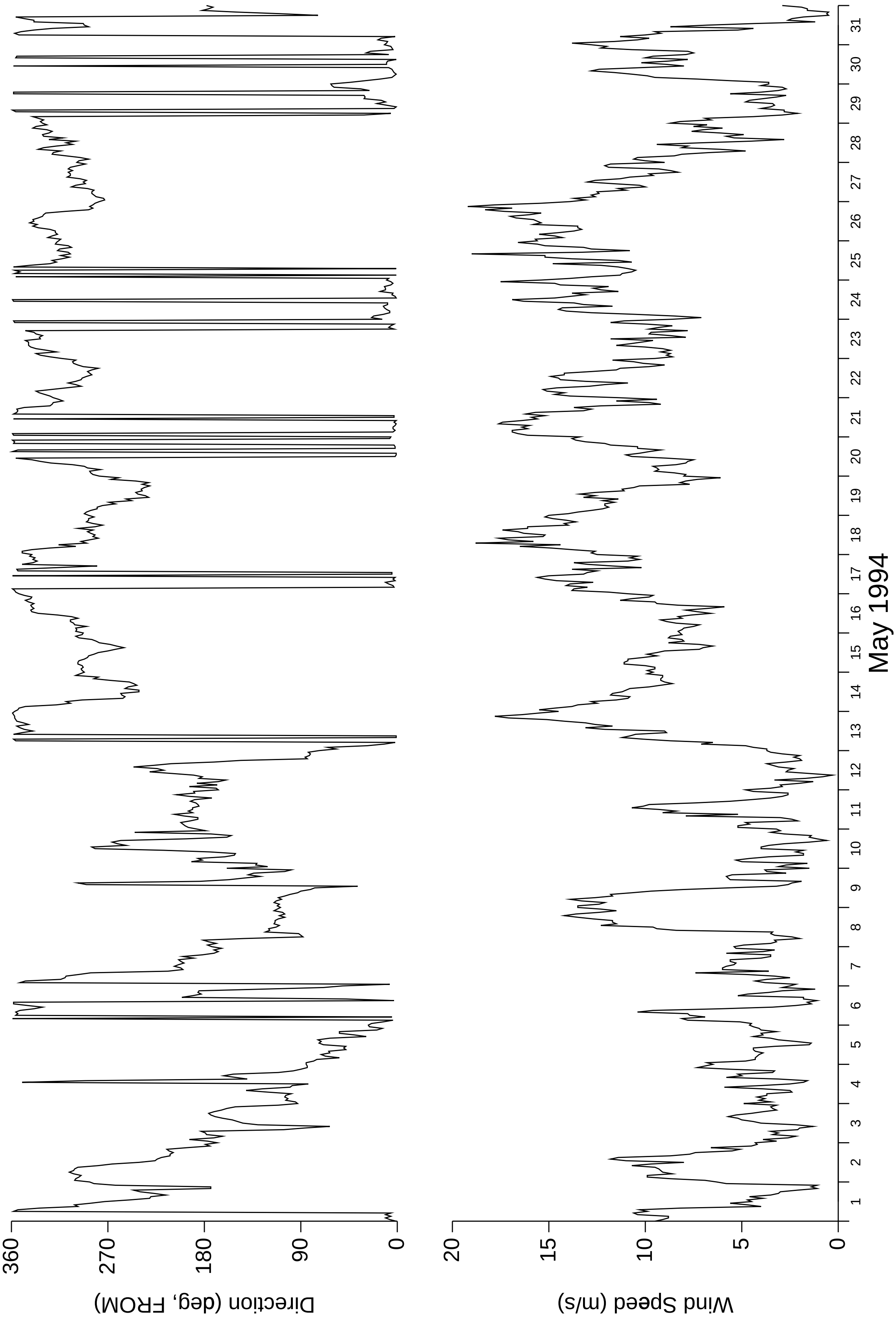

Figure 8: Measured winds at Hovell Pile, used (along with Point Wilson, Point Cook and Fawkner Beacon) to provide data to drive the model.

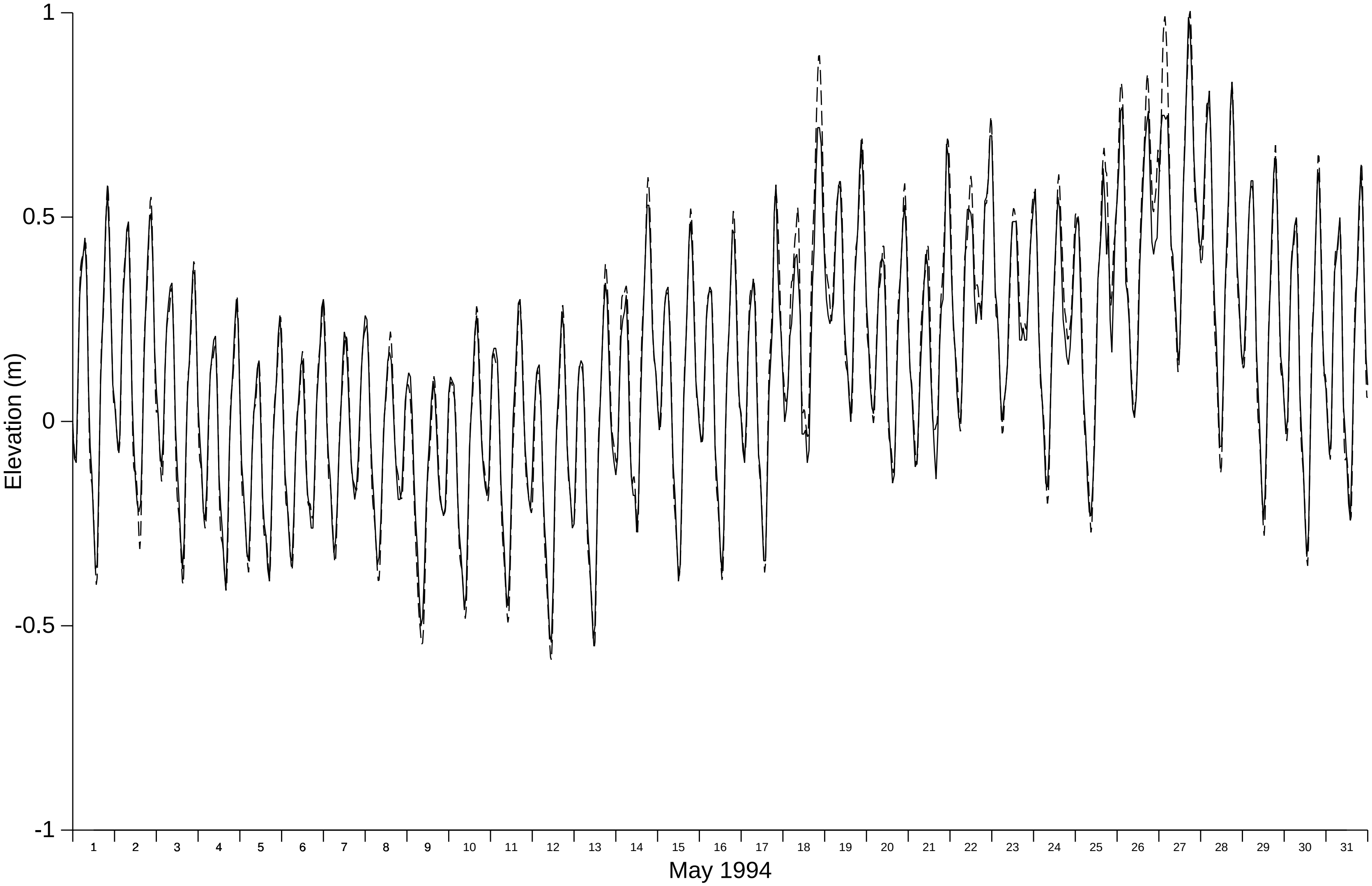

Figure 9: Measured (solid) and modelled (dashed) elevation at Geelong, May 1994

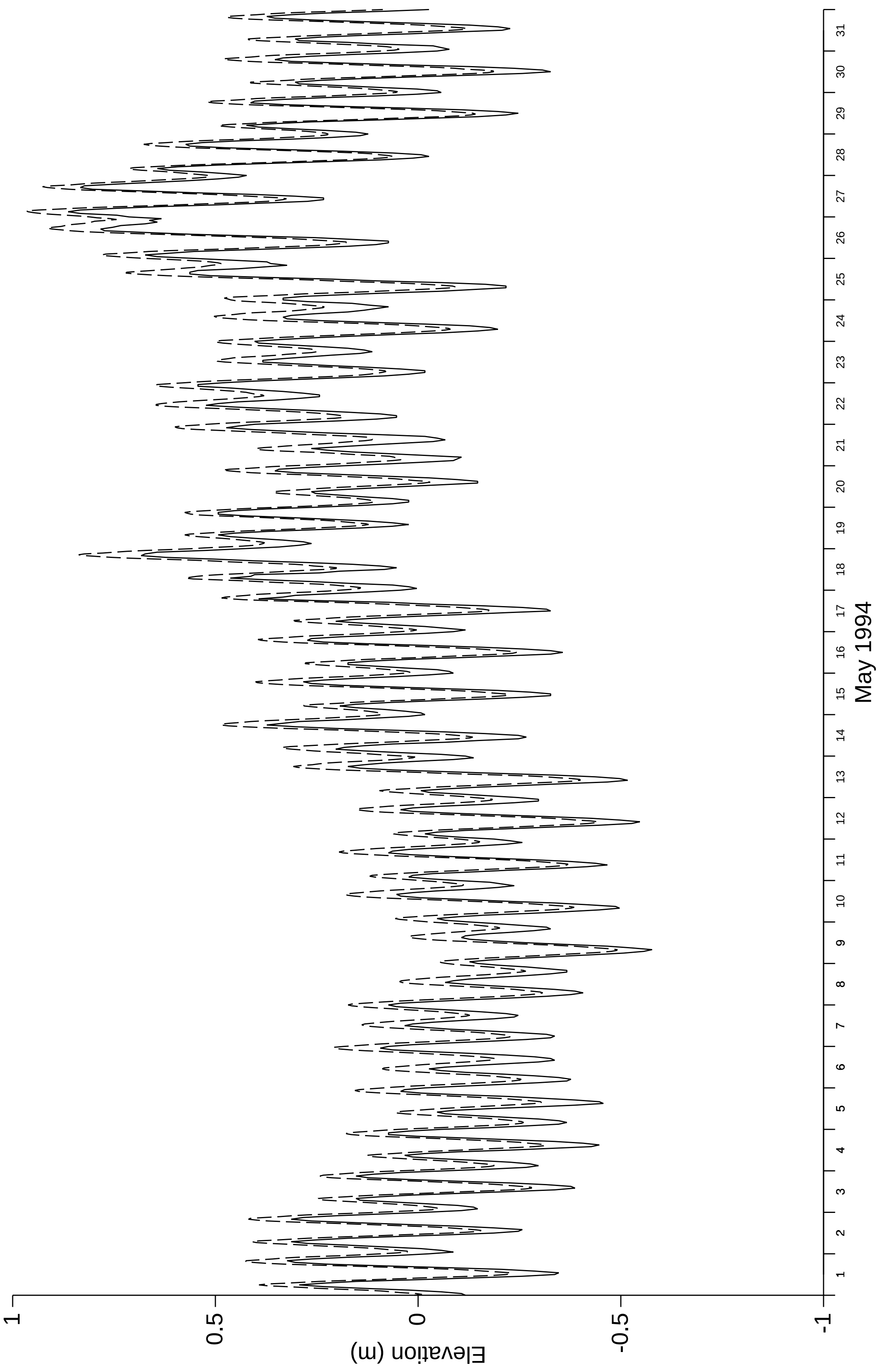

Figure 10: Measured (solid) and modelled (dashed) elevation at Hovell Pile, May 1994

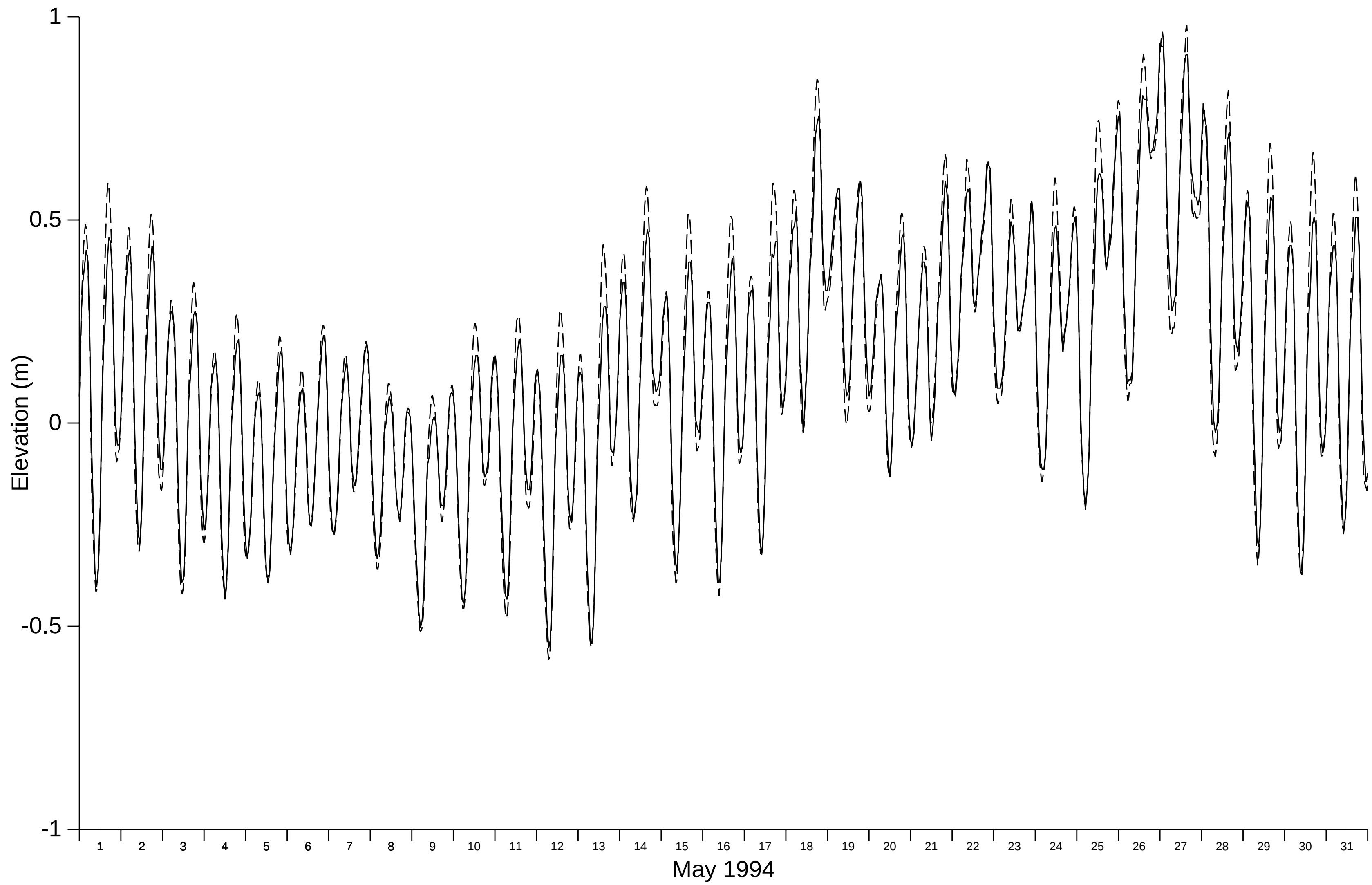

Figure 11: Measured (solid) and modelled (dashed) elevation at Queenscliff, May 1994

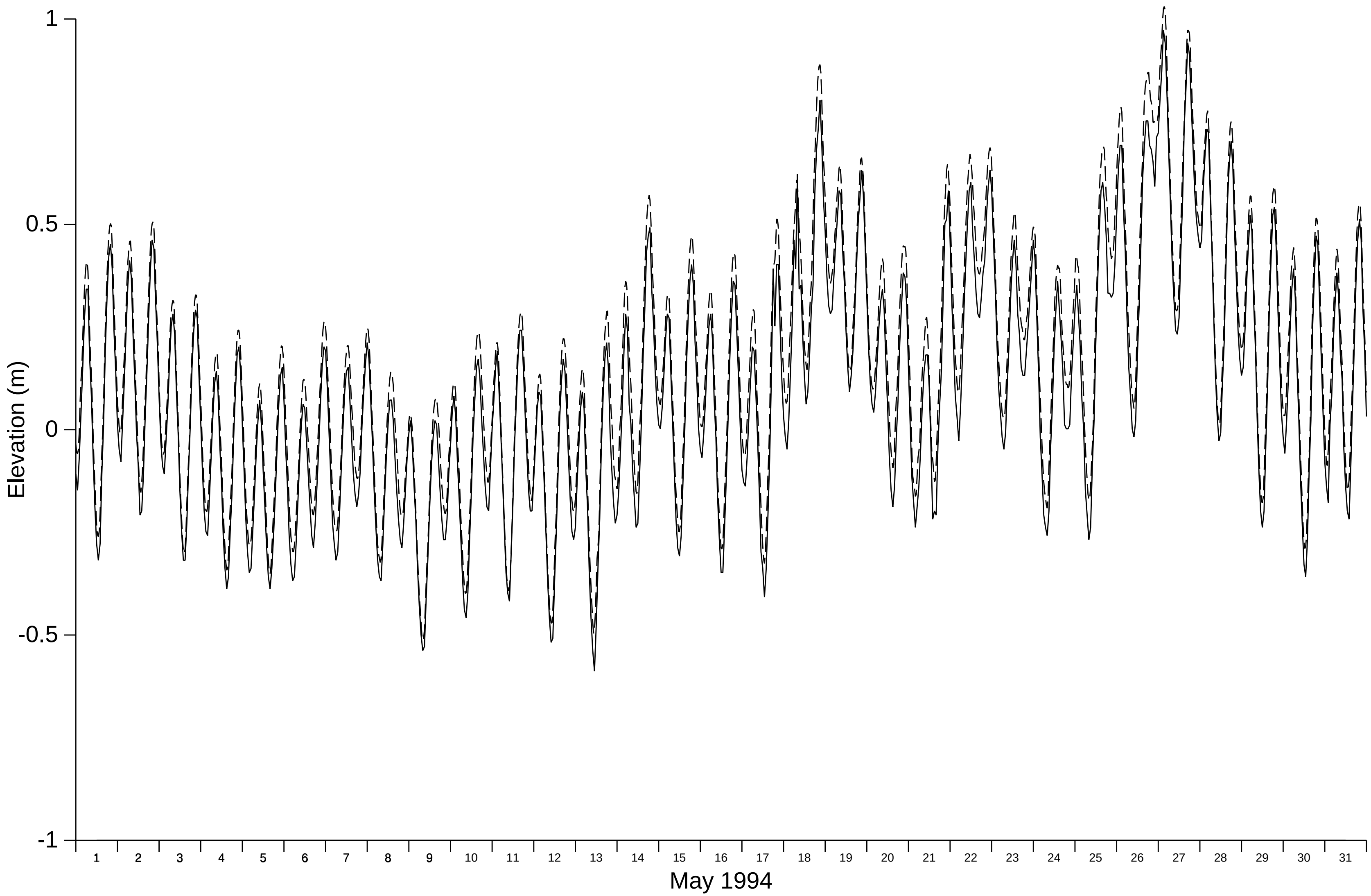

Figure 12: Measured (solid) and modelled (dashed) elevation at Victoria Dock, May 1994

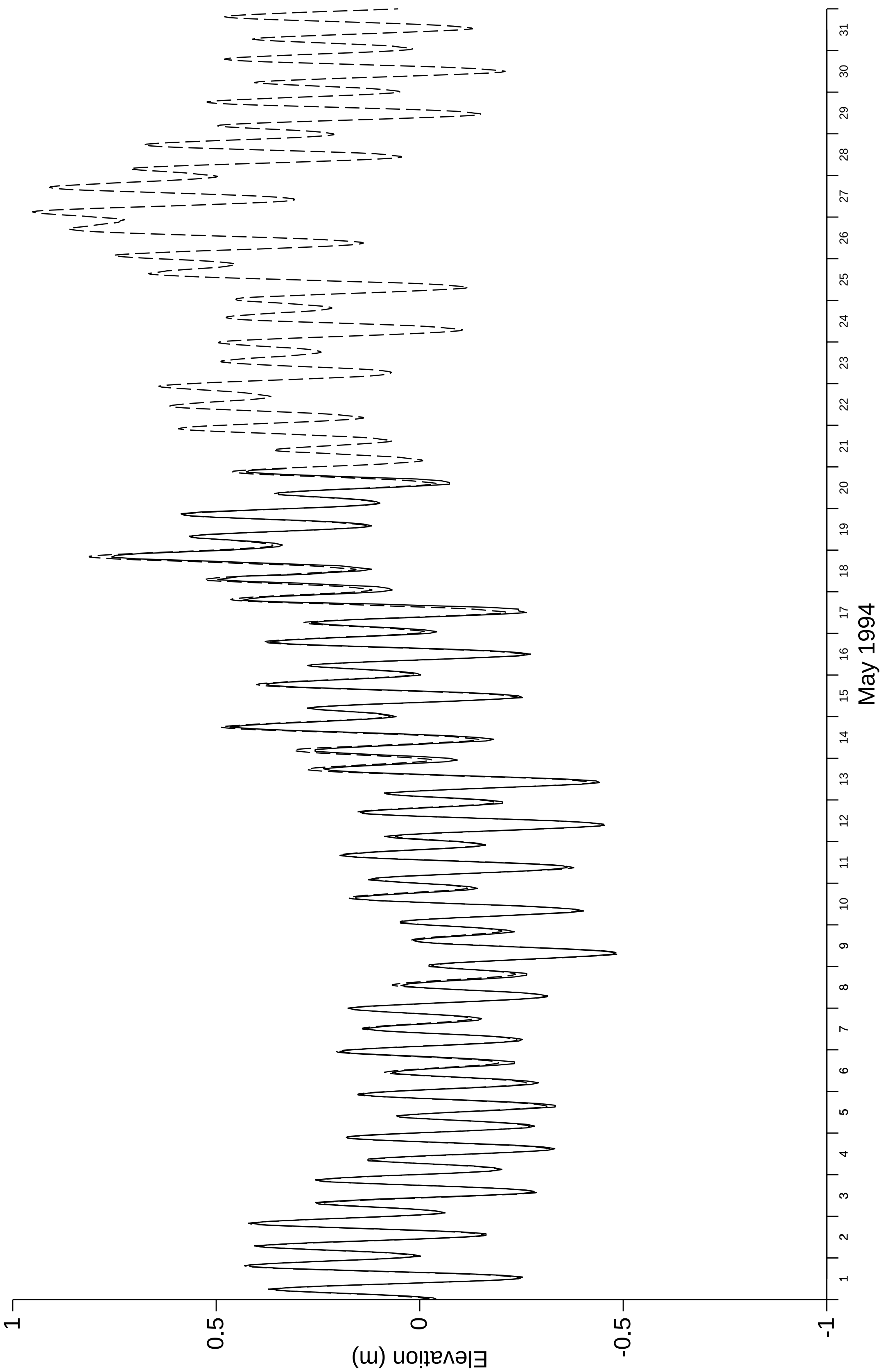

Figure 13: Measured (solid) and modelled (dashed) elevation at West Channel Pile, May 1994

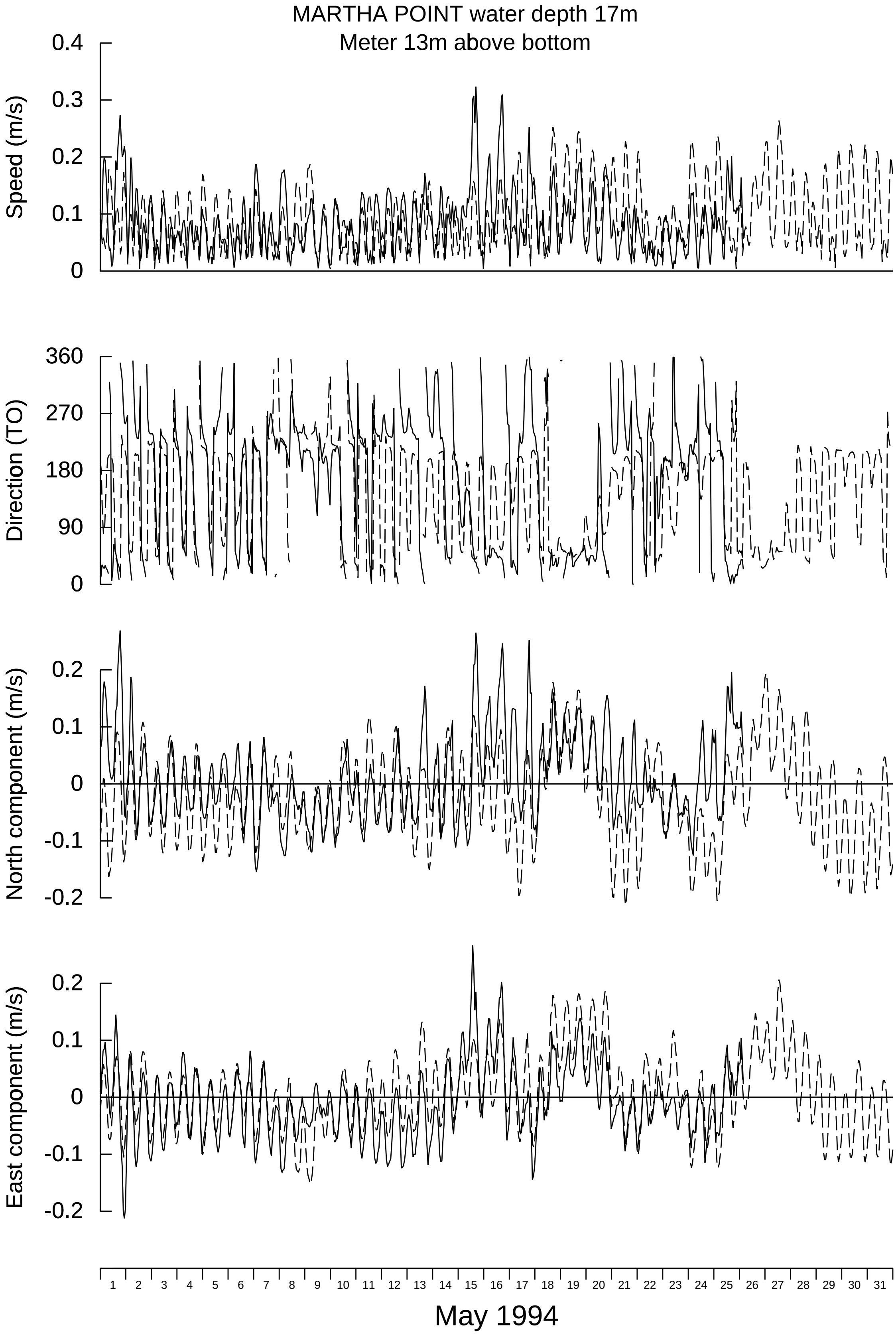

Figure 14: Measured (solid) and modelled (dashed) currents at the Martha Point site, upper meter, May 1994.

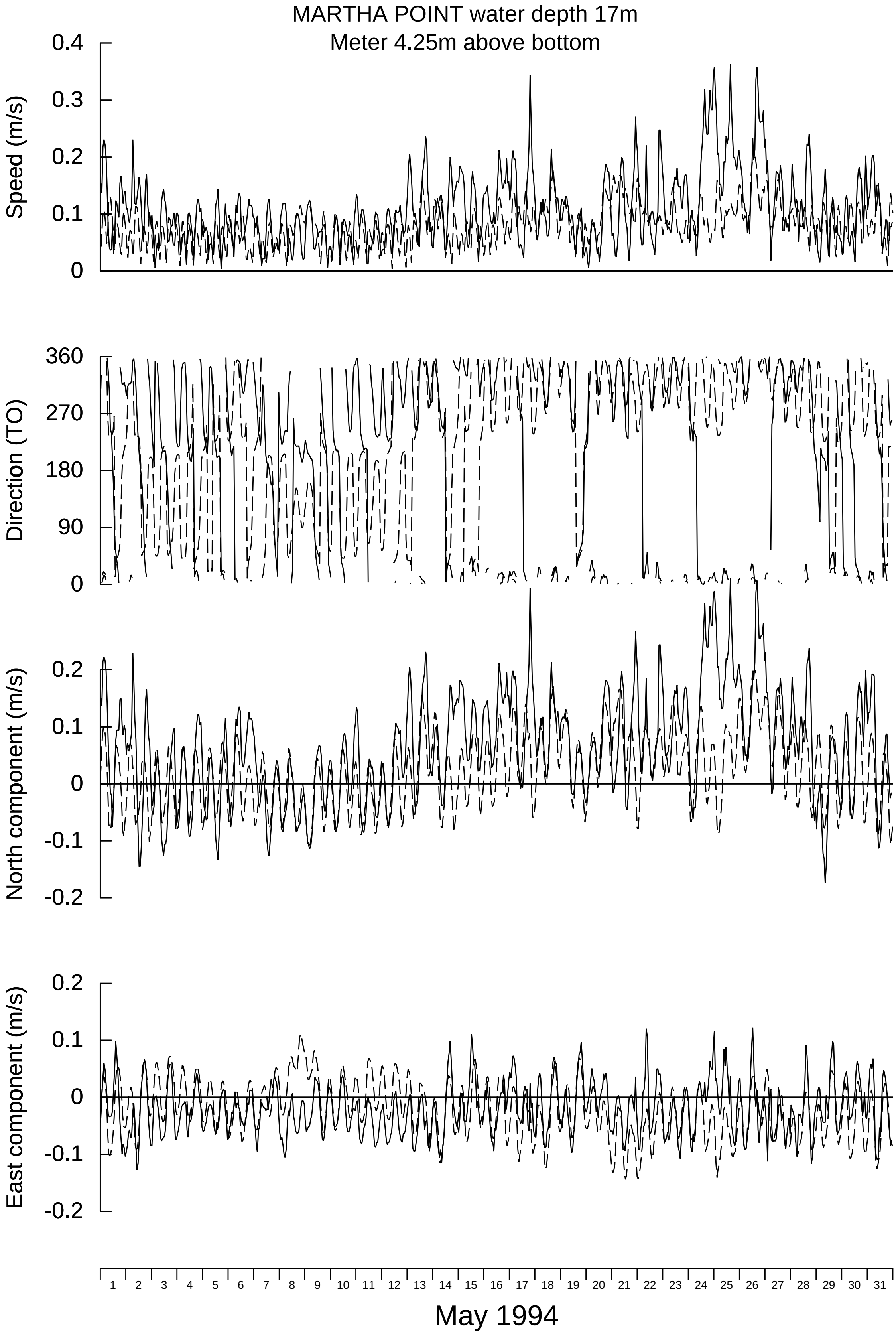

Figure 15: Measured (solid) and modelled (dashed) currents at the Martha Point site, lower meter, May 1994.

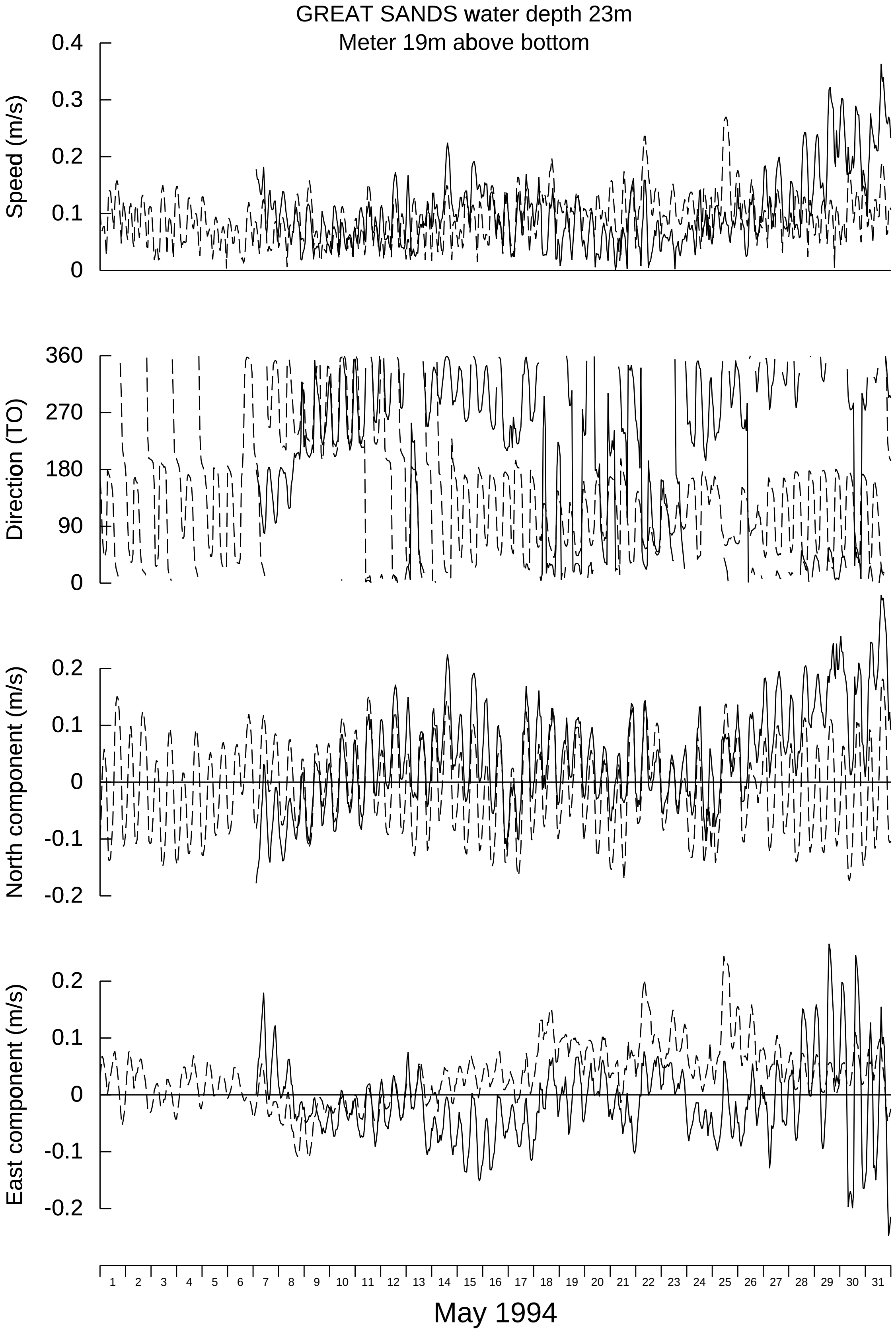

Figure 16: Measured (solid) and modelled (dashed) currents at the Great Sands site, upper meter, May 1994.

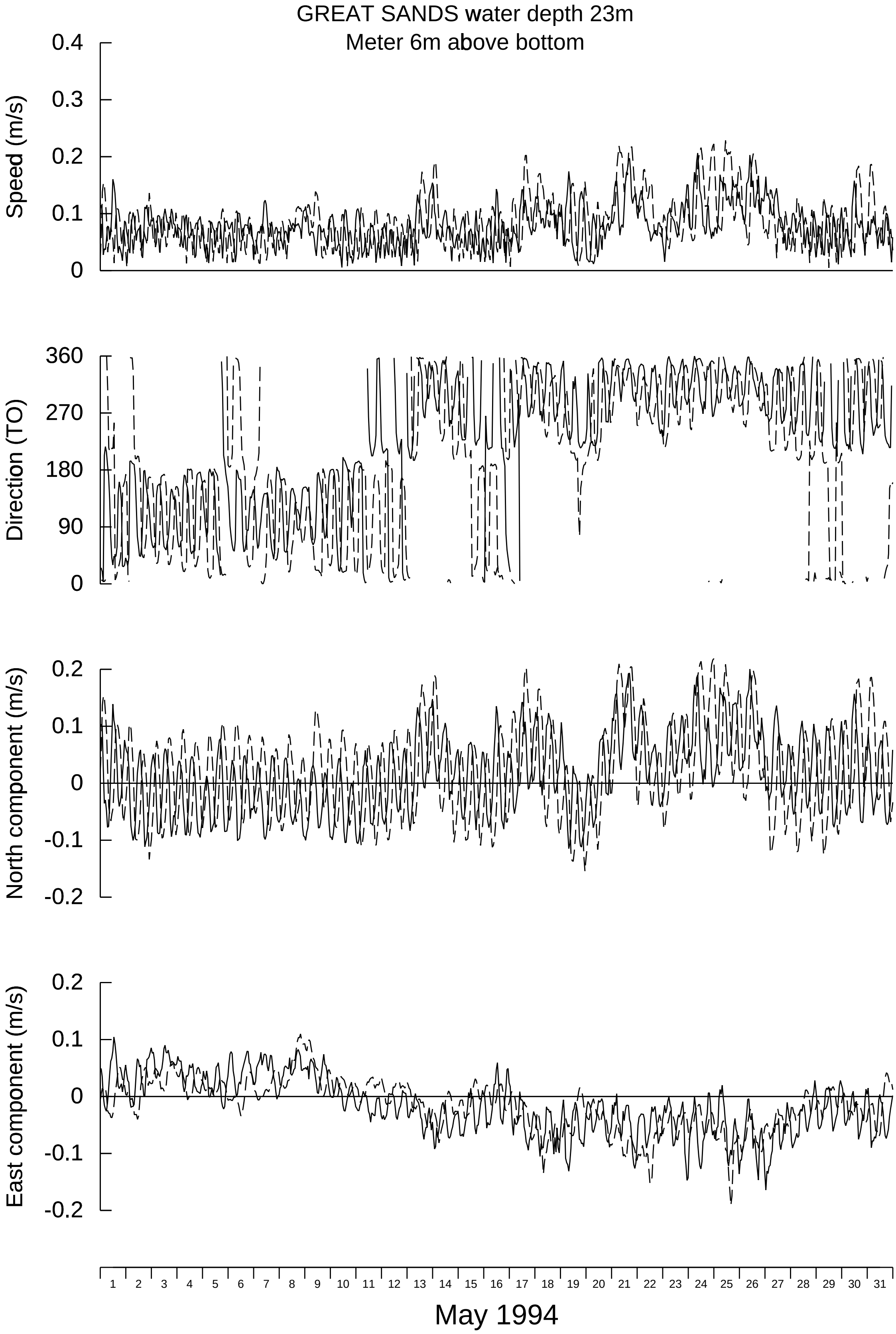

Figure 17: Measured (solid) and modelled (dashed) currents at the Great Sands site, lower meter, May 1994. Note that the measured data appears to have a significant timing error when compared to both the model and the upper meter at this site.

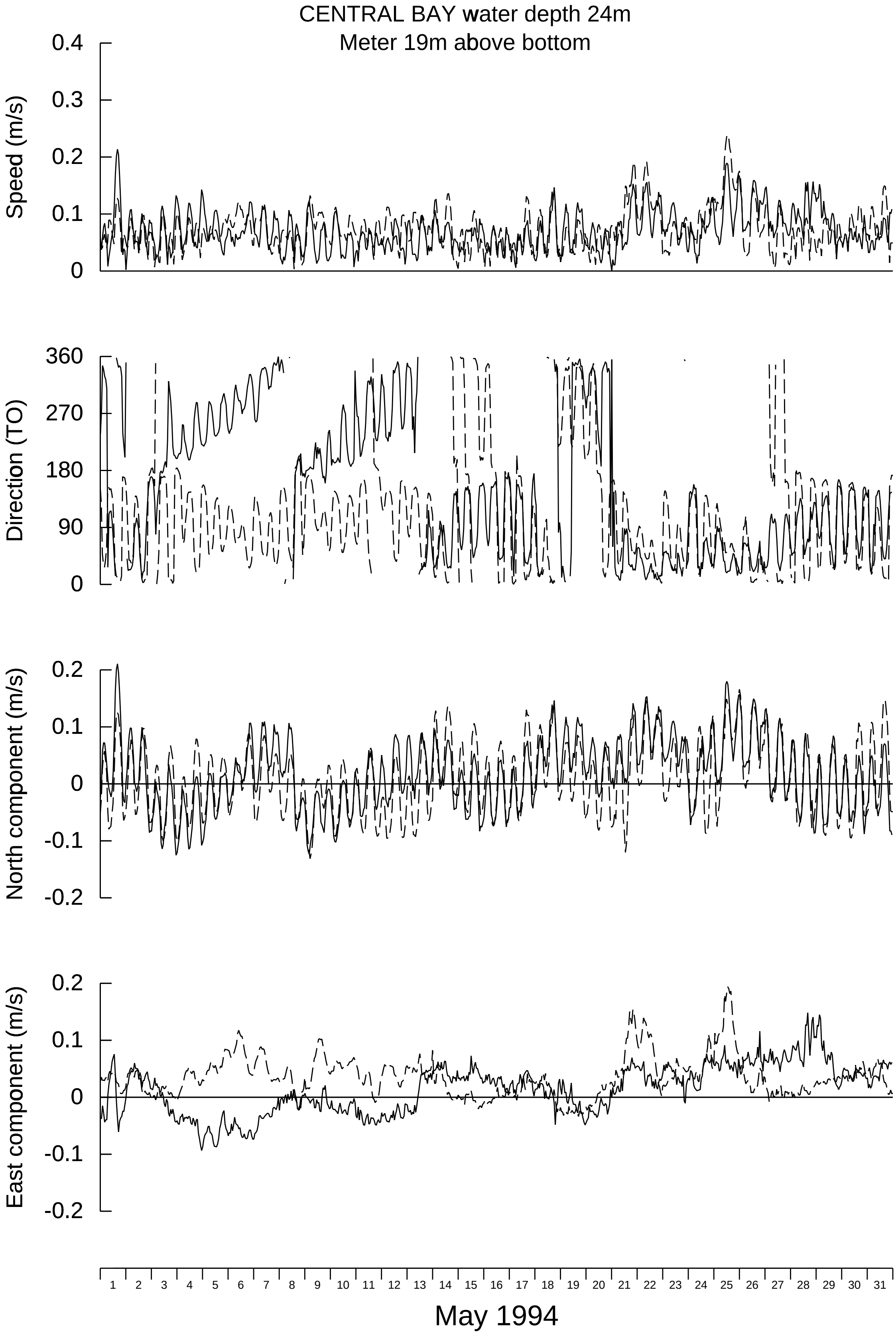

Figure 18: Measured (solid) and modelled (dashed) currents at the Central Bay site, upper meter, May 1994.

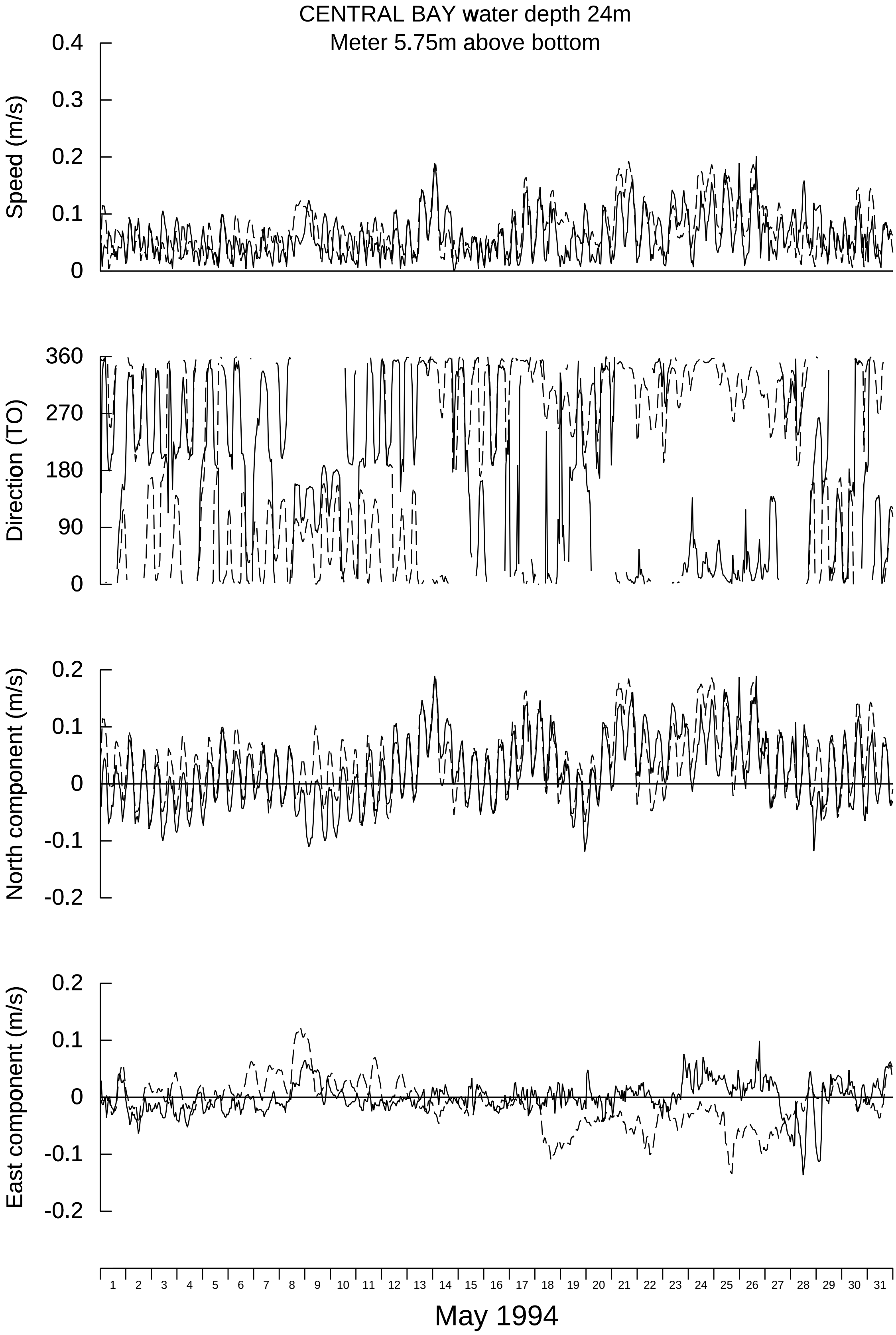

Figure 19: Measured (solid) and modelled (dashed) currents at the Central Bay site, lower meter, May 1994.

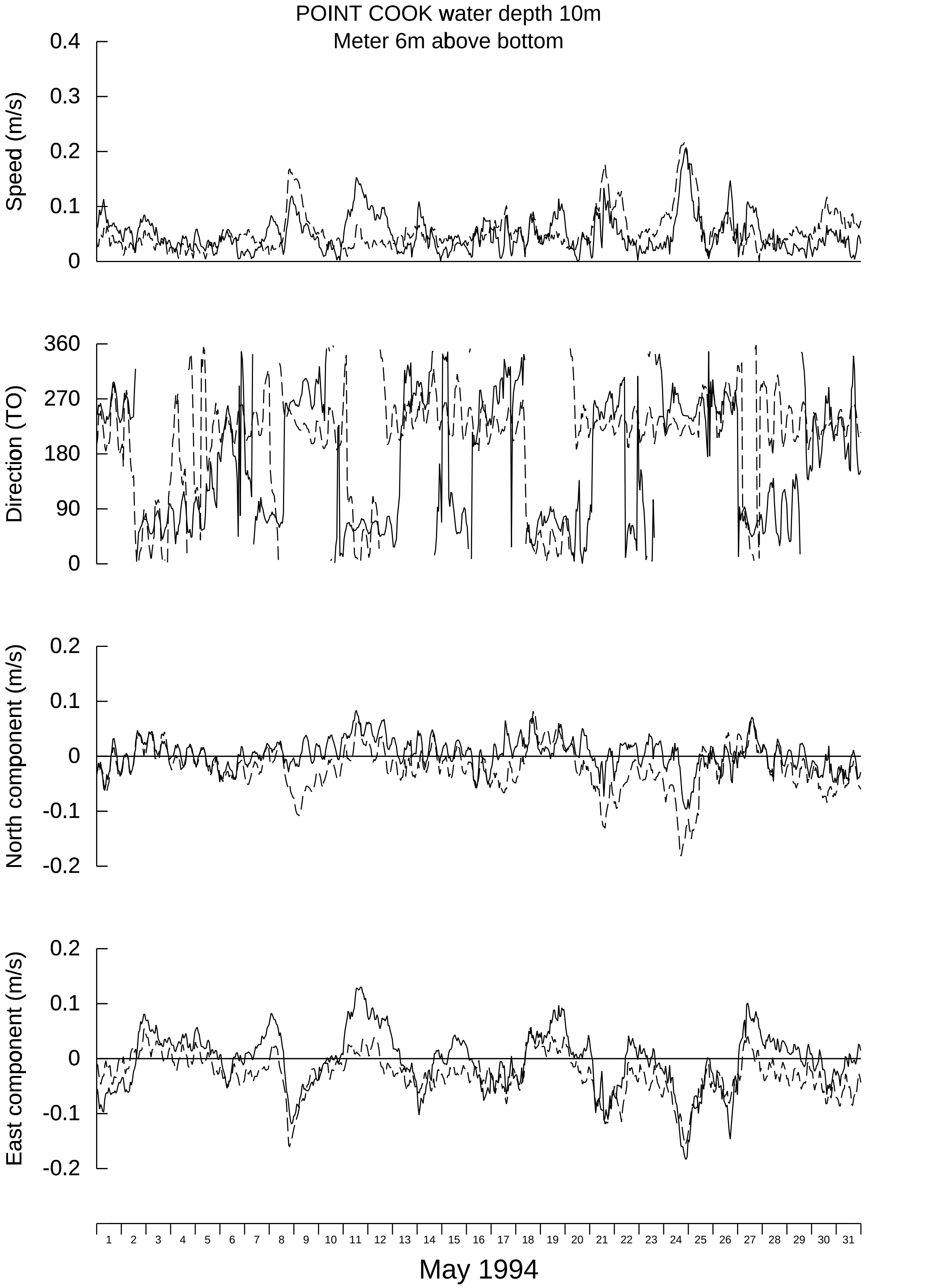

Figure 20: Measured (solid) and modelled (dashed) currents at the Point Cook site, upper meter, May 1994.

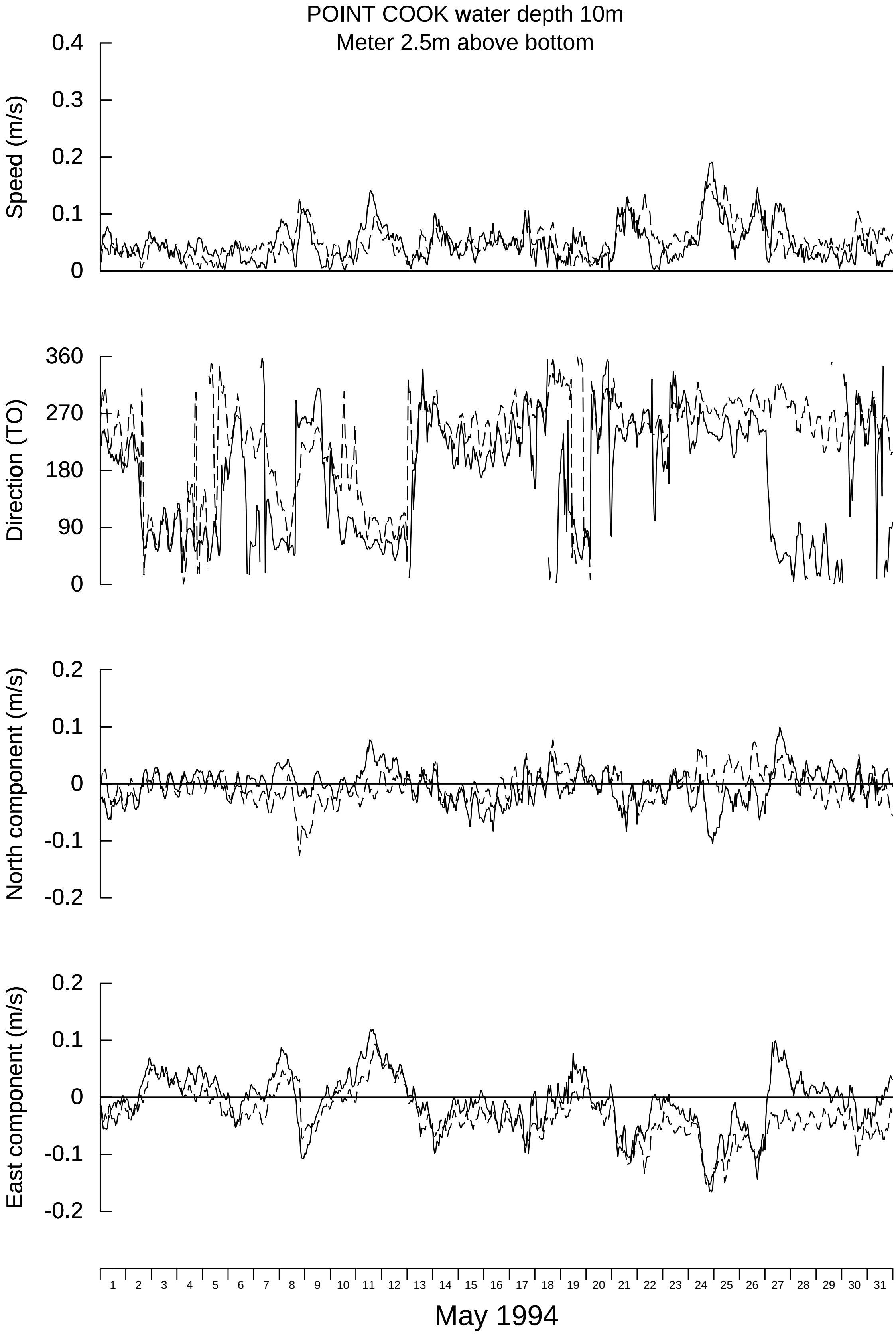

Figure 21: Measured (solid) and modelled (dashed) currents at the Point Cook site, lower meter, May 1994.

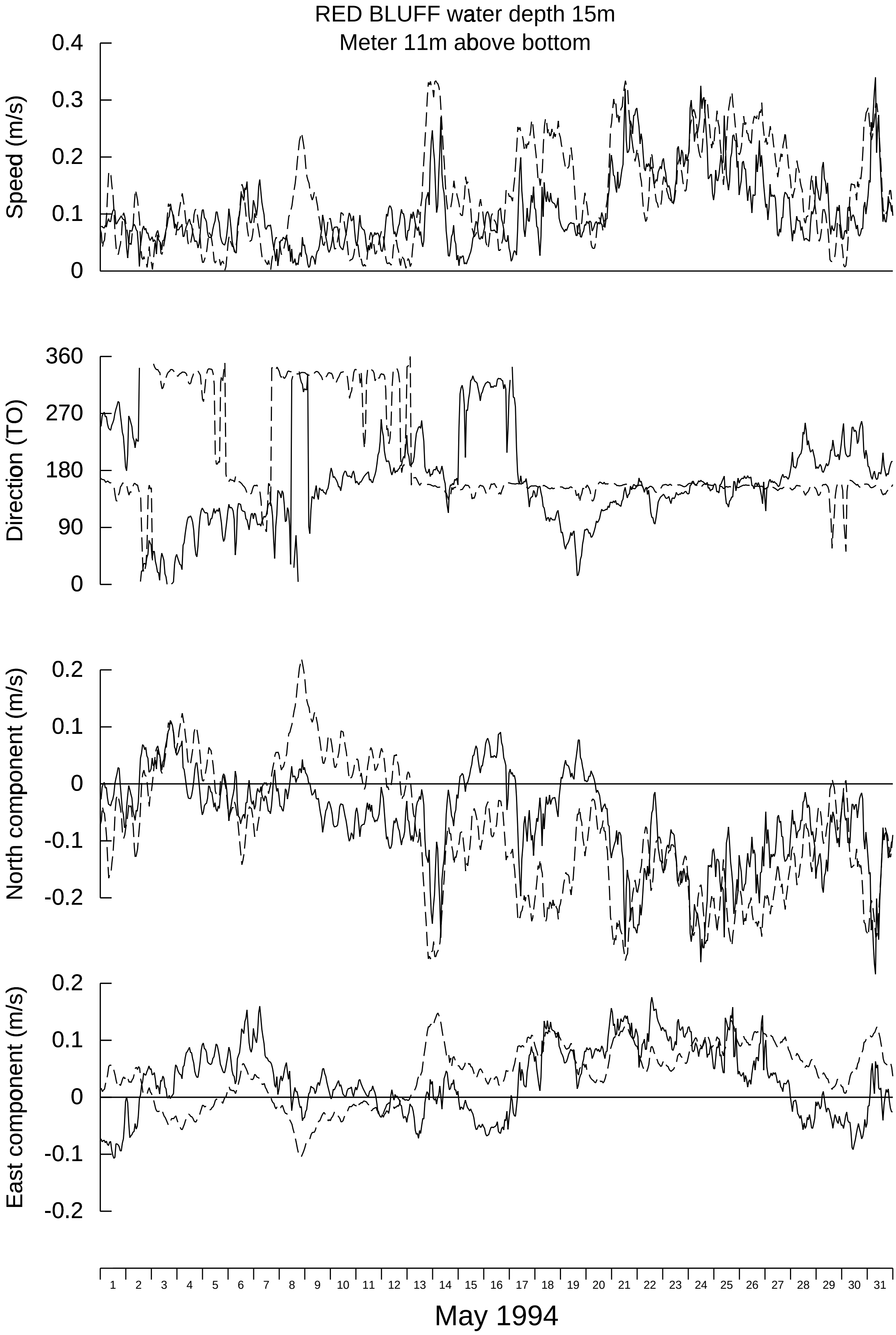

Figure 22: Measured (solid) and modelled (dashed) currents at the Red Bluff site, upper meter, May 1994.

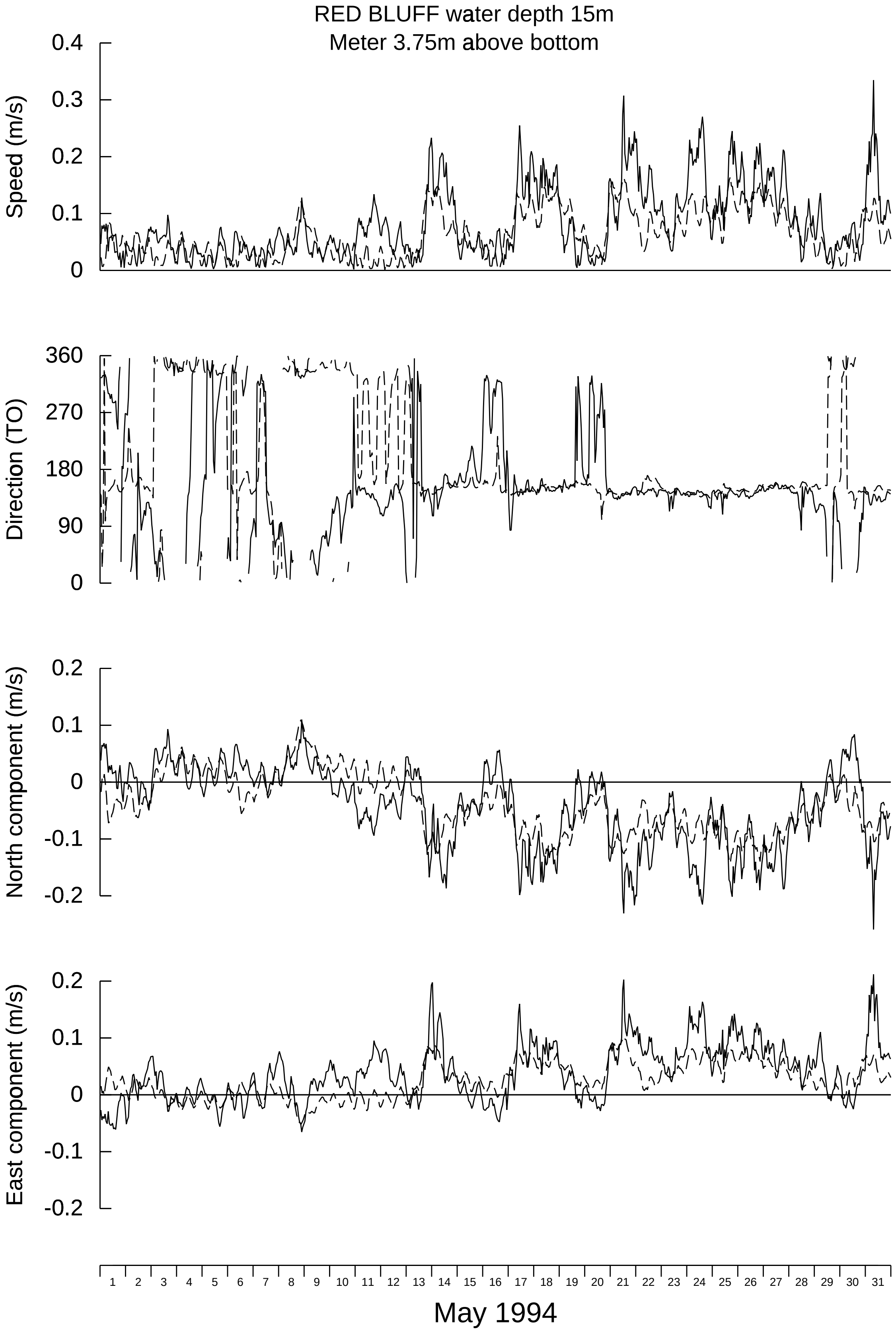

Figure 23: Measured (solid) and modelled (dashed) currents at the Red Bluff site, lower meter, May 1994.

Figure 24: Sites where COSRAD currents were compared with model currents, May 1994.

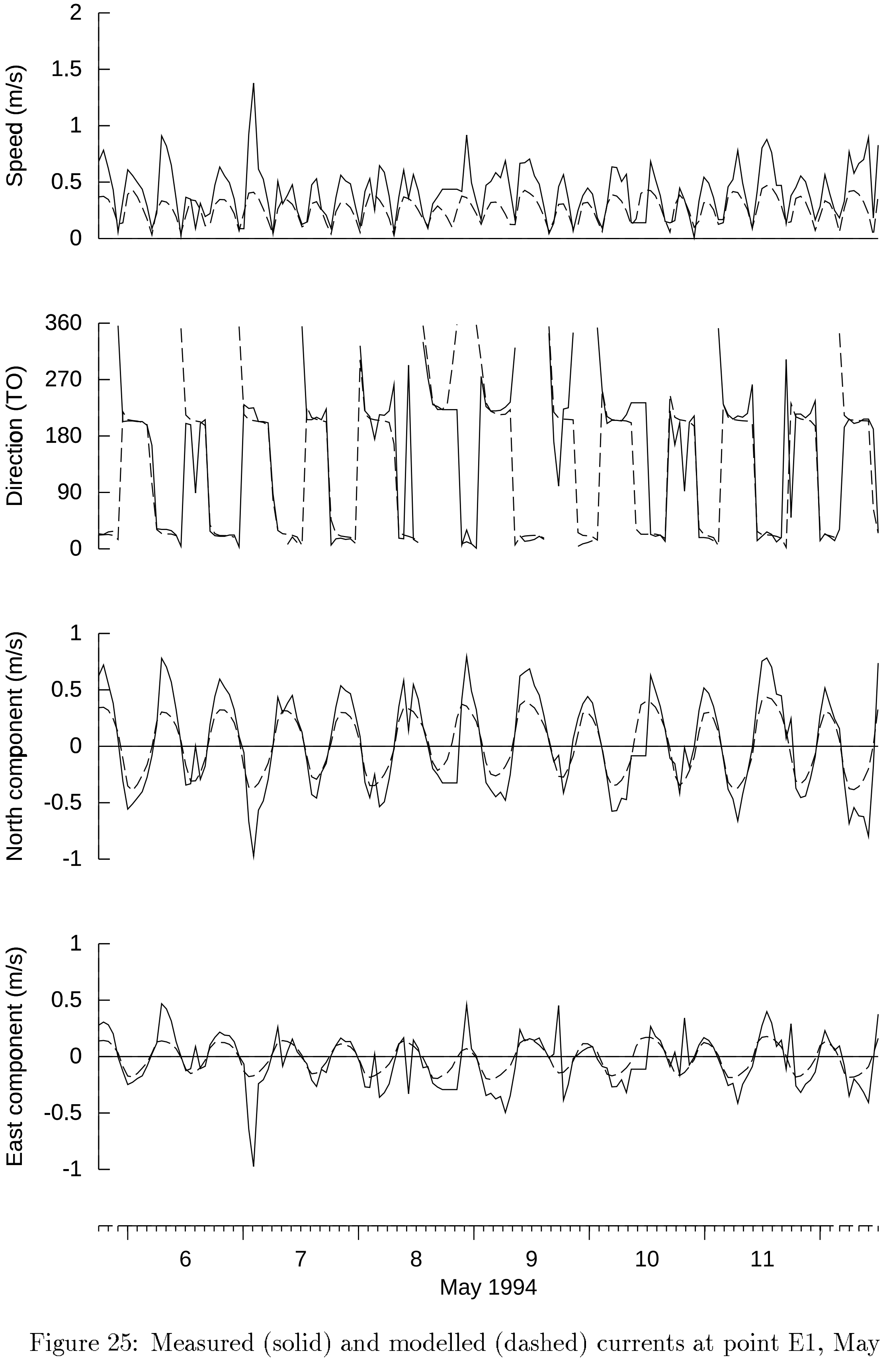

Figure 25: Measured (solid) and modelled (dashed) currents at point E1, May 1994.

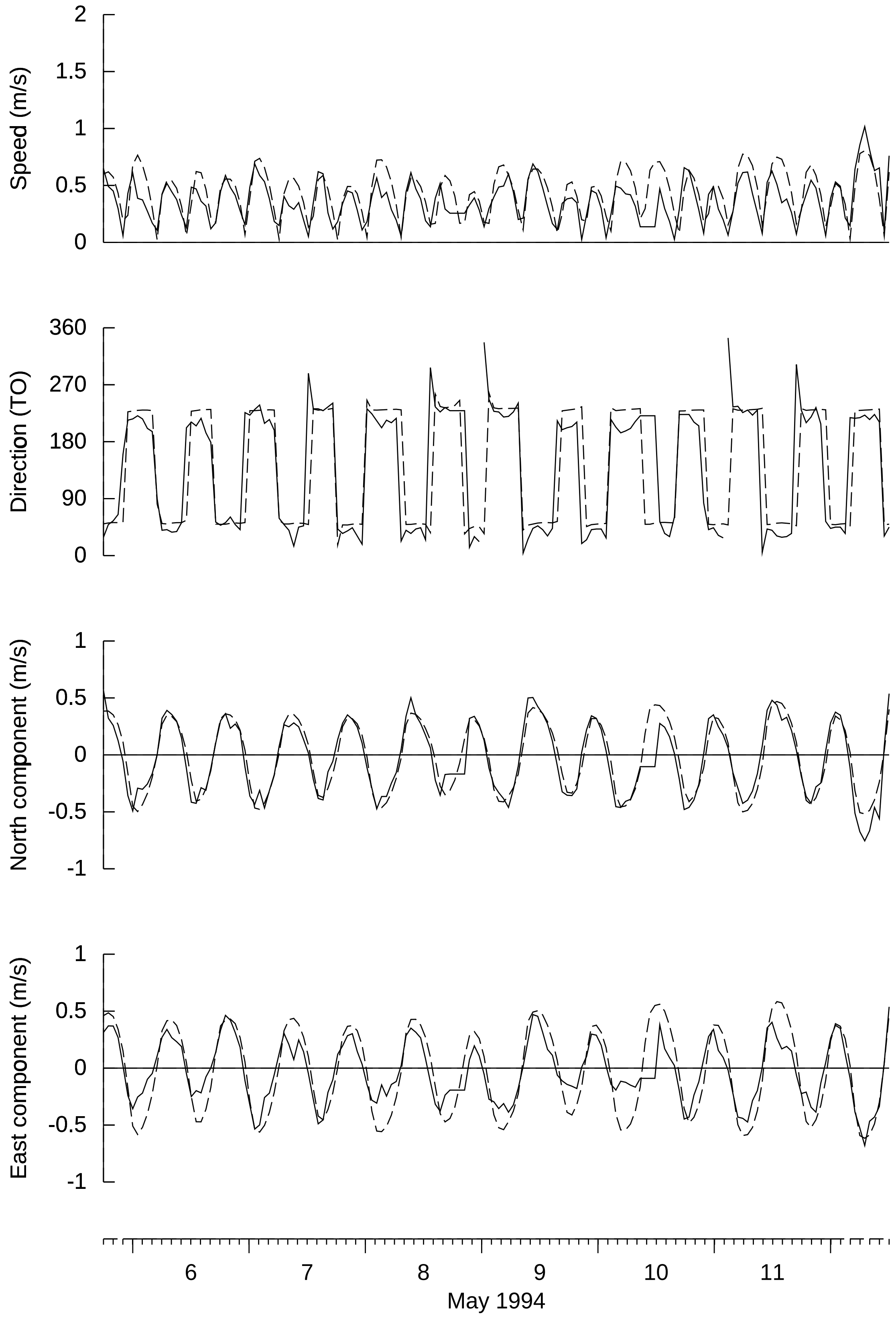

Figure 26: Measured (solid) and modelled (dashed) currents at point E2, May 1994.

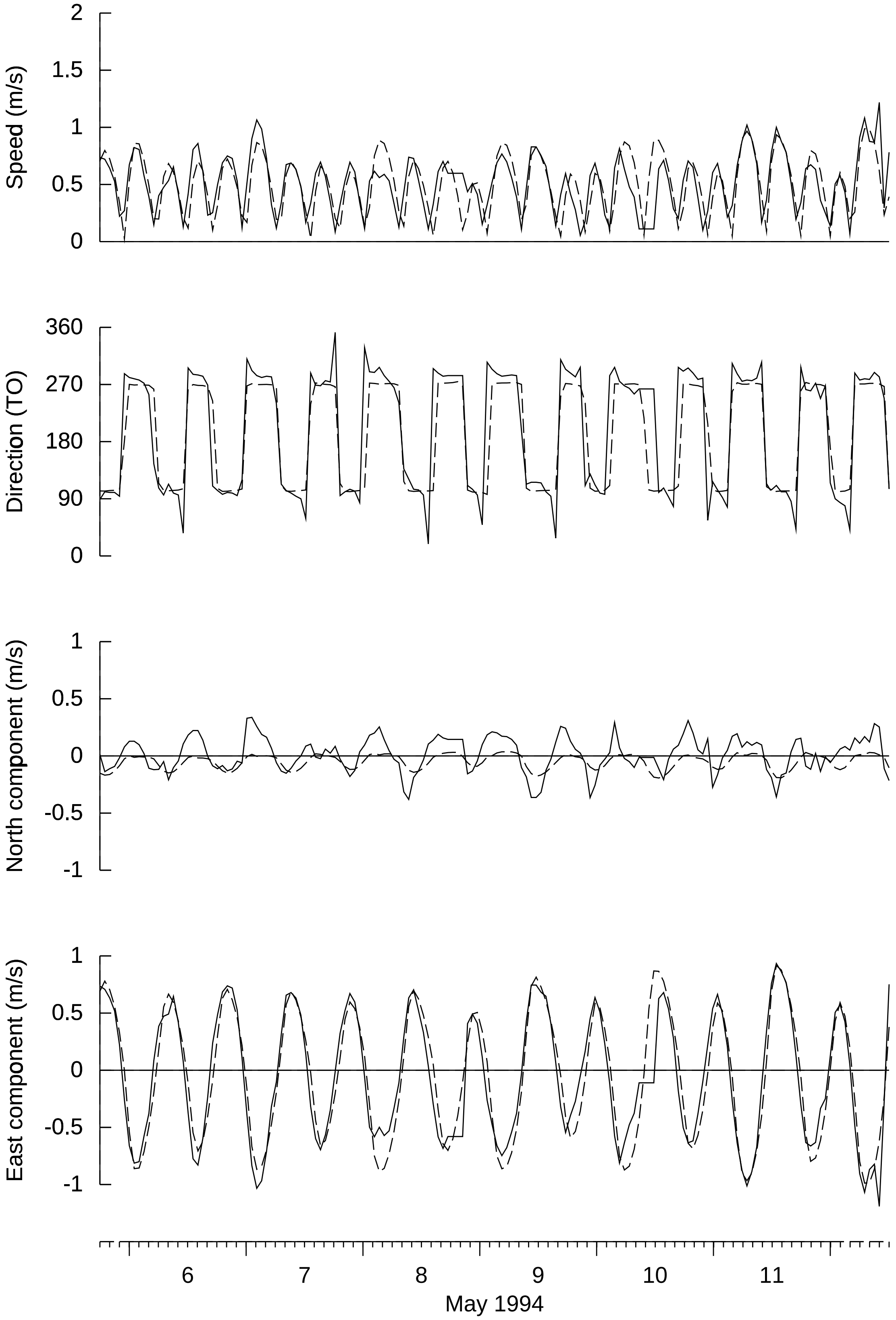

Figure 27: Measured (solid) and modelled (dashed) currents at point E3, May 1994.

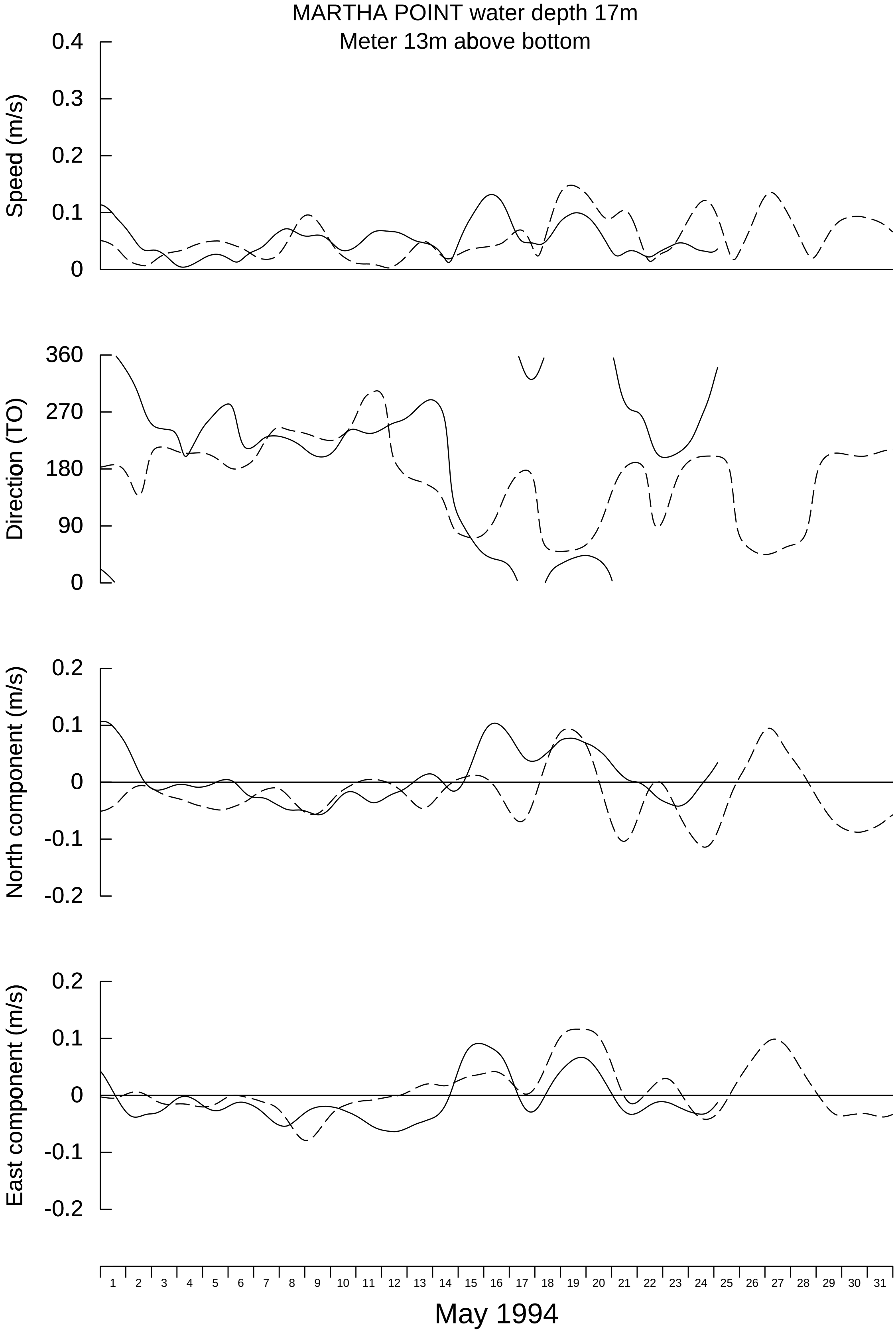

Figure 28: Measured (solid) and modelled (dashed) low pass filtered currents at the Martha Point site, upper meter, May 1994.

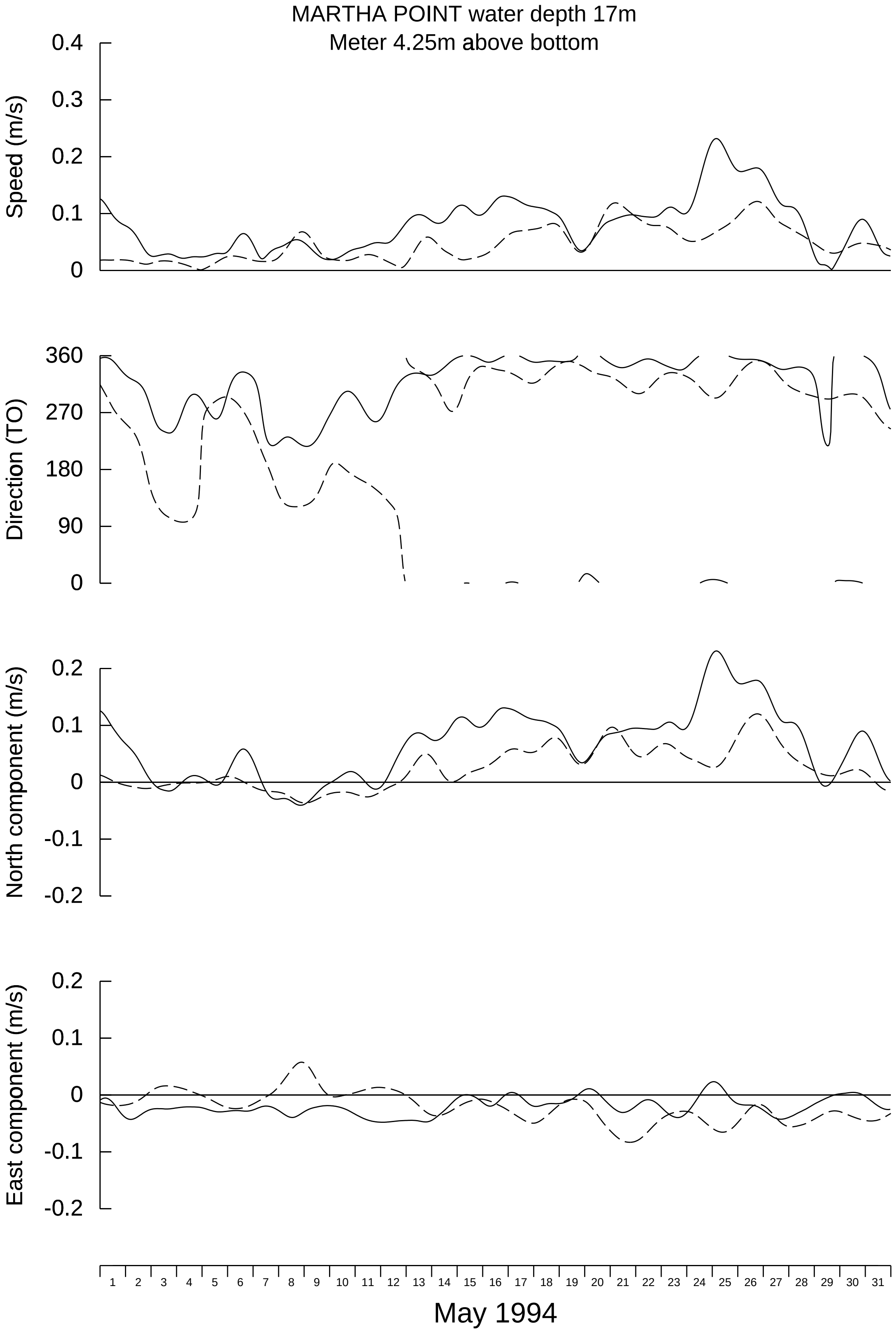

Figure 29: Measured (solid) and modelled (dashed) low pass filtered currents at the Martha Point site, lower meter, May 1994.

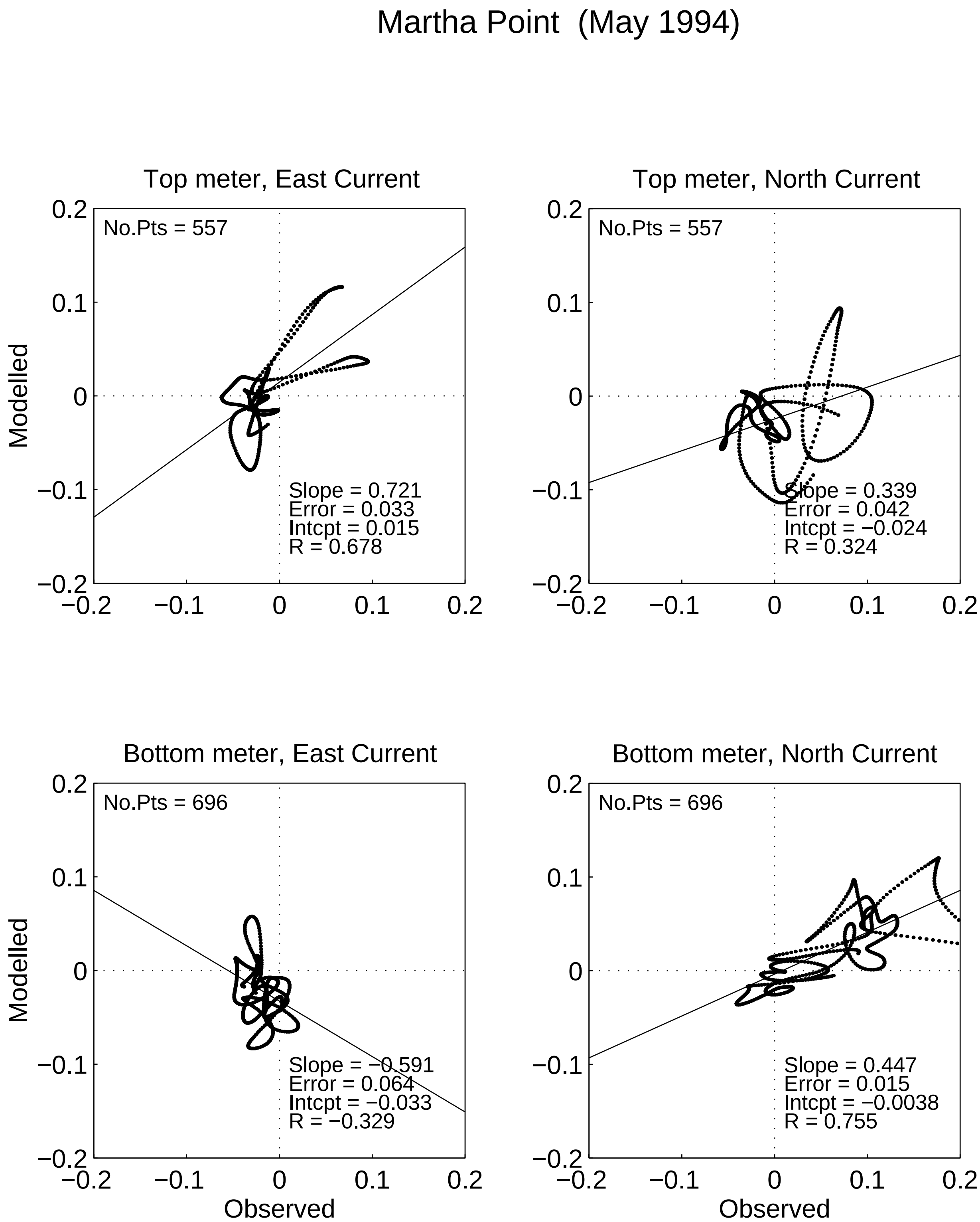

Figure 30: Observed (x-axis) versus modelled (y-axis) low pass filtered current components for the Martha Point mooring, May 1994.

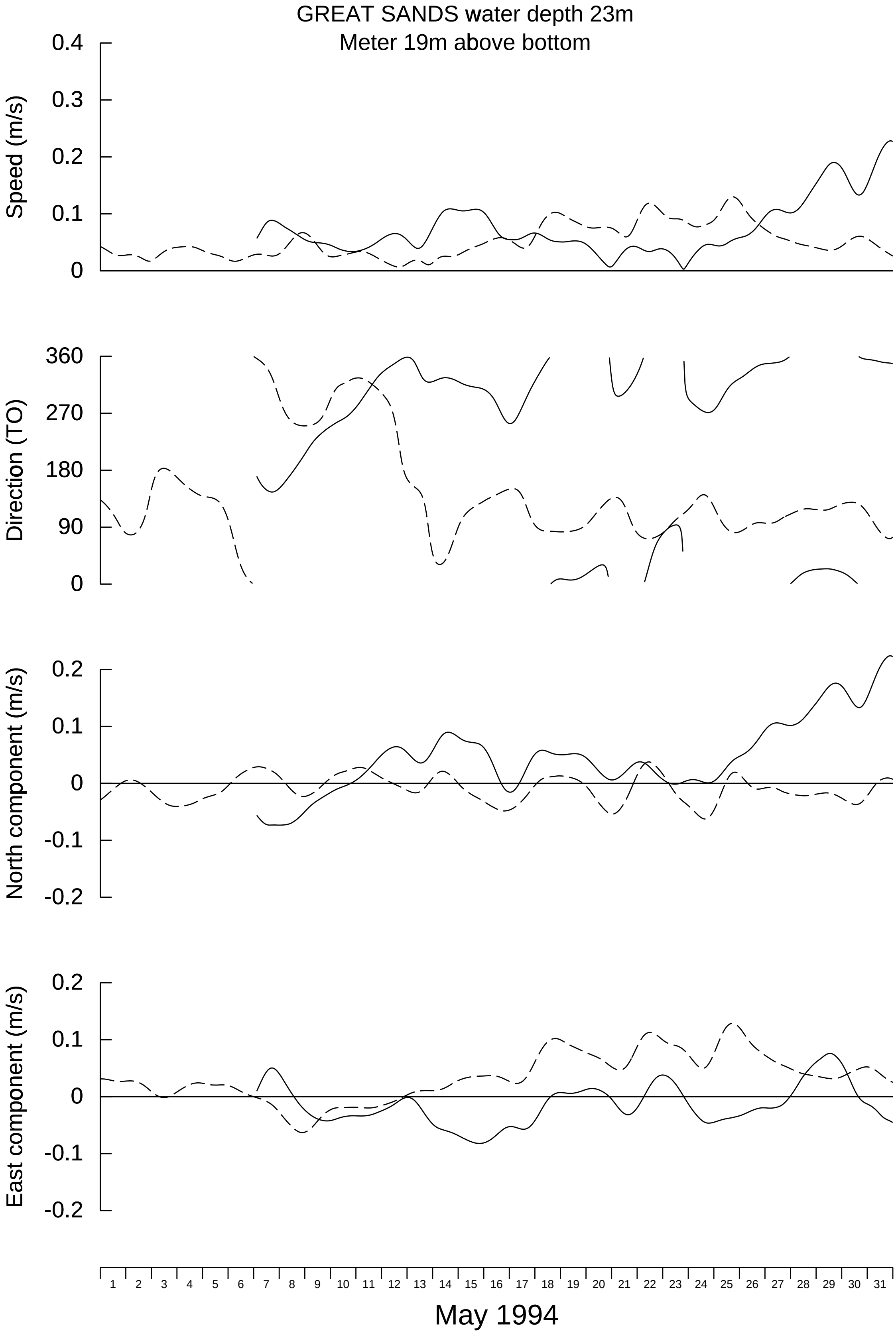

Figure 31: Measured (solid) and modelled (dashed) low pass filtered currents at the Great Sands site, upper meter, May 1994.

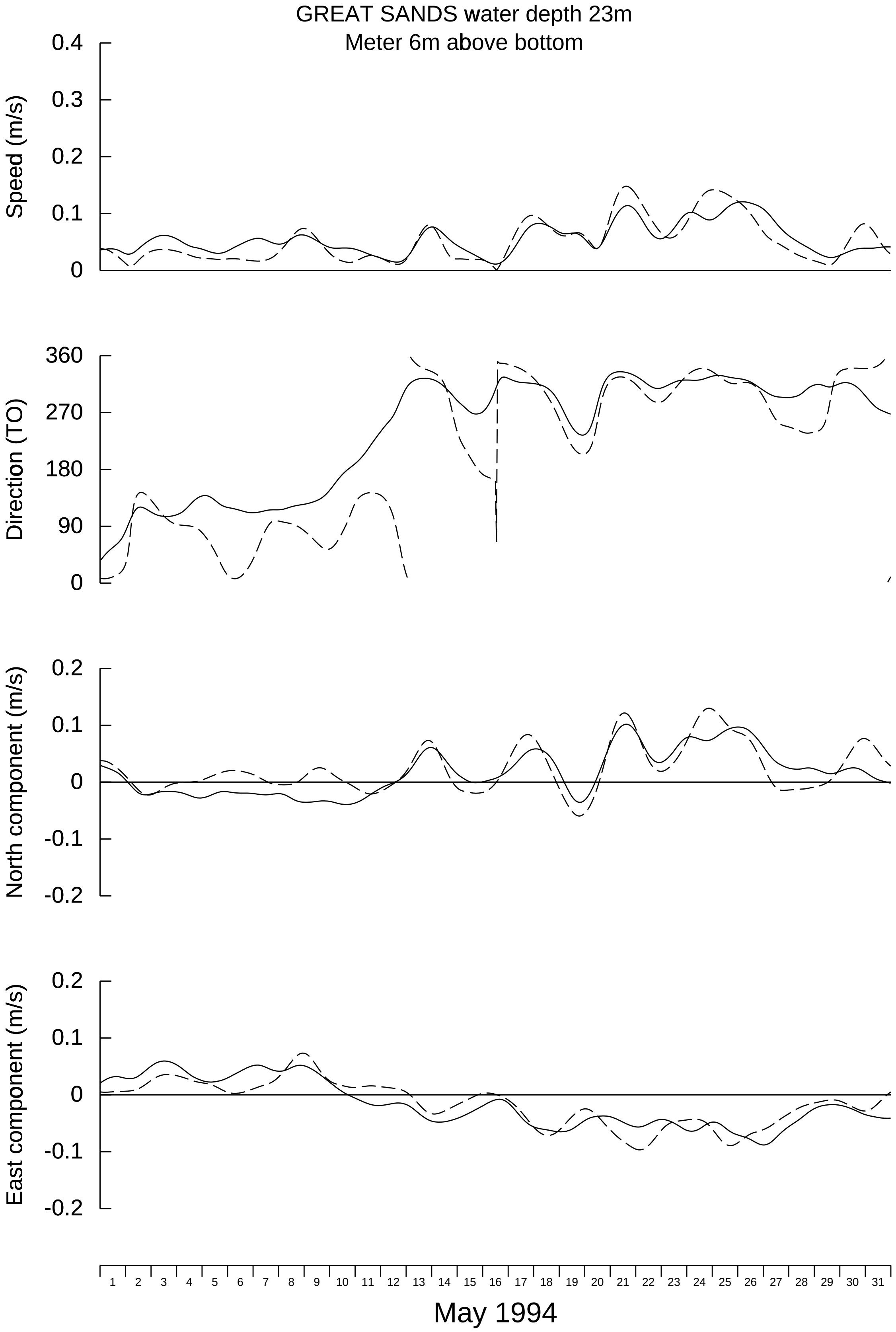

Figure 32: Measured (solid) and modelled (dashed) low pass filtered currents at the Great Sands site, lower meter, May 1994.

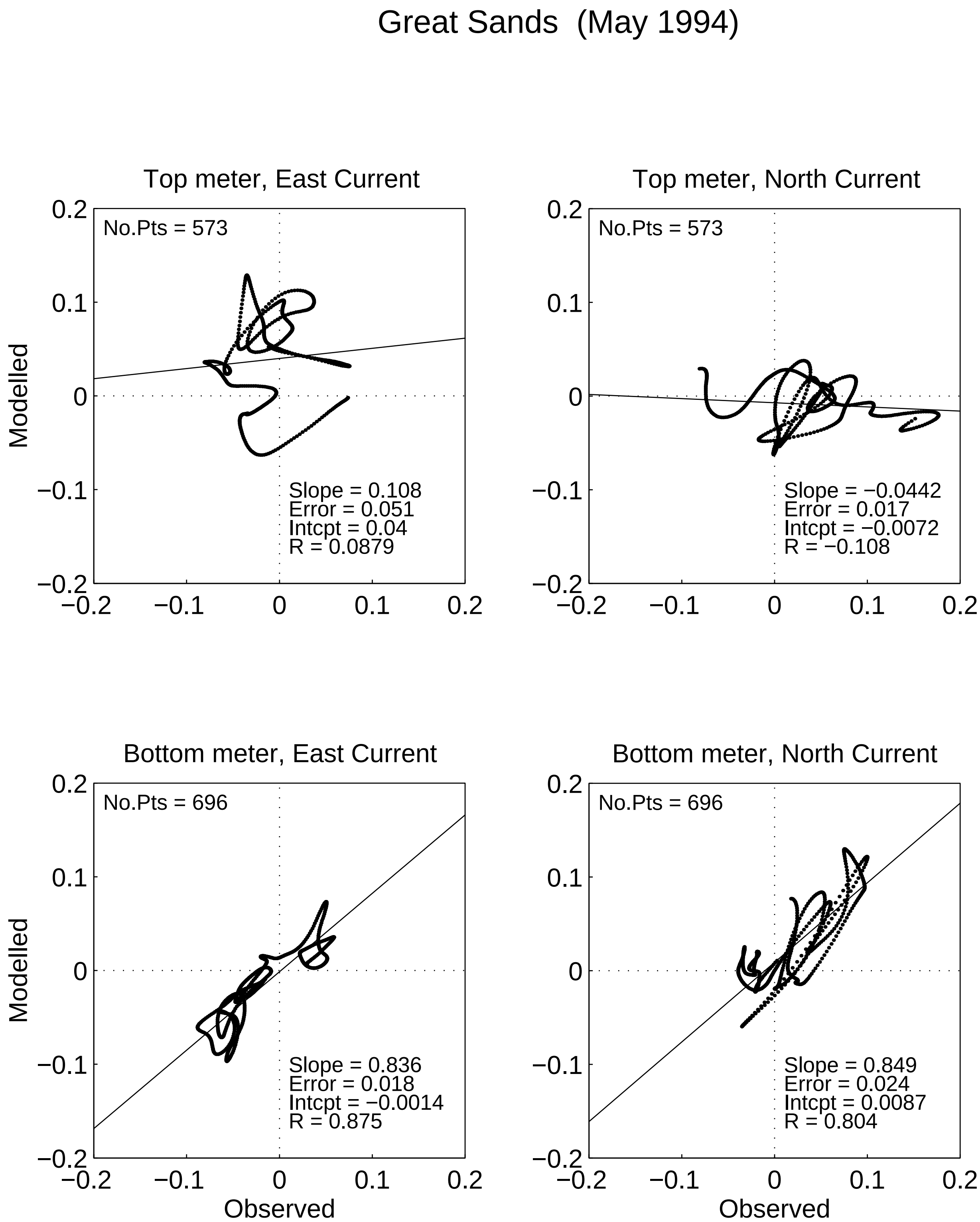

Figure 33: Observed (x-axis) versus modelled (y-axis) low pass filtered current components for the Great Sands mooring, May 1994.

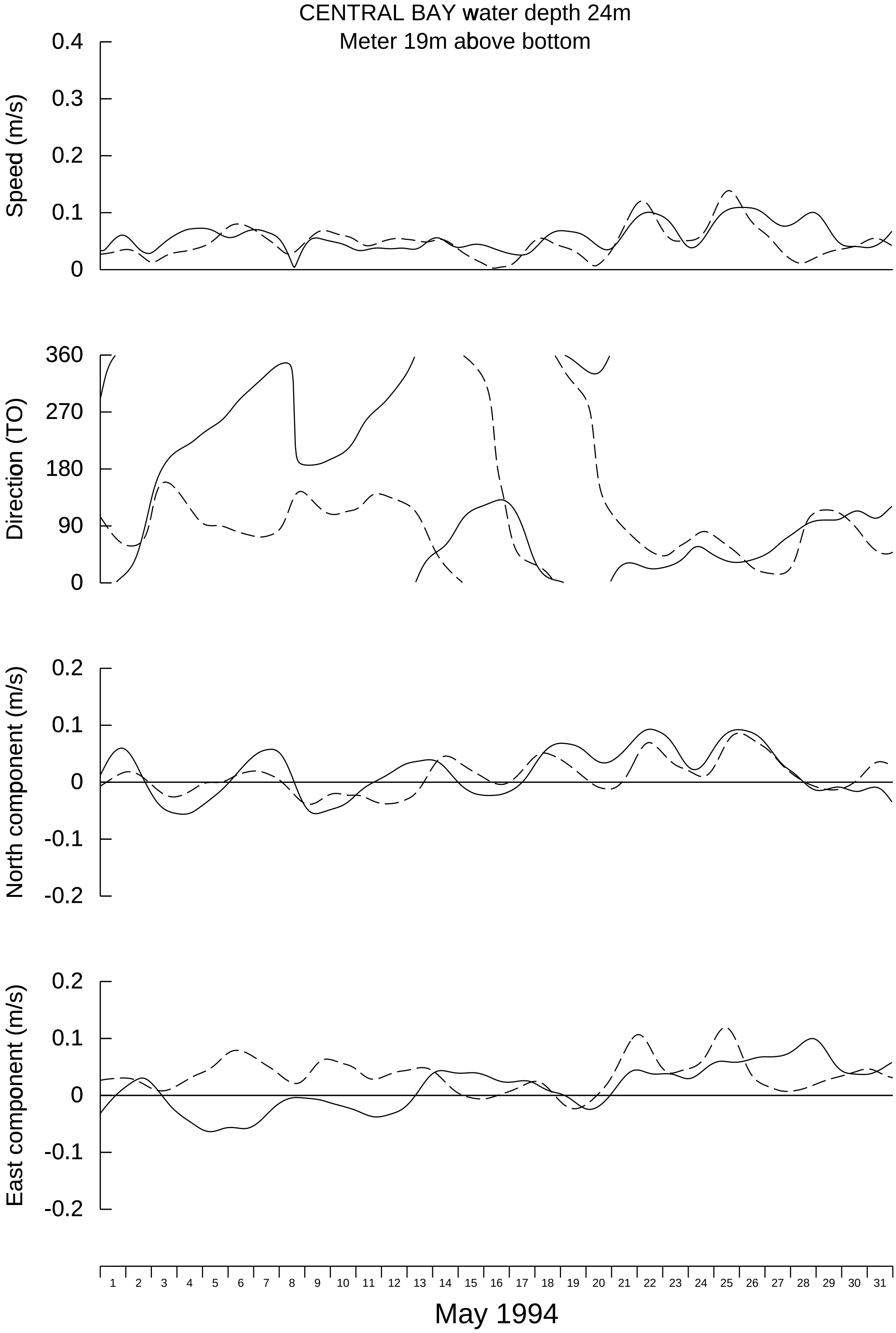

Figure 34: Measured (solid) and modelled (dashed) low pass filtered currents at the Central Bay site, upper meter, May 1994.

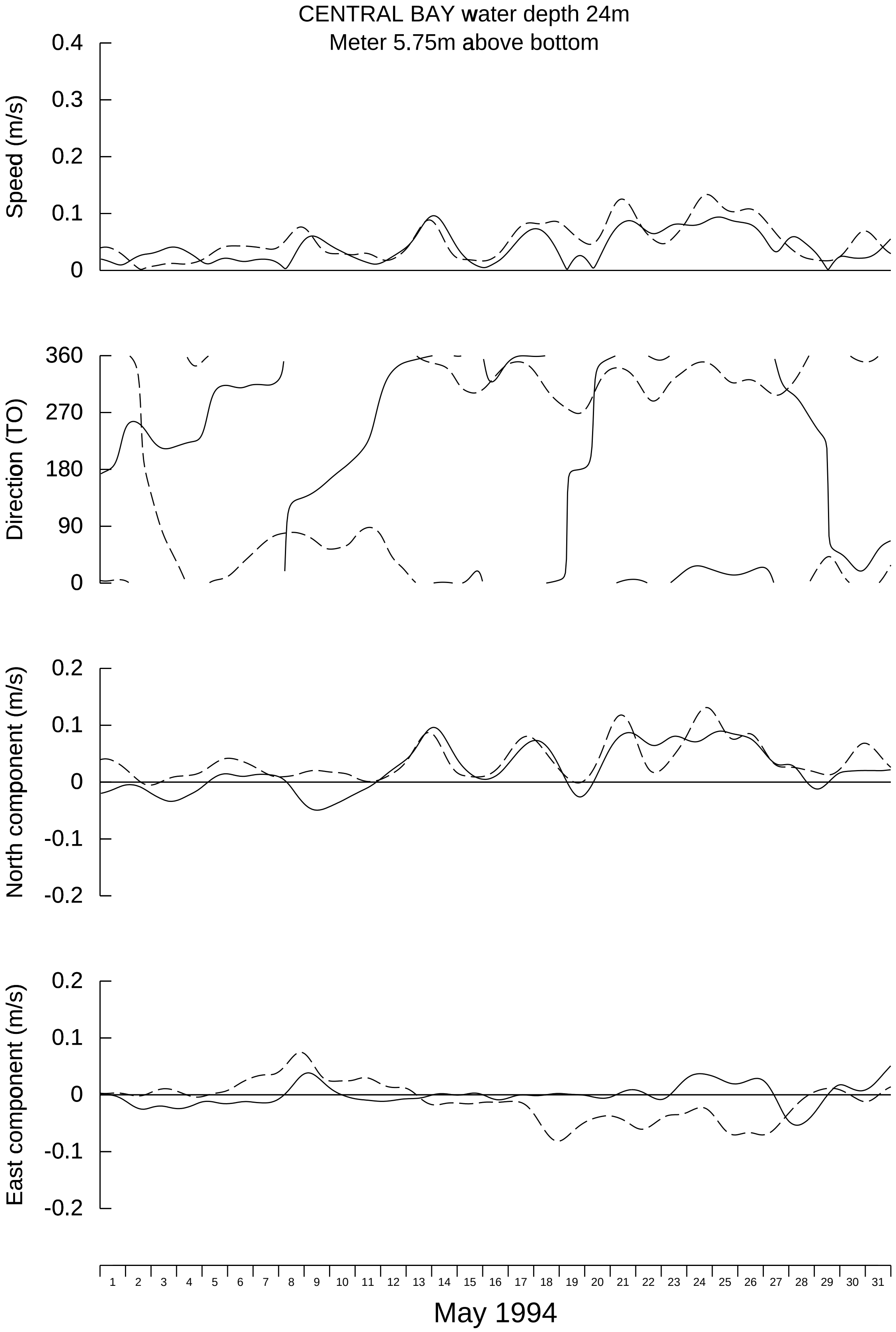

Figure 35: Measured (solid) and modelled (dashed) low pass filtered currents at the Central Bay site, lower meter, May 1994.

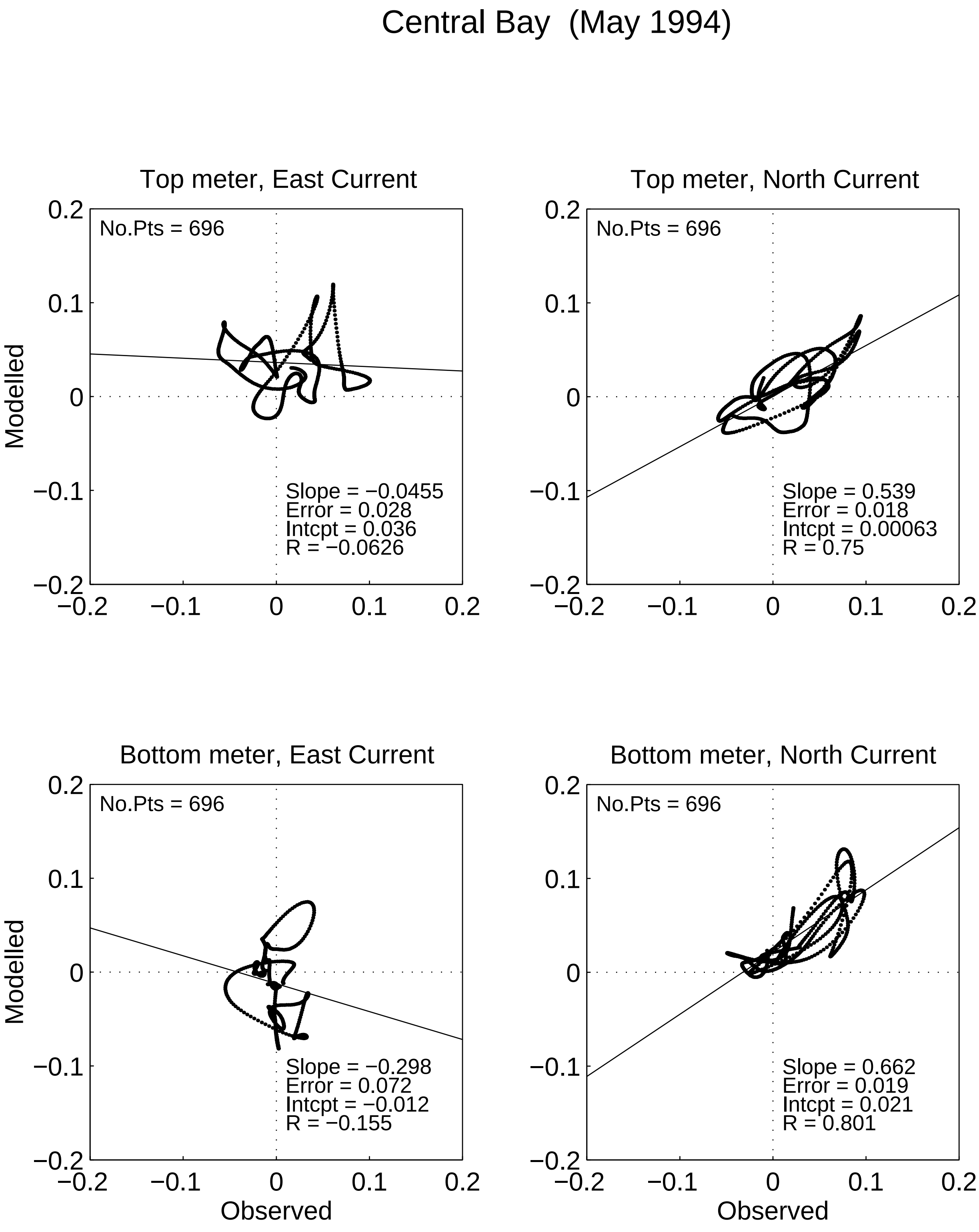

Figure 36: Observed (x-axis) versus modelled (y-axis) low pass filtered current components for the Central Bay mooring, May 1994.

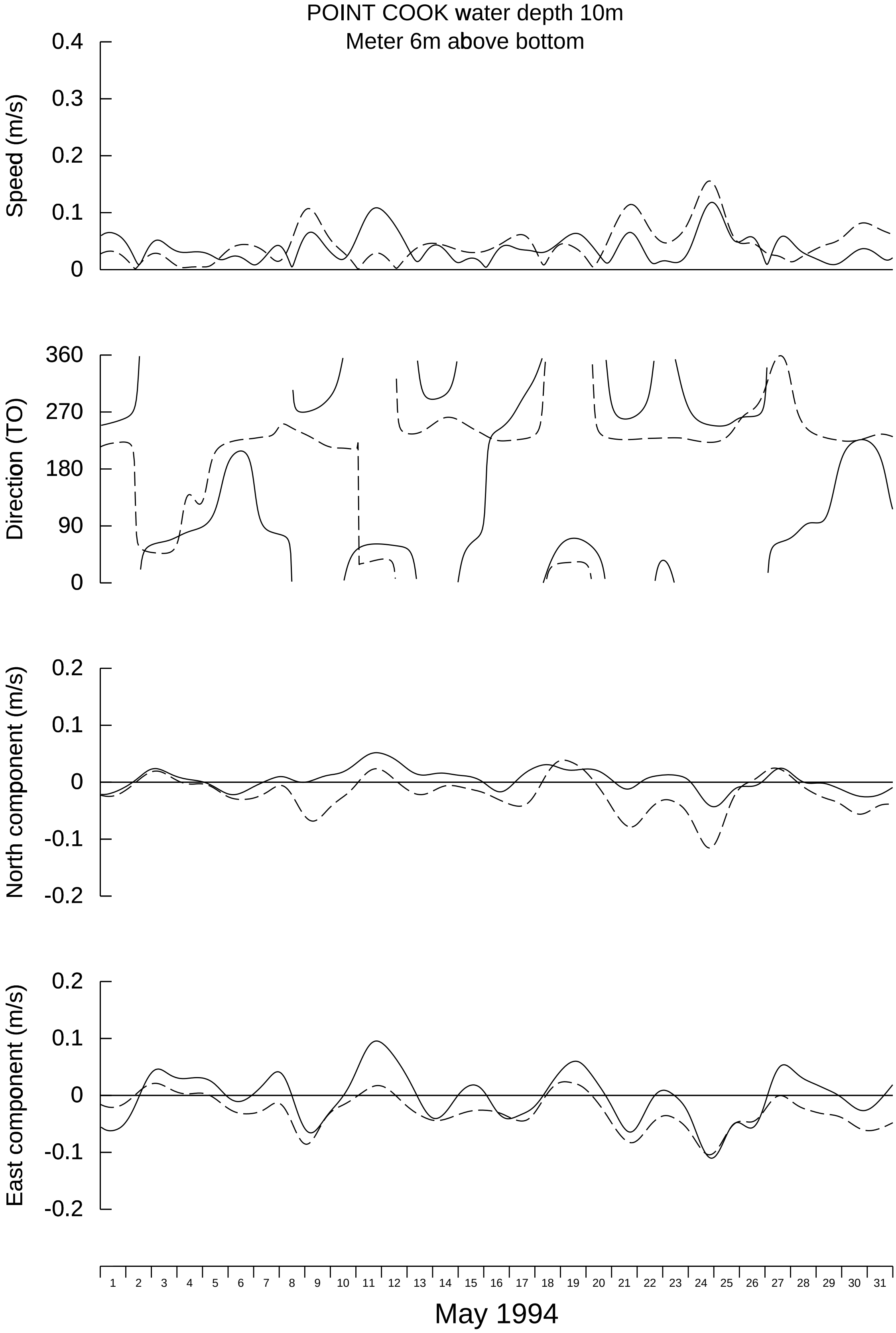

Figure 37: Measured (solid) and modelled (dashed) low pass filtered currents at the Point Cook site, upper meter, May 1994.

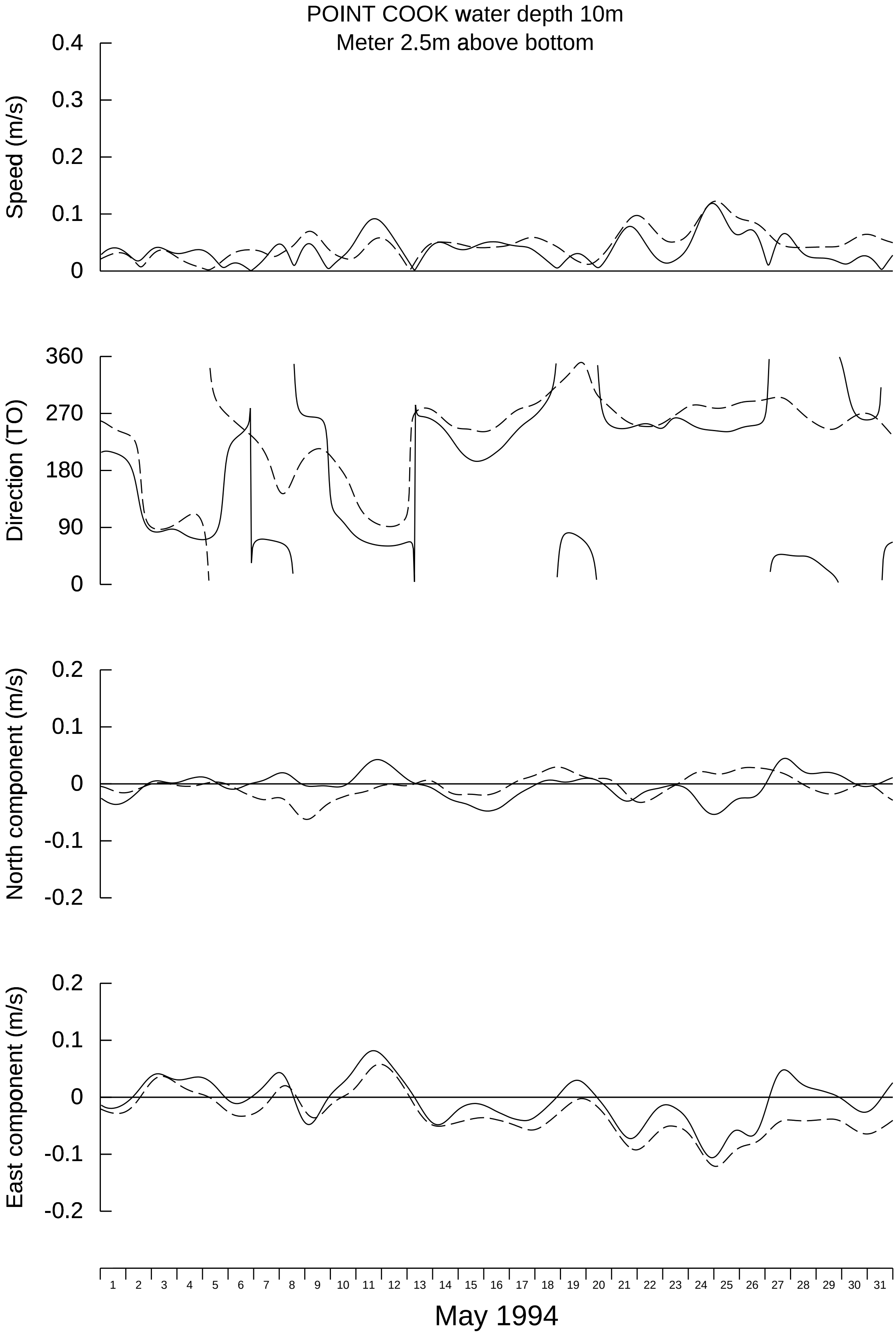

Figure 38: Measured (solid) and modelled (dashed) low pass filtered currents at the Point Cook site, lower meter, May 1994.

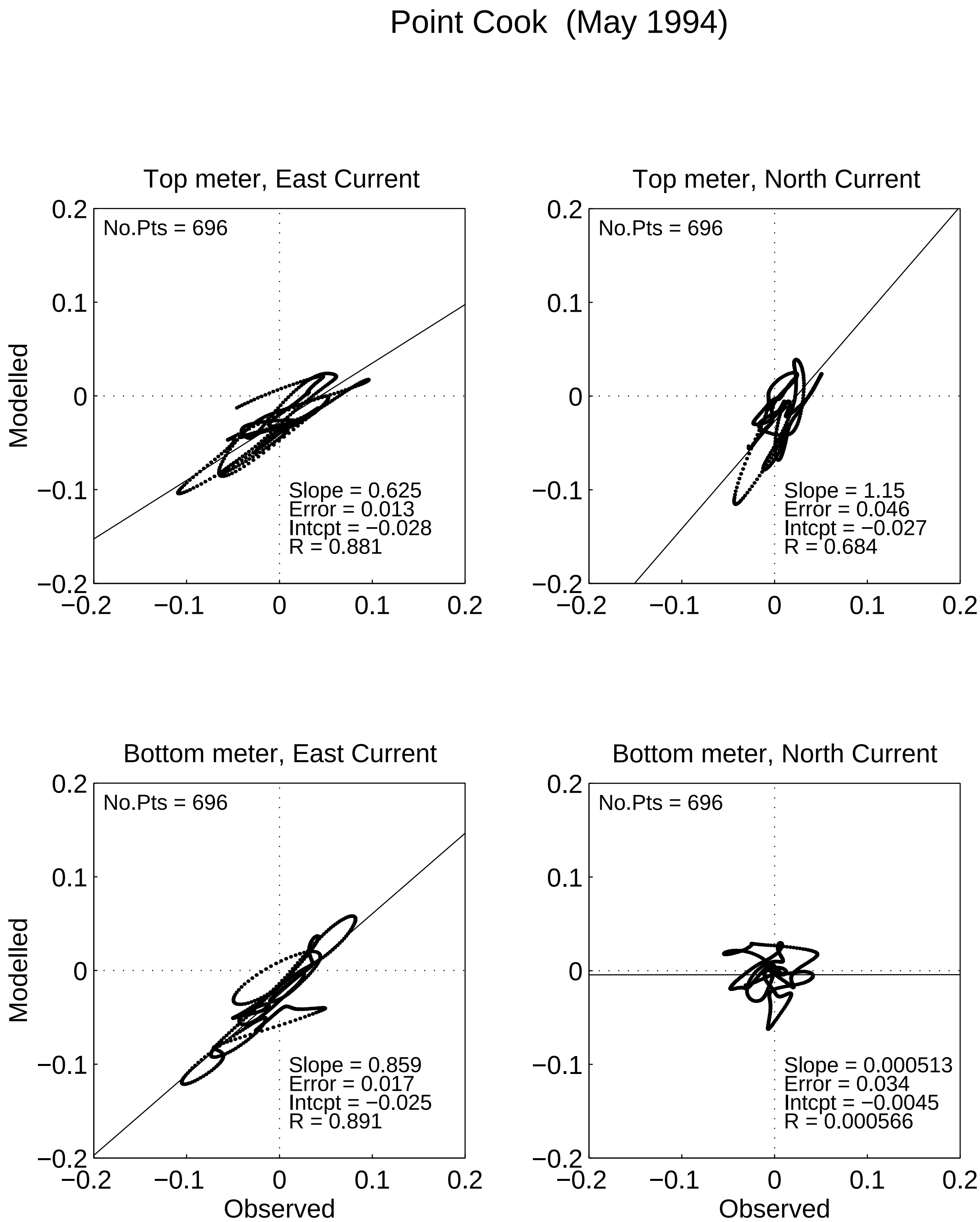

Figure 39: Observed (x-axis) versus modelled (y-axis) low pass filtered current components for the Point Cook mooring, May 1994.

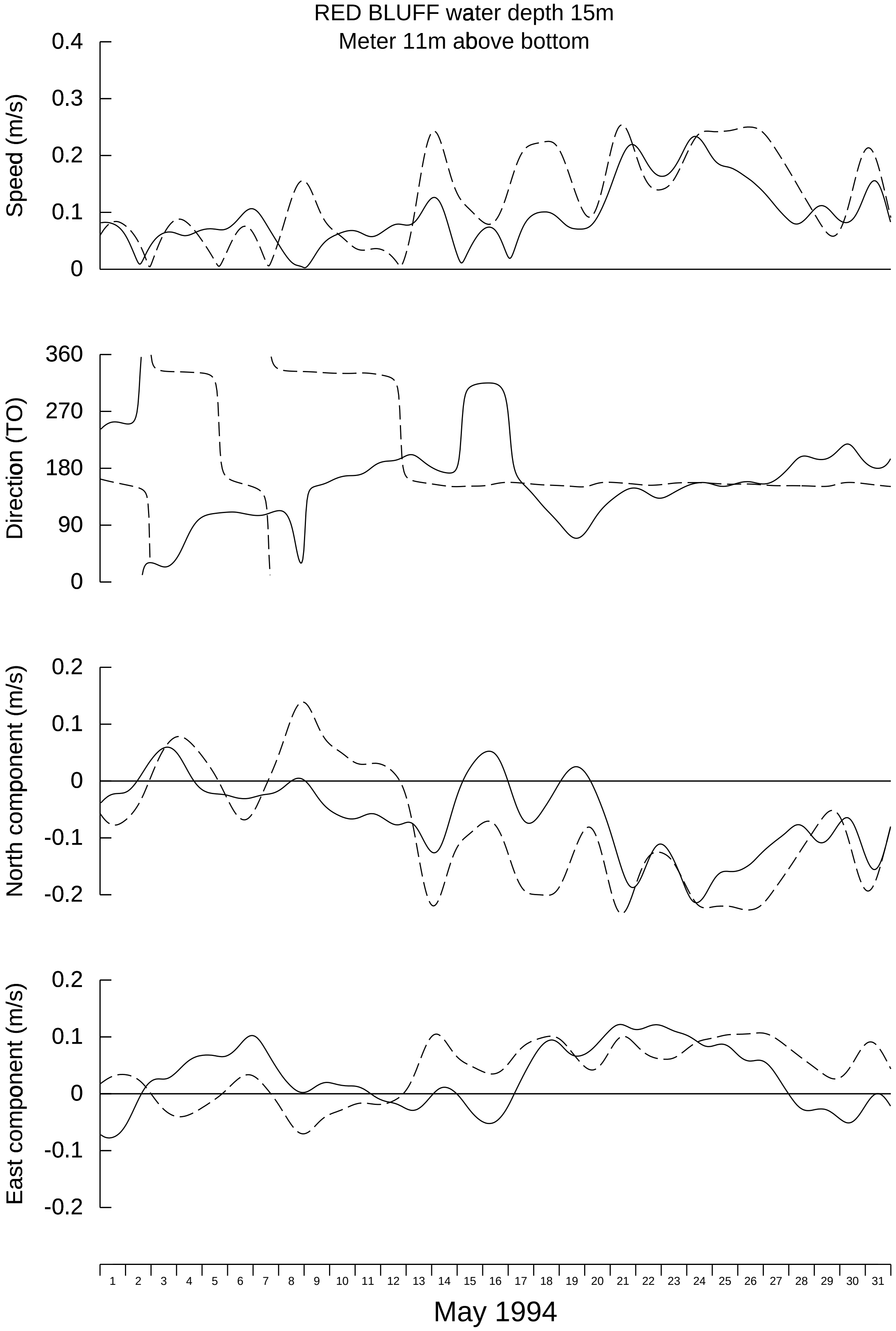

Figure 40: Measured (solid) and modelled (dashed) low pass filtered currents at the Red Bluff site, upper meter, May 1994.

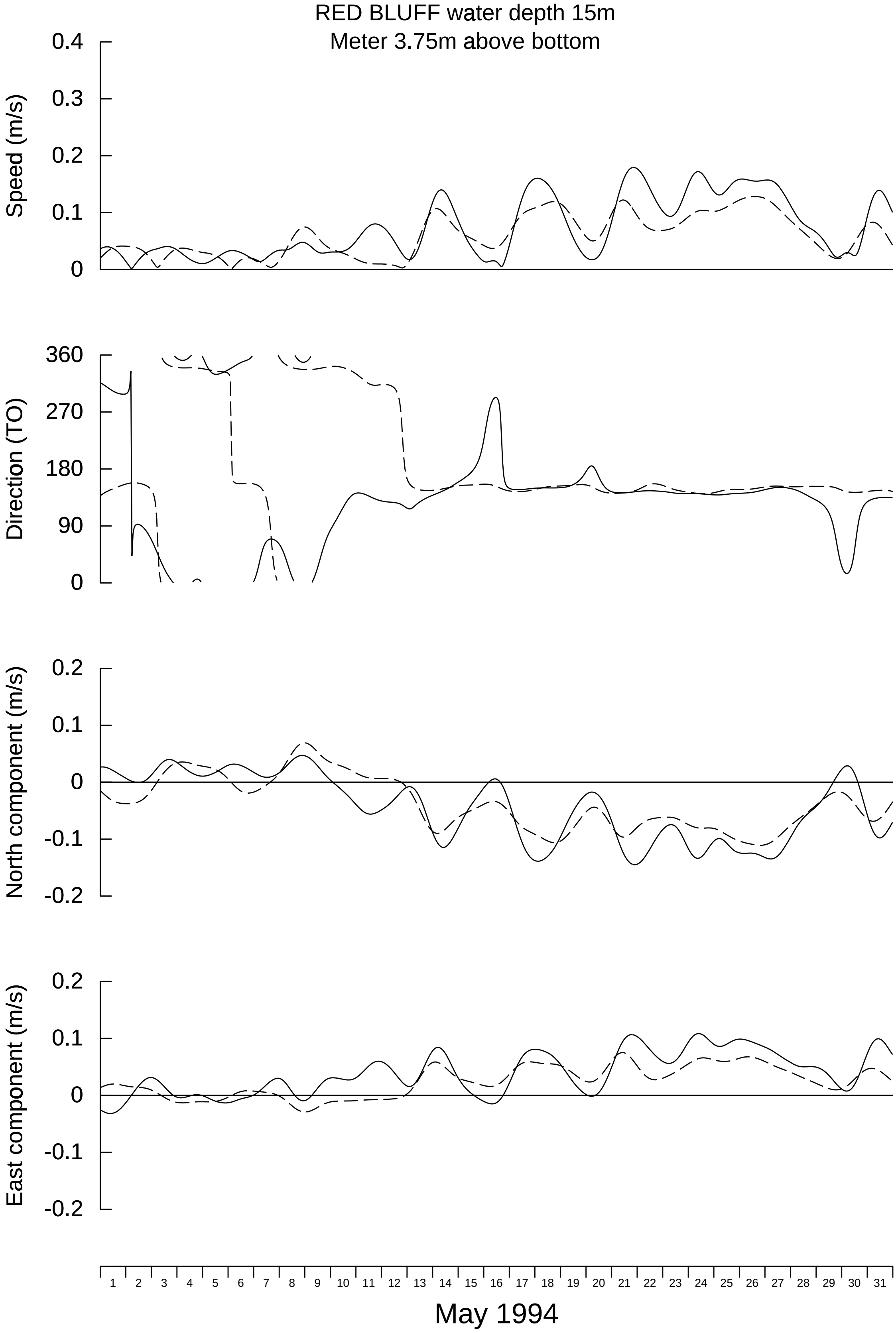

Figure 41: Measured (solid) and modelled (dashed) low pass filtered currents at the Red Bluff site, lower meter, May 1994.

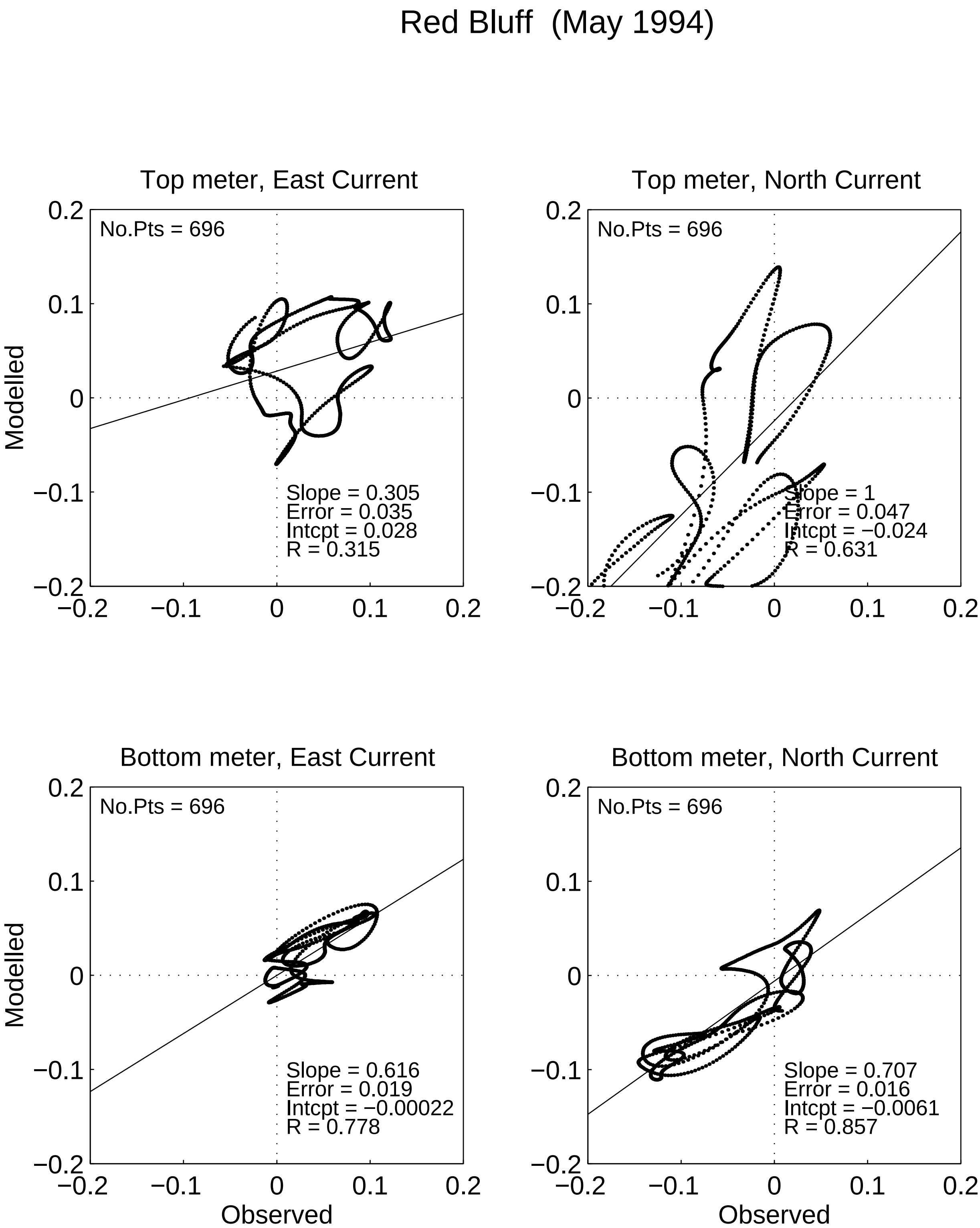

Figure 42: Observed (x-axis) versus modelled (y-axis) low pass filtered current components for the Red Bluff mooring, May 1994.

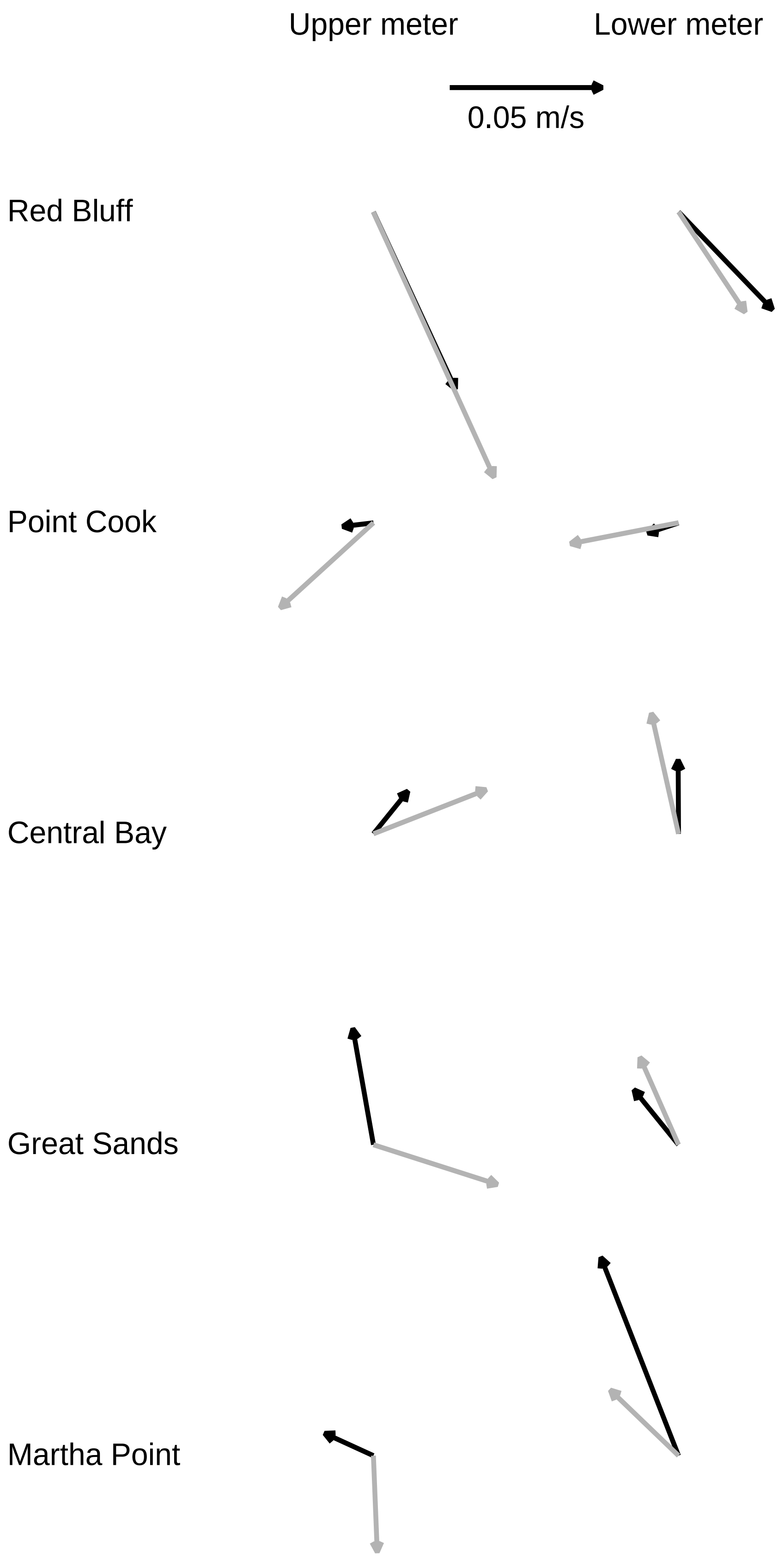

Figure 43: Vector mean currents for the entire May 1994 current meter deployment period. Measured data are shown as black arrows, model results are shown as grey arrows. The arrow at the top of the figure indicates a magnitude of 0.05 m/s. North is towards the top of the page.

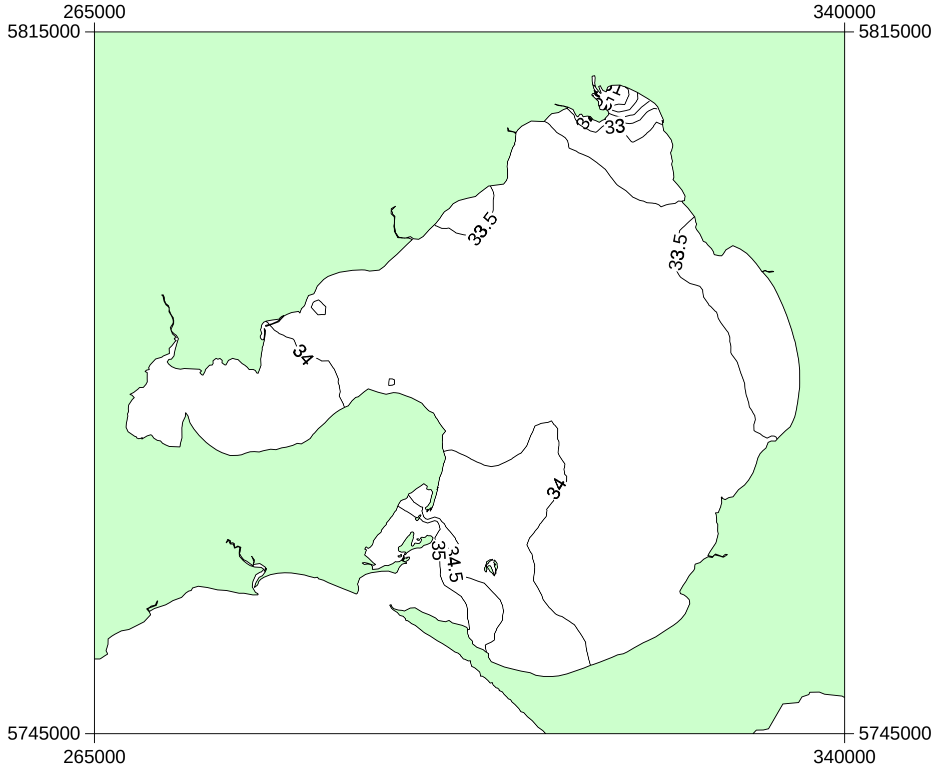

Figure 44: Surface (0-2m) salinity measured by CTD, 3-4 May 1994.

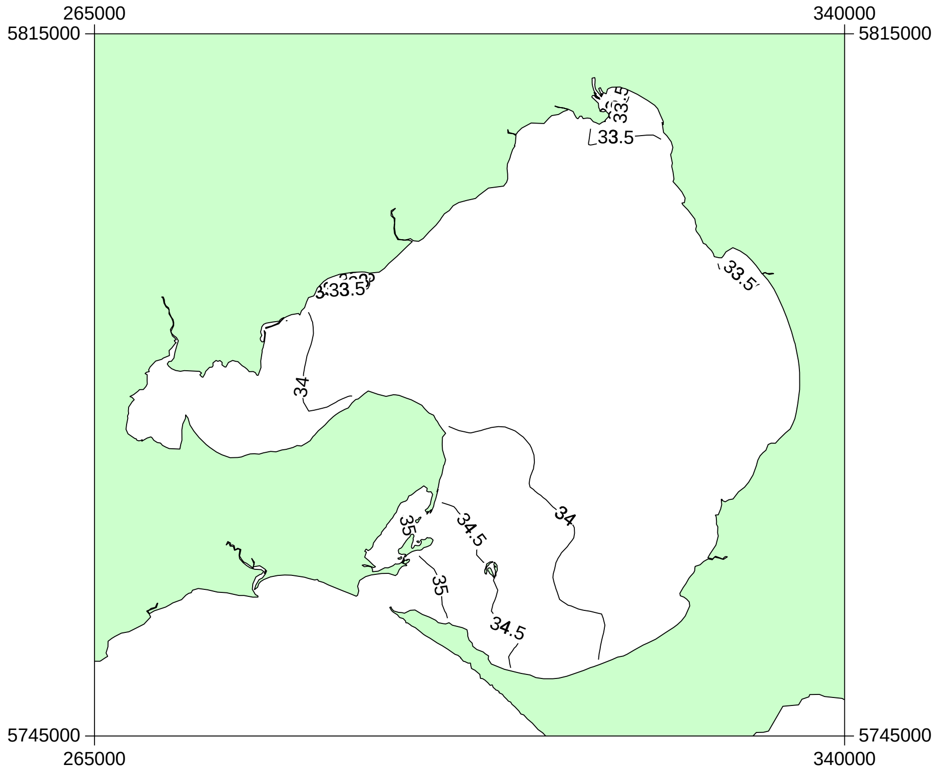

Figure 45: Surface (0-2m) salinity from model, 00:00 4 May 1994

.

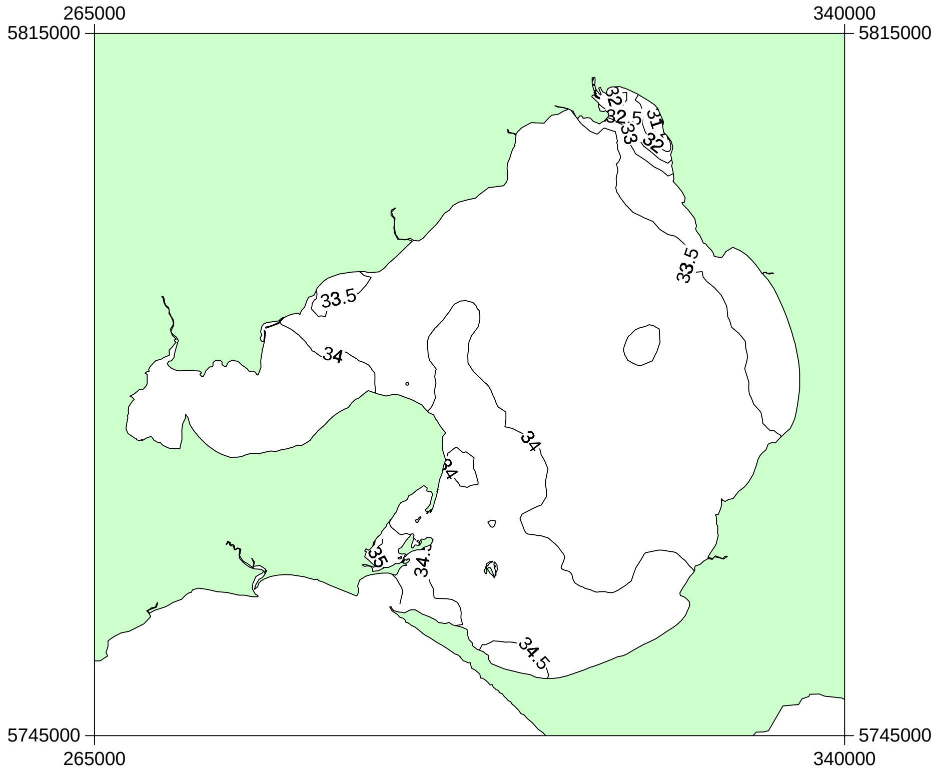

Figure 46: Surface (0-2m) salinity measured by CTD, 12-16 May 1994.

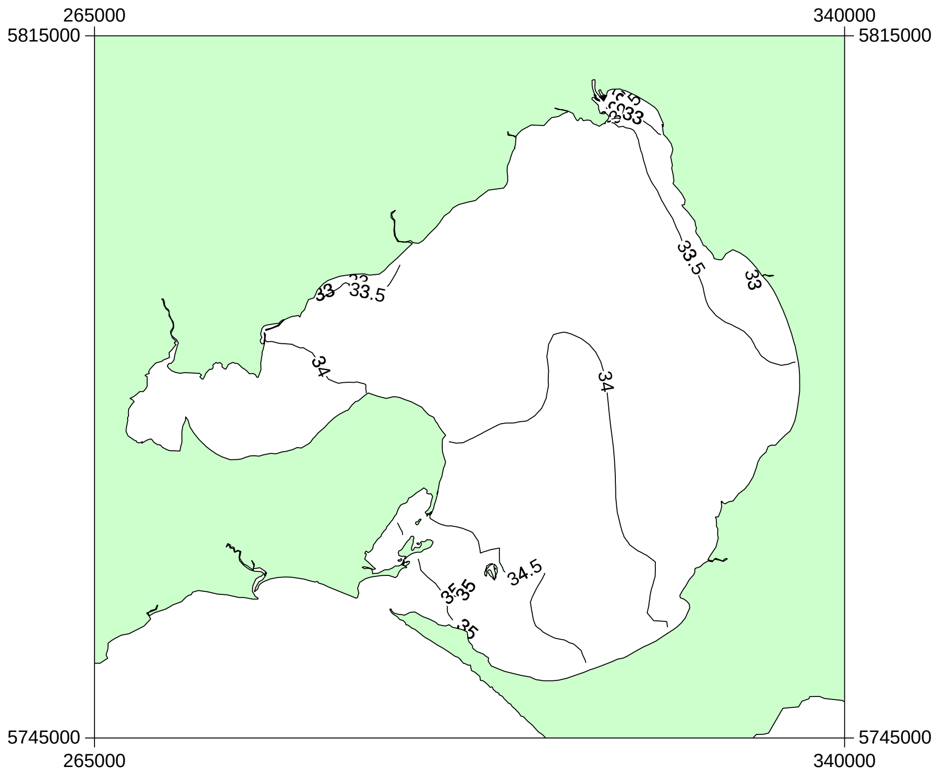

Figure 47: Surface (0-2m) salinity from model, 00:00 16 May 1994

.

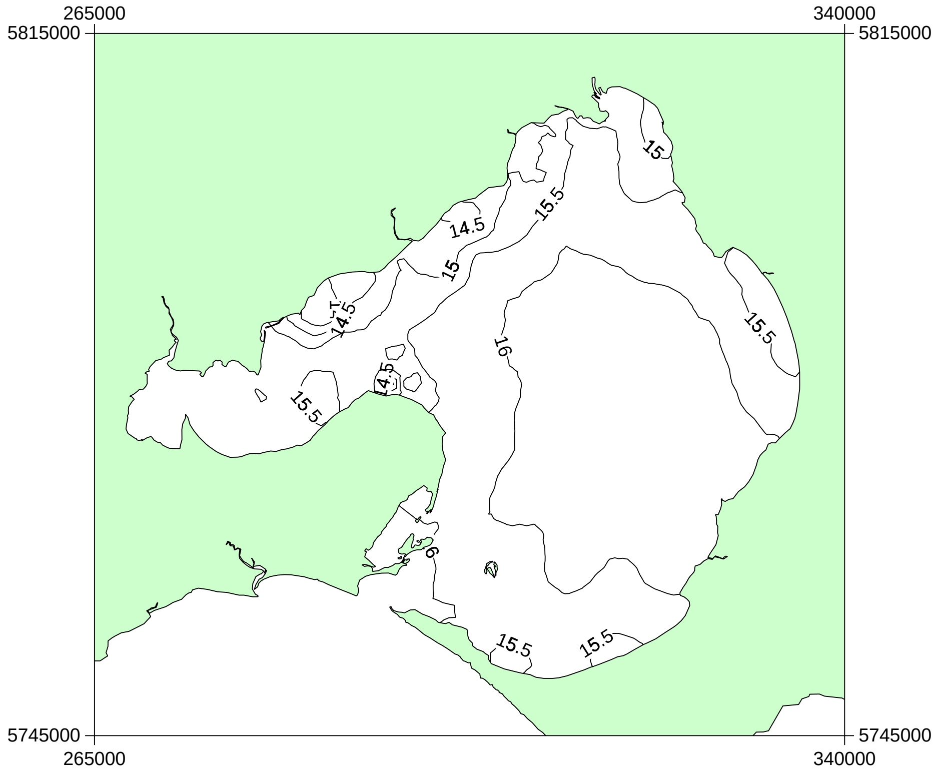

Figure 48: Surface (0-2m) temperature measured by CTD, 3-4 May 1994.

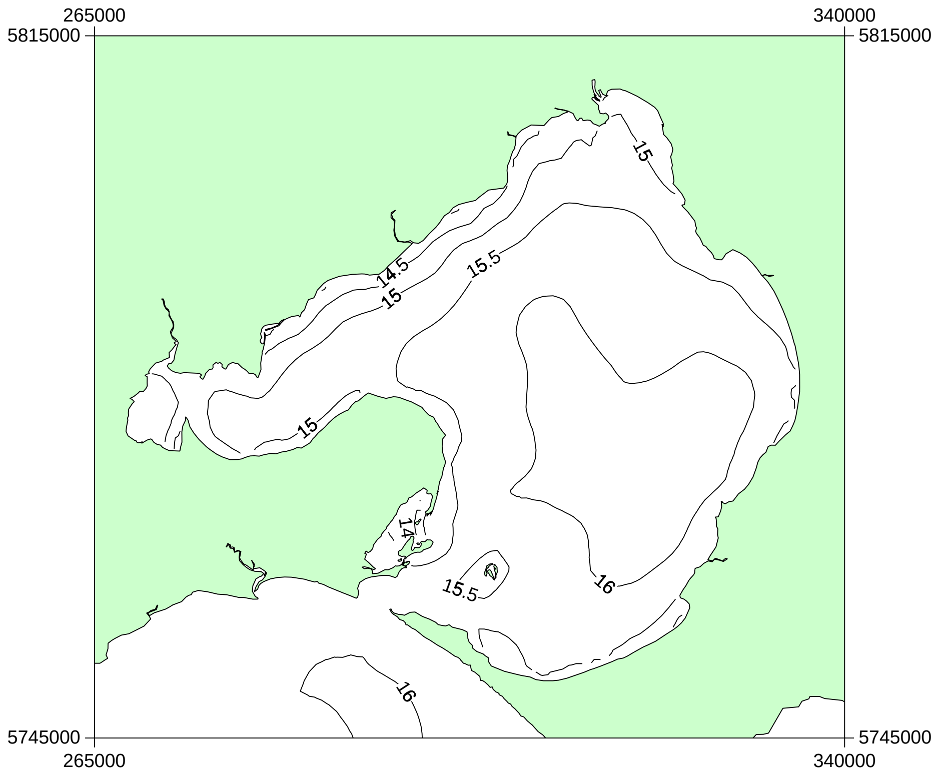

Figure 49: Surface (0-2m) temperature from model, 00:00 4 May 1994

.

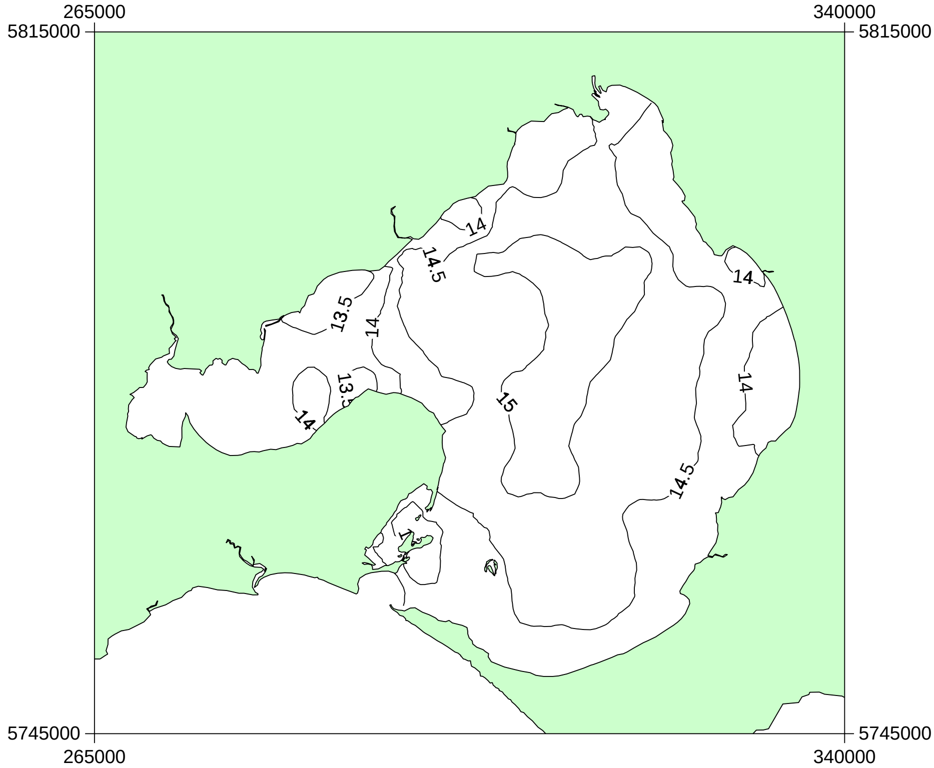

Figure 50: Surface (0-2m) temperature measured by CTD, 12-16 May 1994.

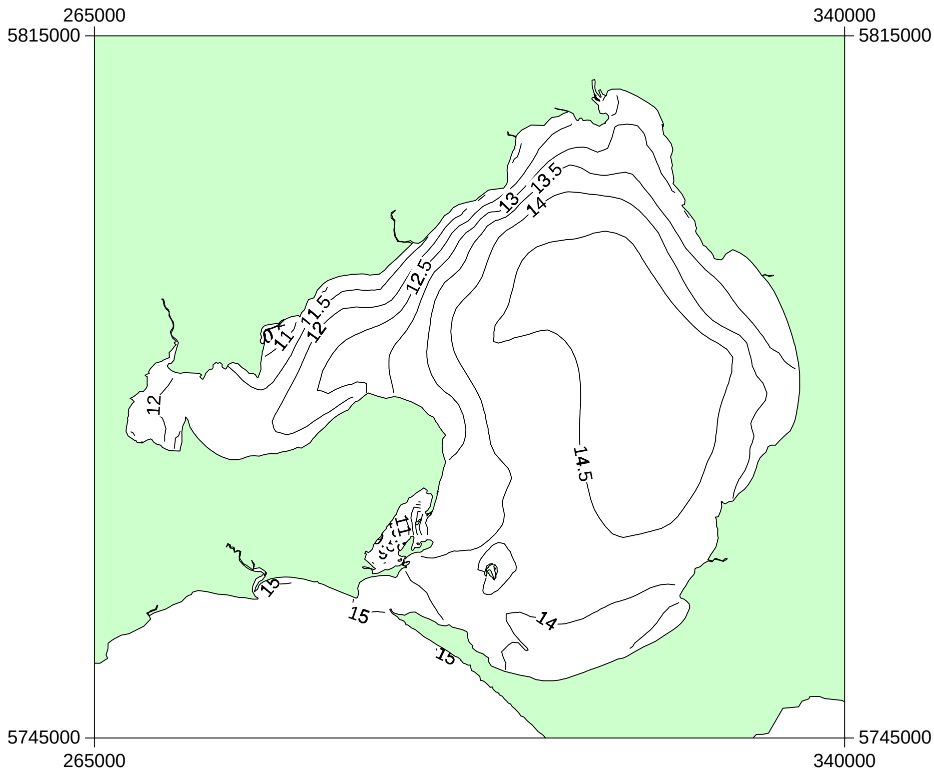

Figure 51: Surface (0-2m) temperature from model, 00:00 16 May 1994

.

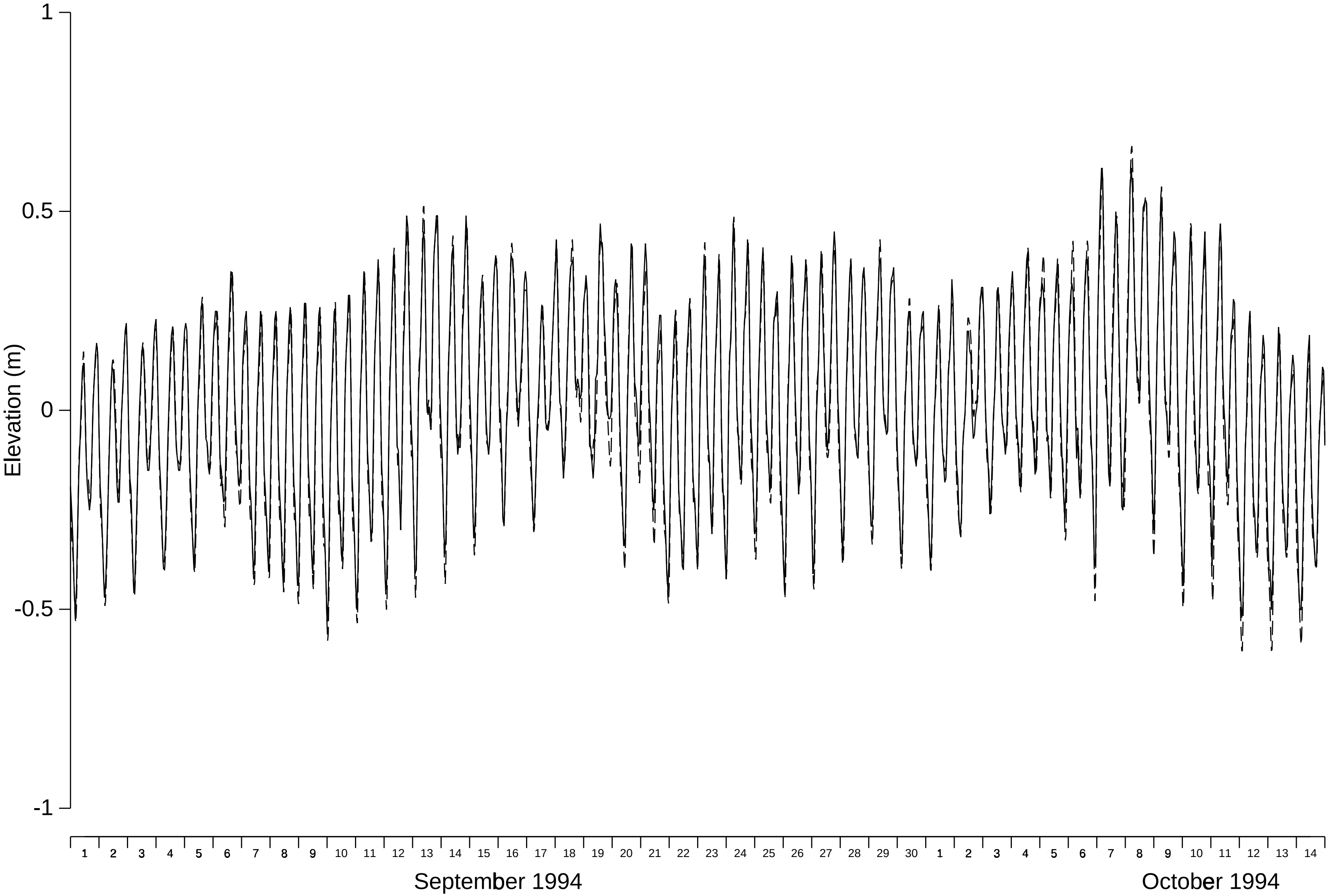

Figure 52: Measured (solid) and modelled (dashed) elevation at Geelong, September 1994

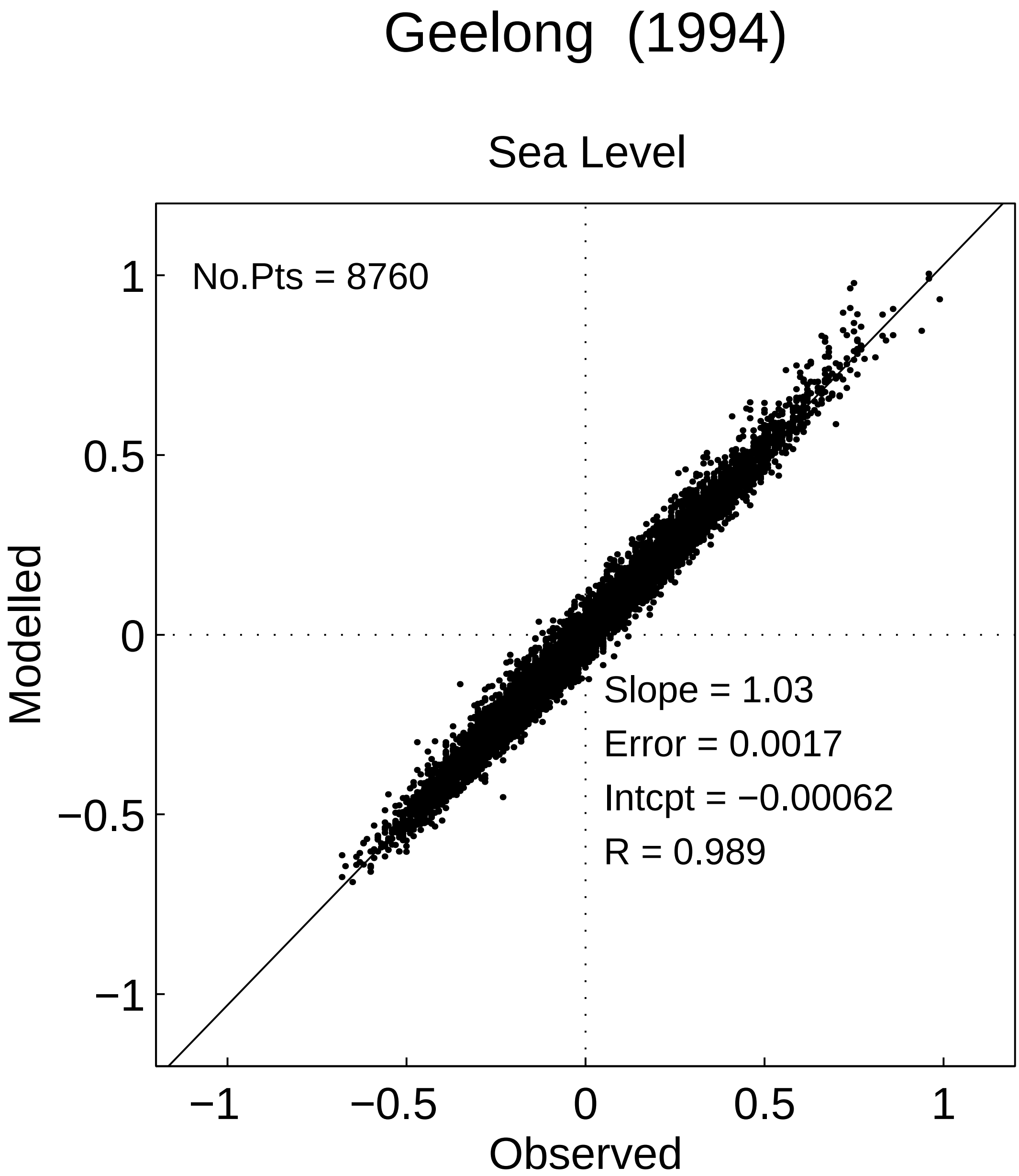

Figure 53: Scatter plot of hourly observed and modelled sea-level at Geelong, 1994

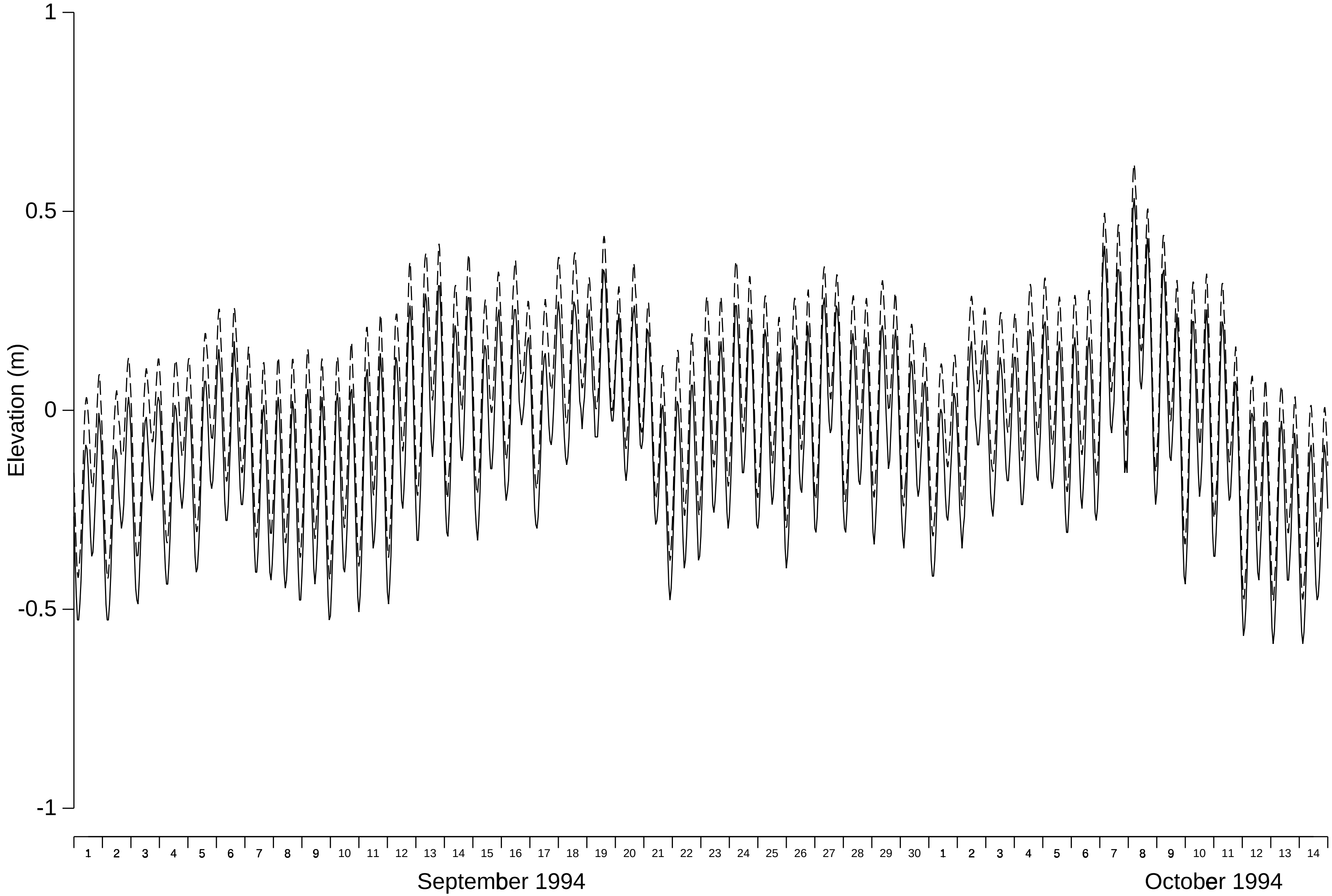

Figure 54: Measured (solid) and modelled (dashed) elevation at Hovell Pile, September 1994

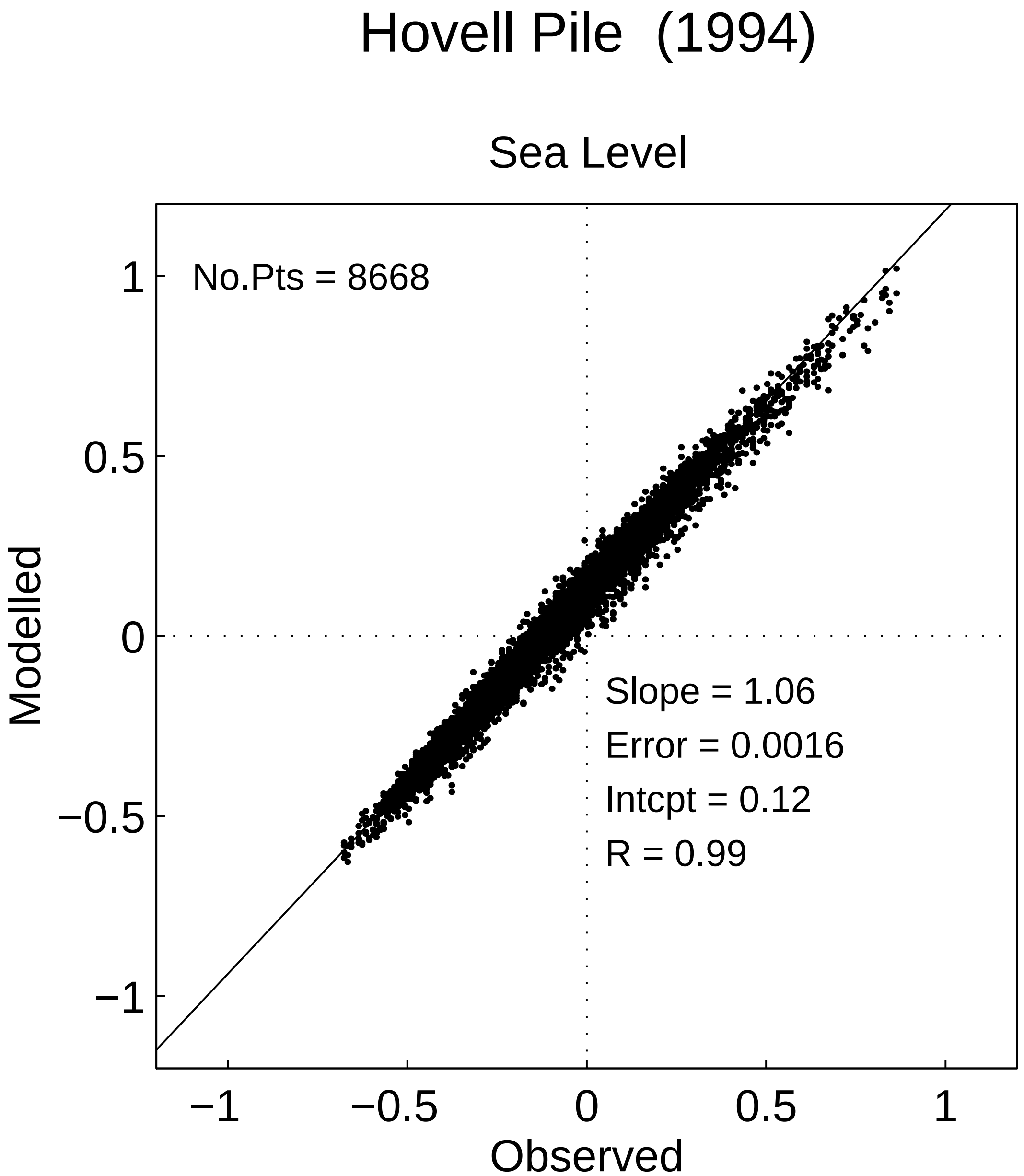

Figure 55: Scatter plot of hourly observed and modelled sea-level at Hovell Pile, 1994

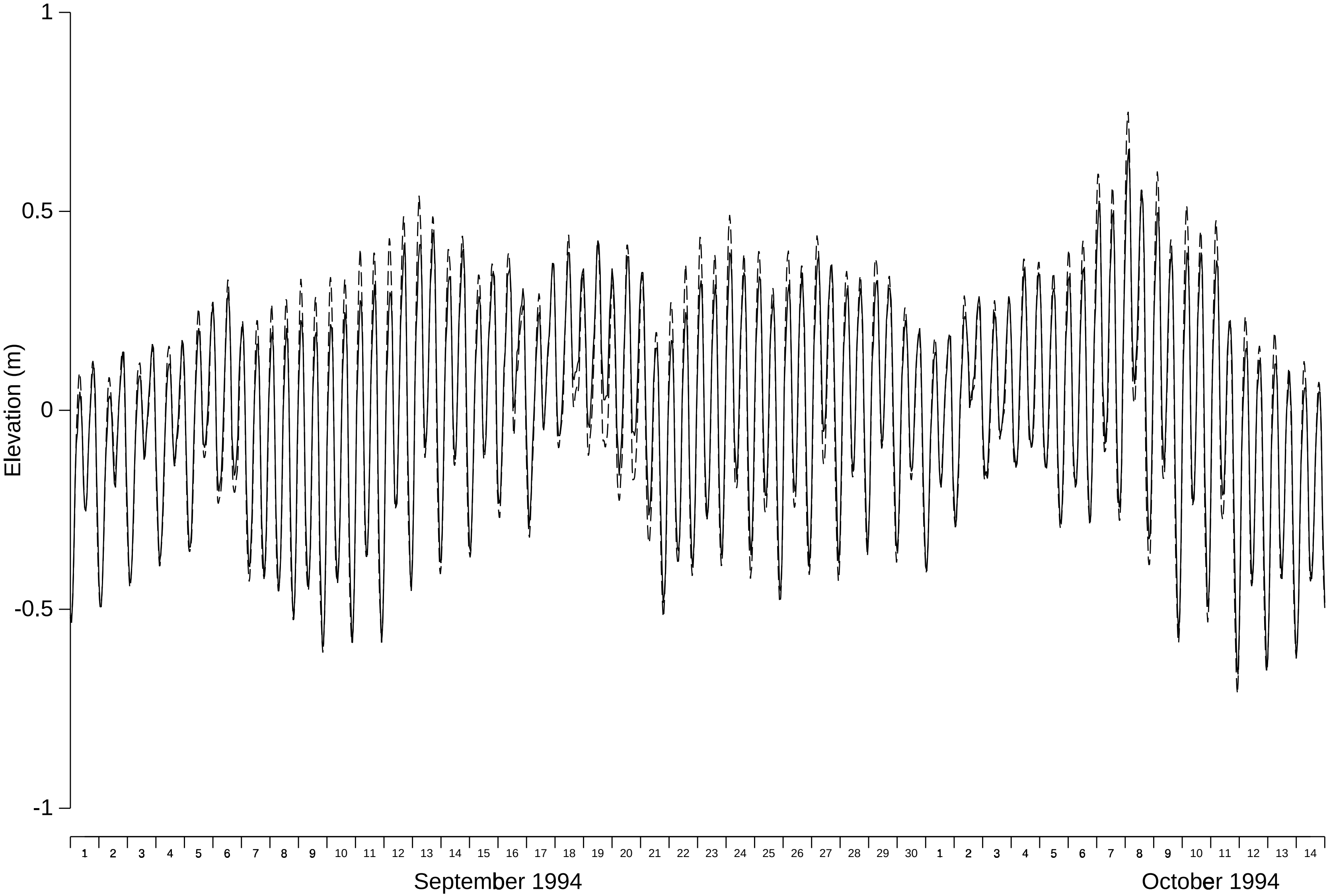

Figure 56: Measured (solid) and modelled (dashed) elevation at Queenscliff, September 1994

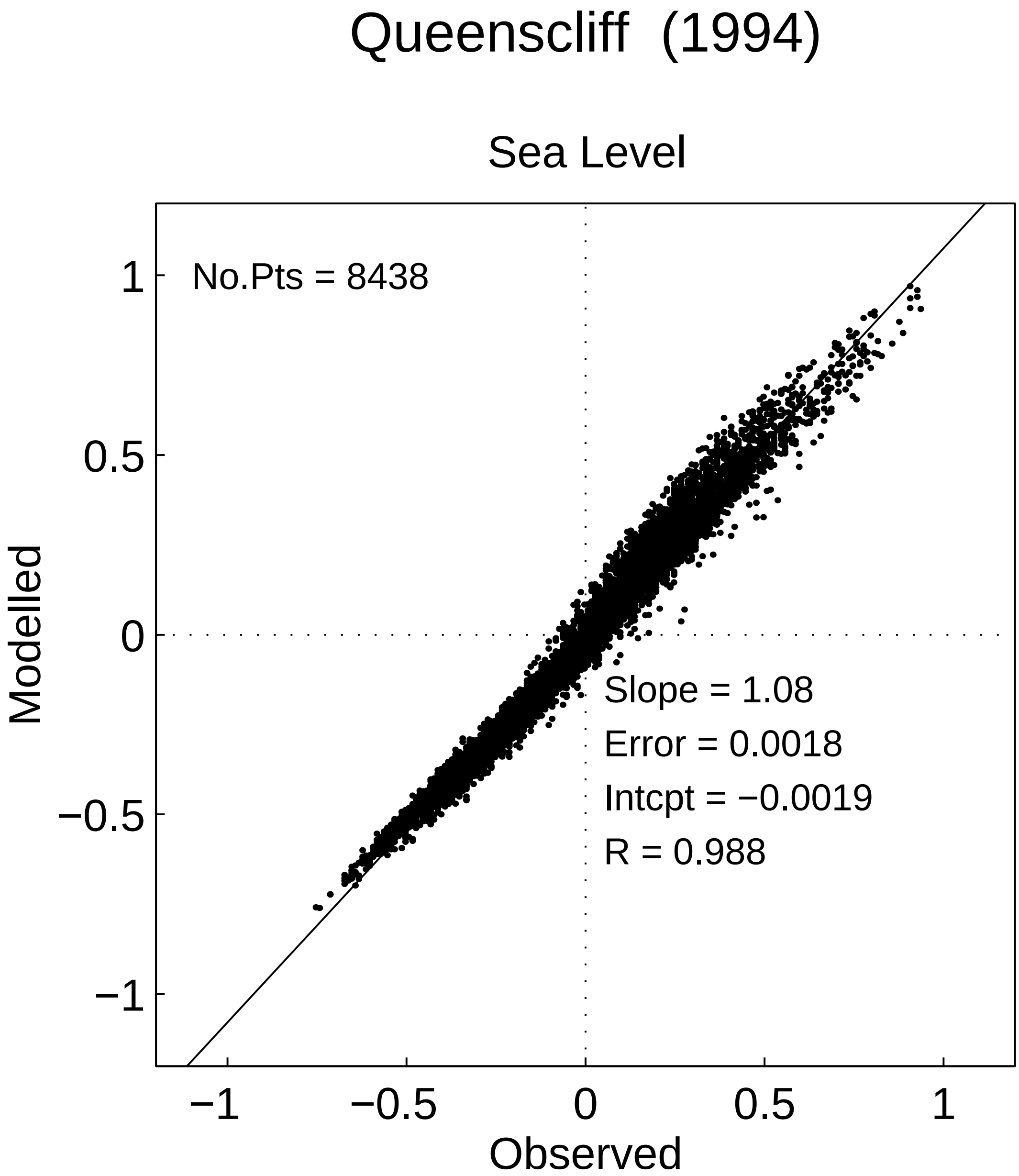

Figure 57: Scatter plot of hourly observed and modelled sea-level at Queenscliff, 1994

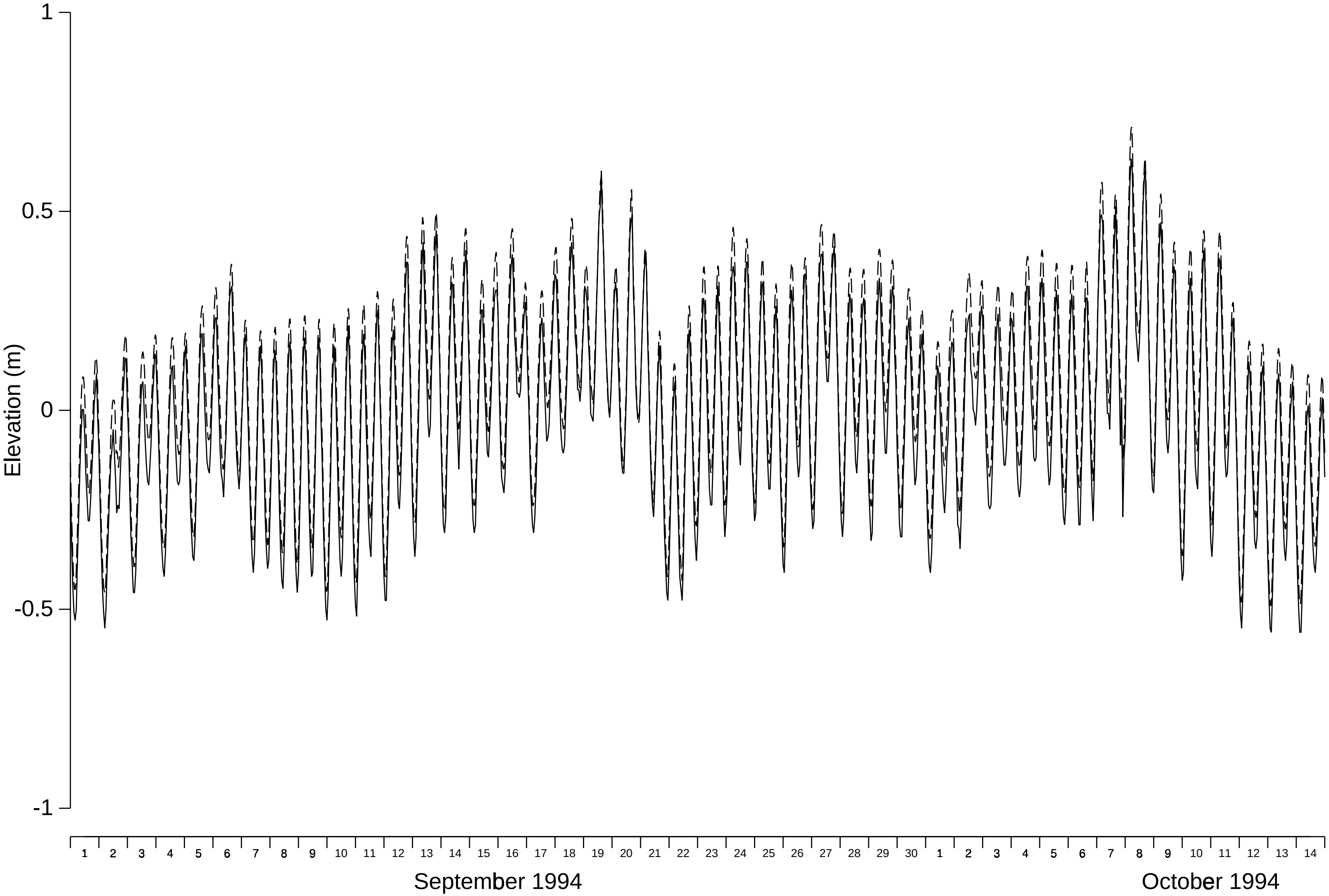

Figure 58: Measured (solid) and modelled (dashed) elevation at Victoria Dock, September 1994

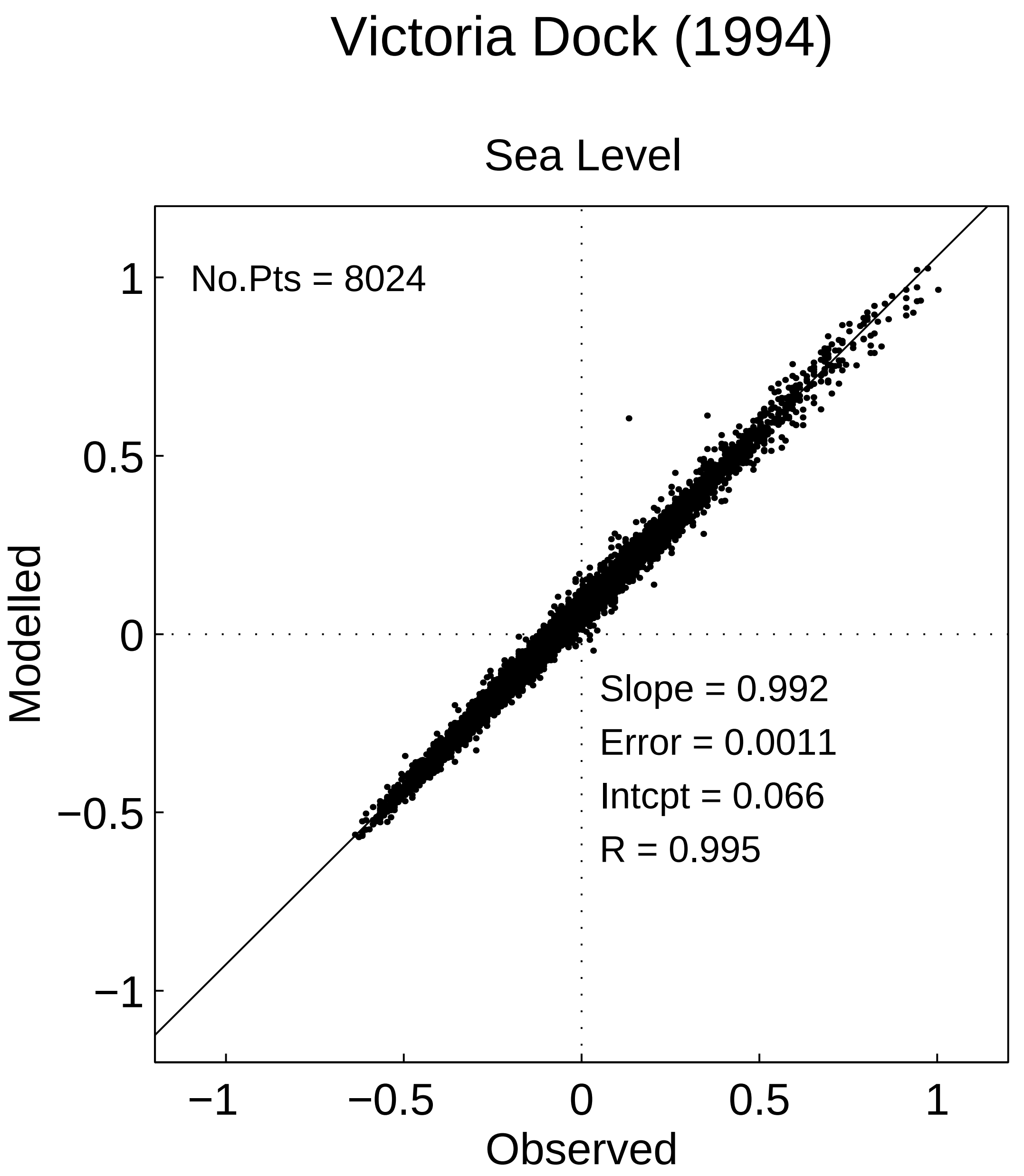

Figure 59: Scatter plot of hourly observed and modelled sea-level at Victoria Dock, 1994

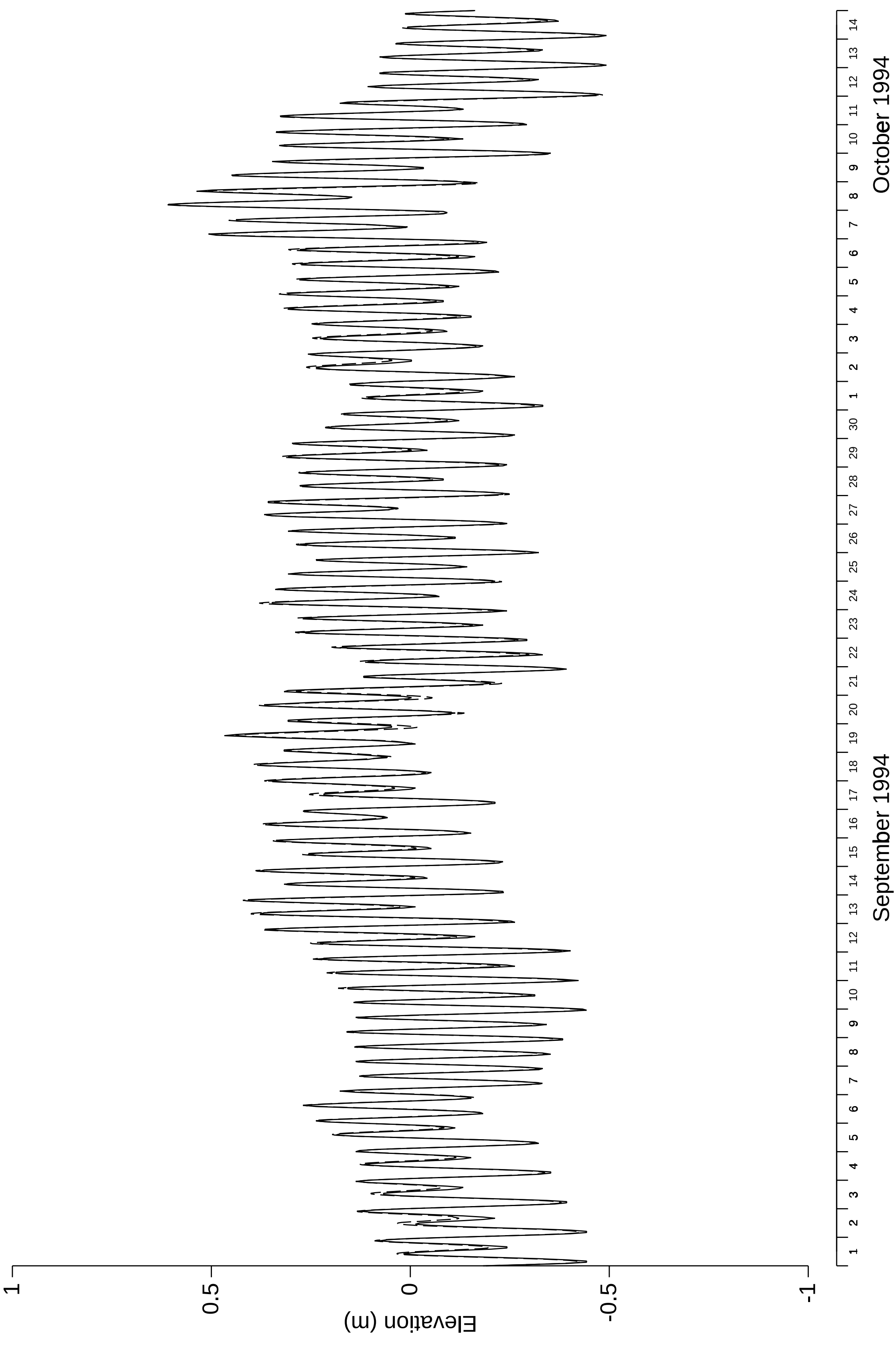

Figure 60: Measured (solid) and modelled (dashed) elevation at West Channel Pile, September 1994

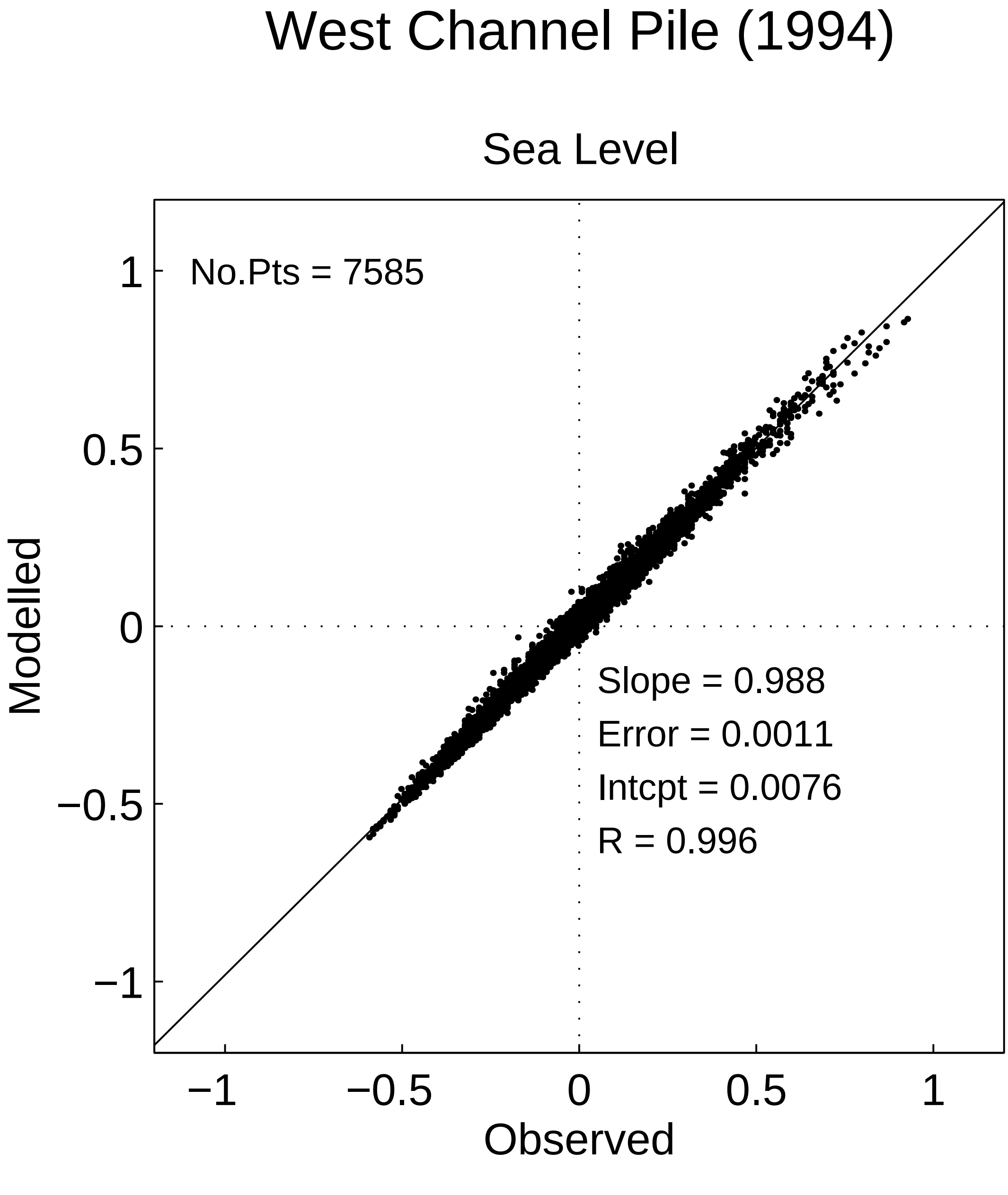

Figure 61: Scatter plot of hourly observed and modelled sea-level at West Channel Pile, 1994

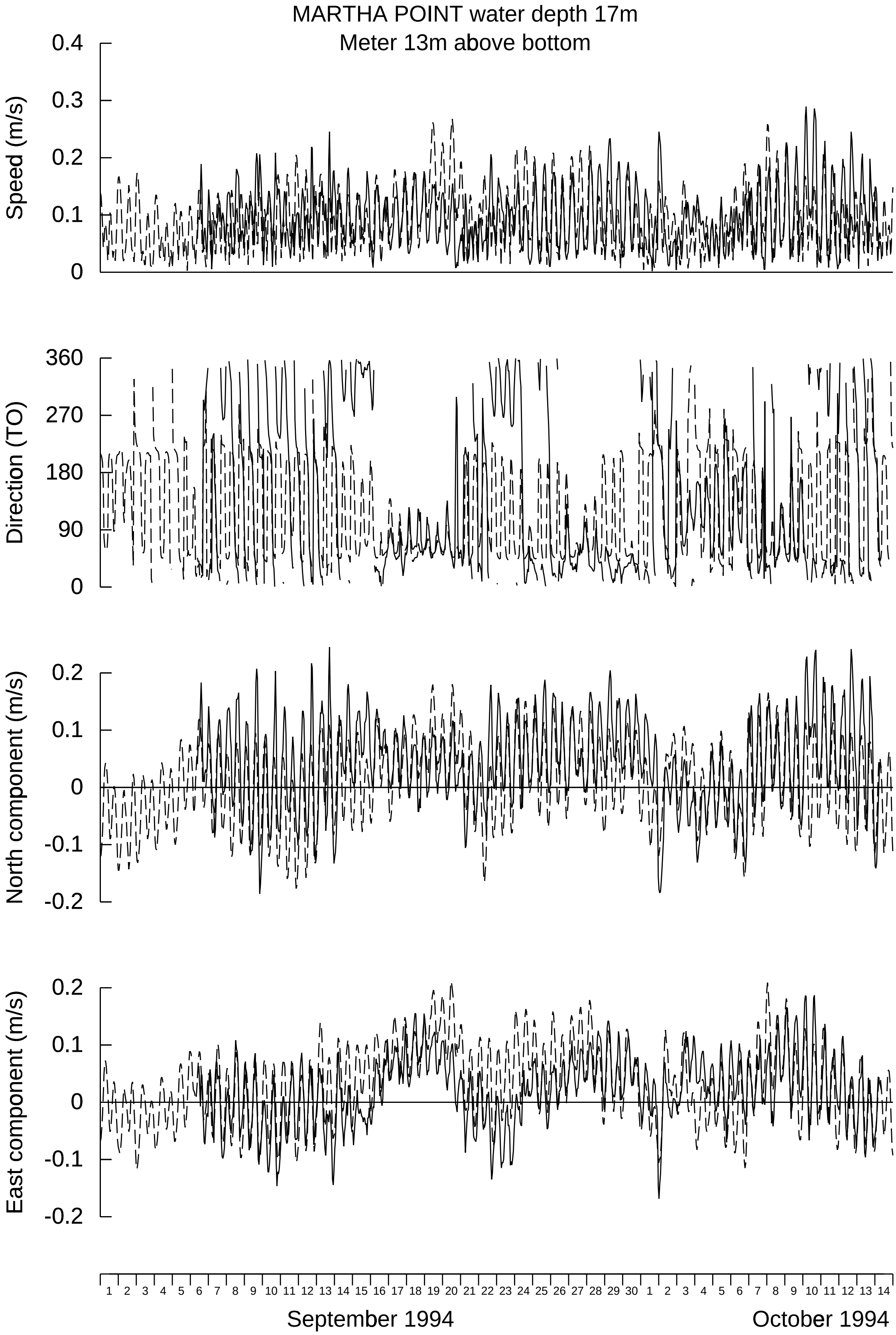

Figure 62: Measured (solid) and modelled (dashed) currents at the Martha Point site, upper meter, September-October 1994.

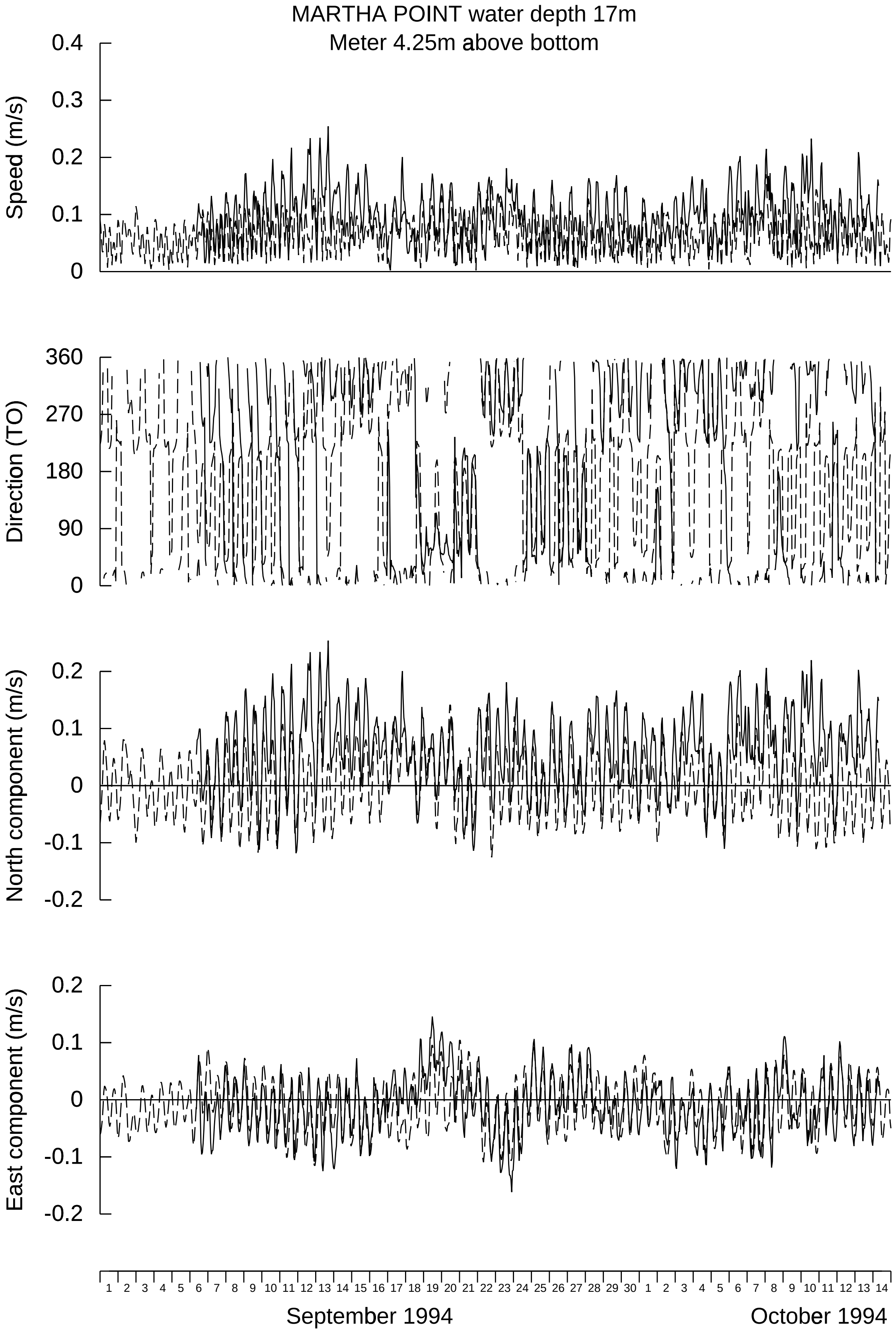

Figure 63: Measured (solid) and modelled (dashed) currents at the Martha Point site, lower meter, September-October 1994.

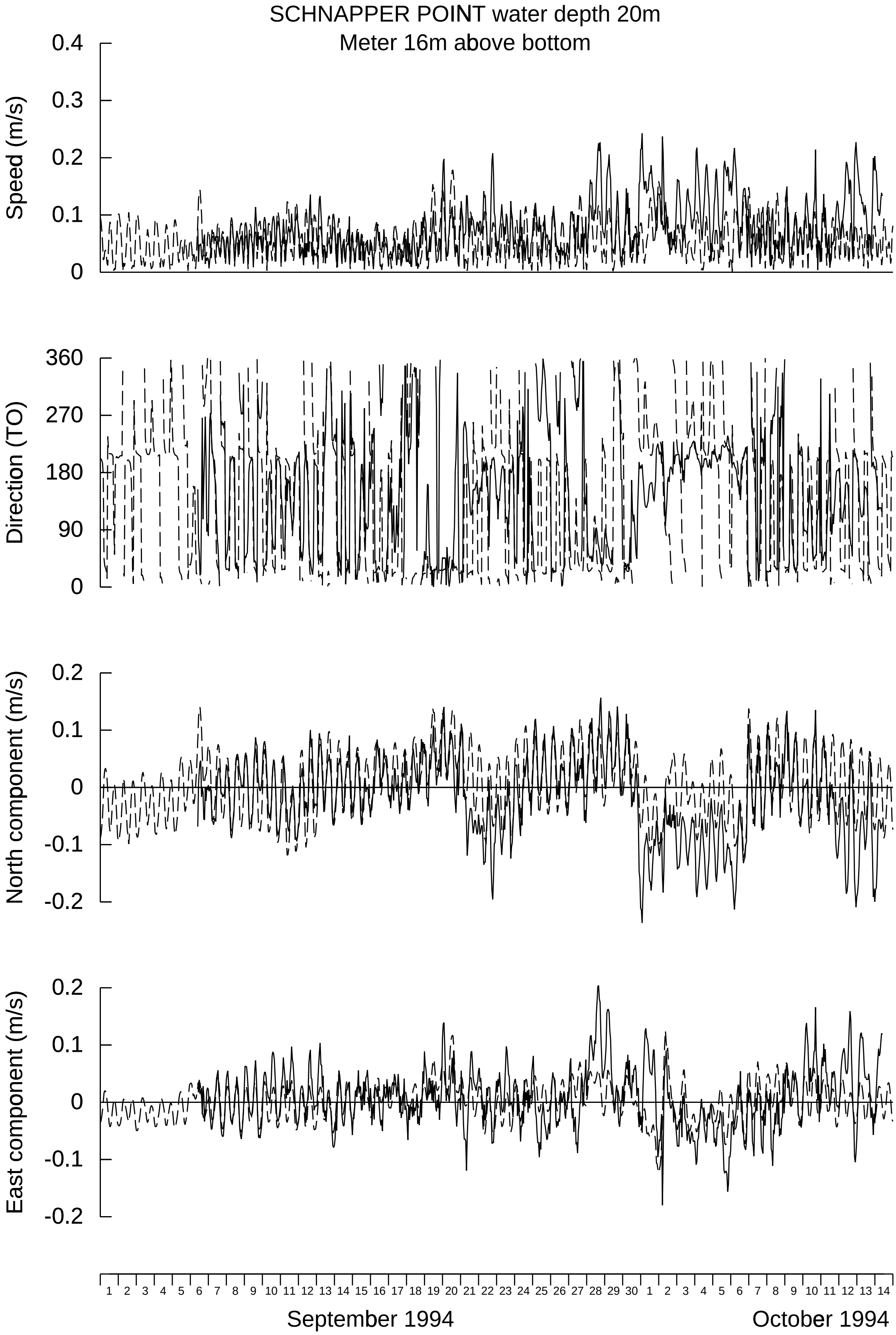

Figure 64: Measured (solid) and modelled (dashed) currents at the Great Sands site, upper meter, September-October 1994.

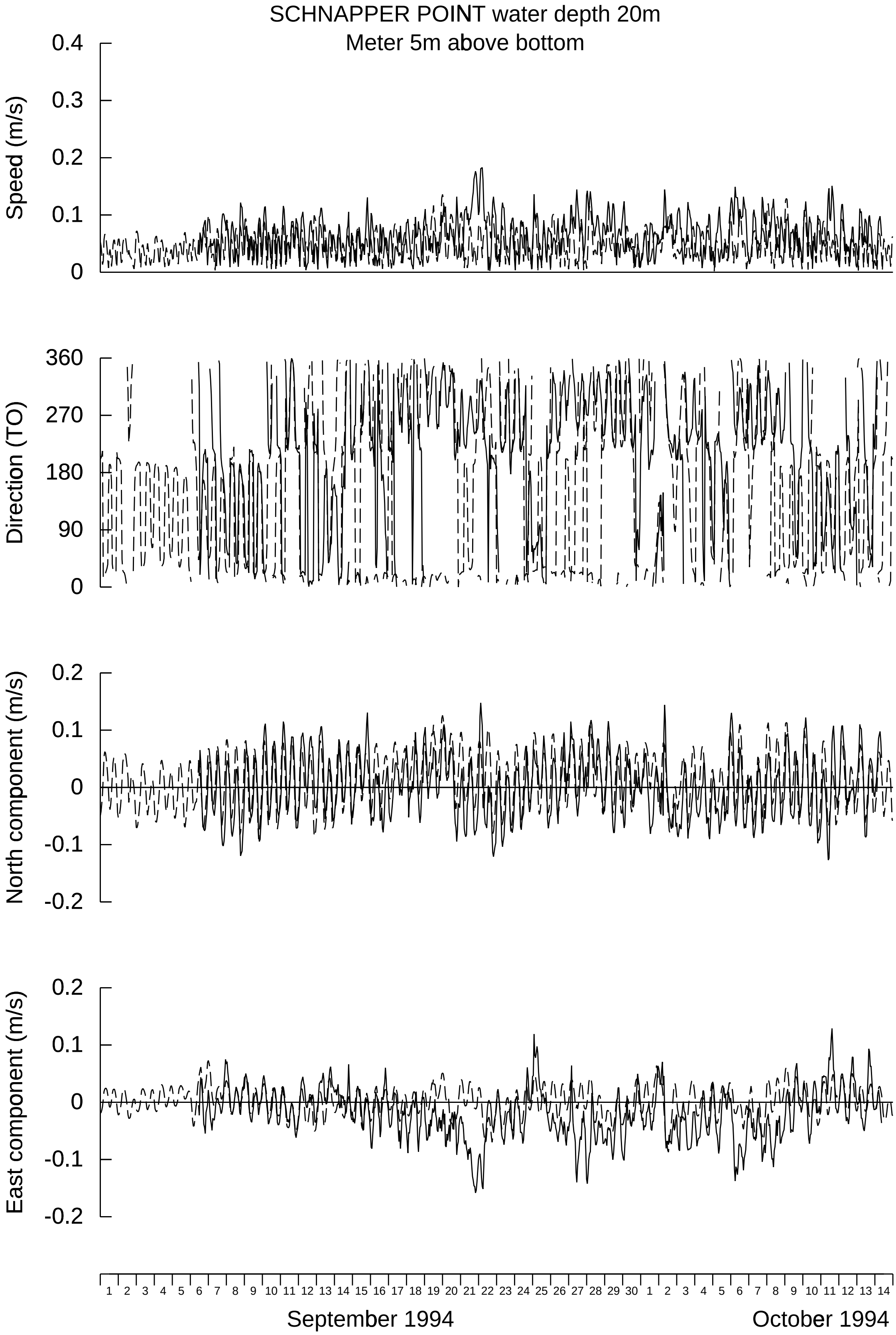

Figure 65: Measured (solid) and modelled (dashed) currents at the Great Sands site, lower meter, September-October 1994.

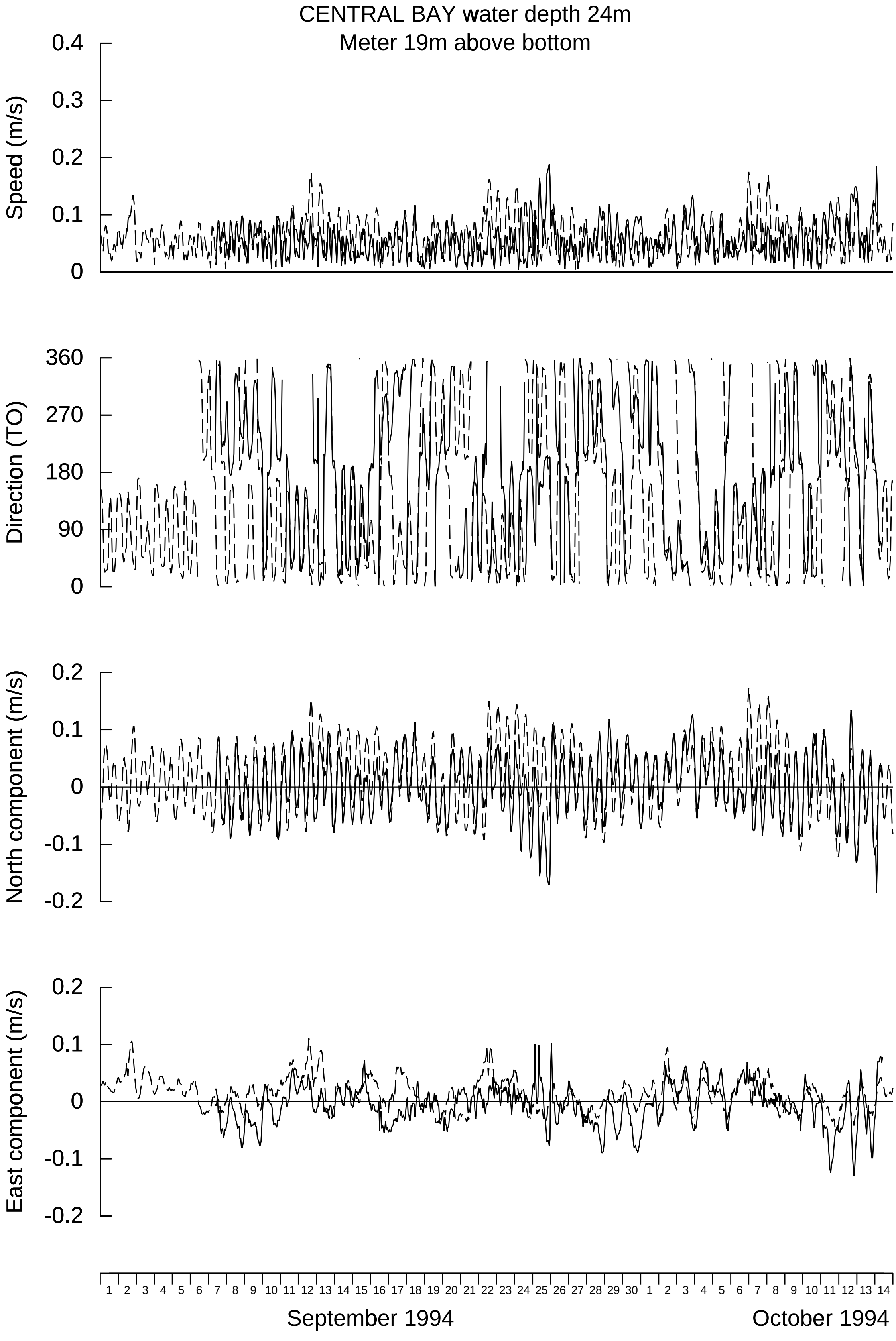

Figure 66: Measured (solid) and modelled (dashed) currents at the Central Bay site, upper meter, September-October 1994.

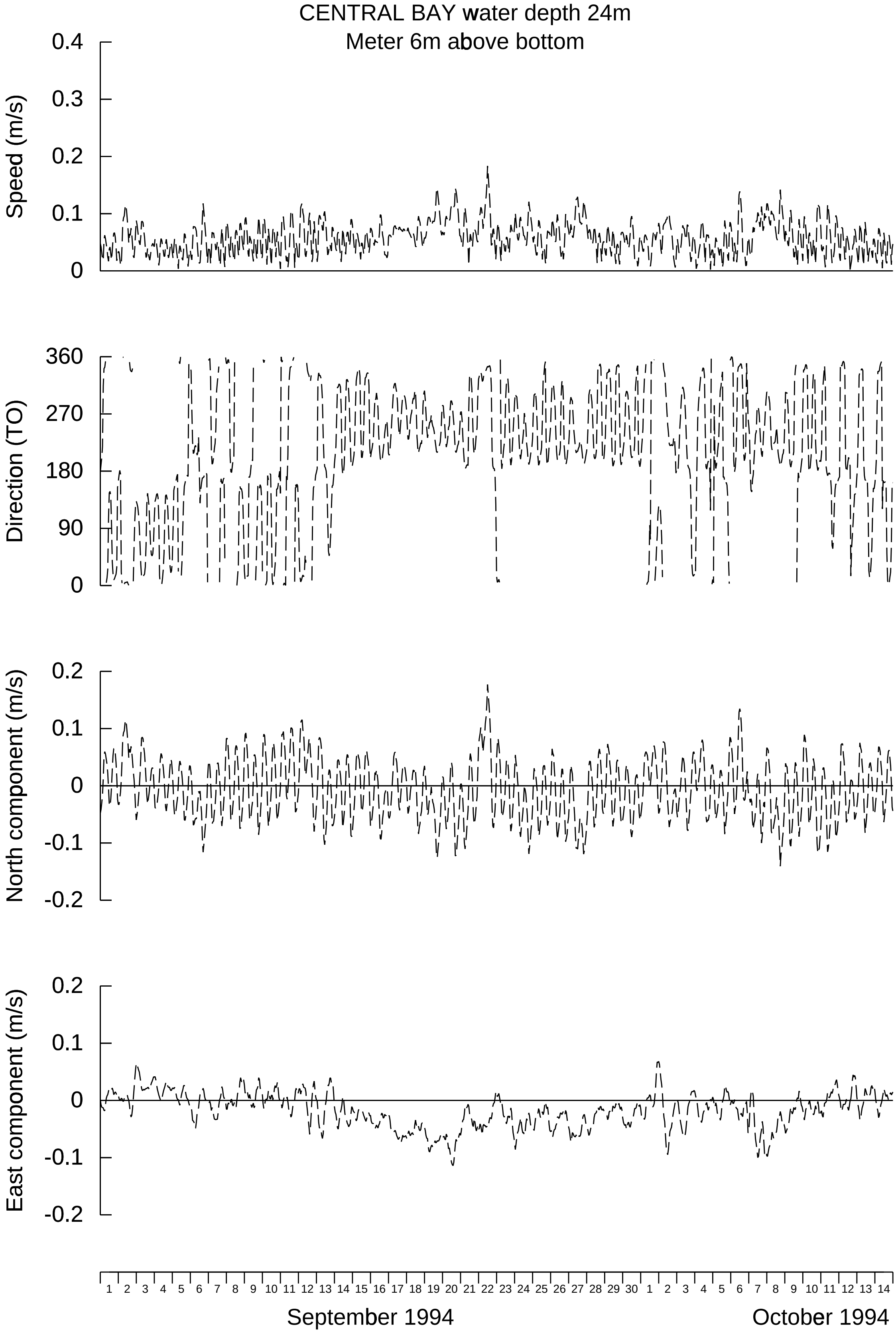

Figure 67: Modelled currents at the Central Bay site, lower meter, September-October 1994. No data was recovered from the meter at this site.

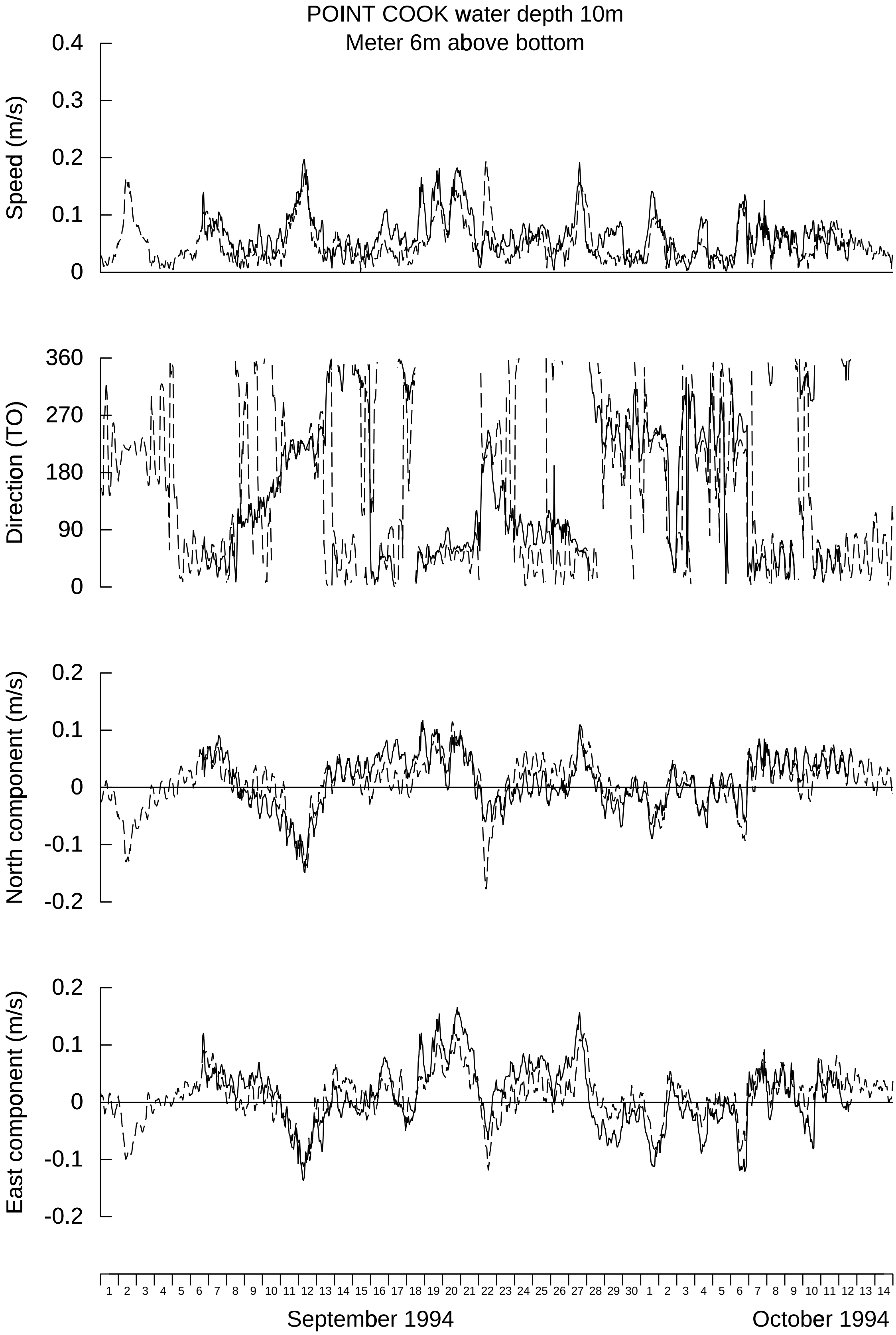

Figure 68: Measured (solid) and modelled (dashed) currents at the Point Cook site, upper meter, September-October 1994.

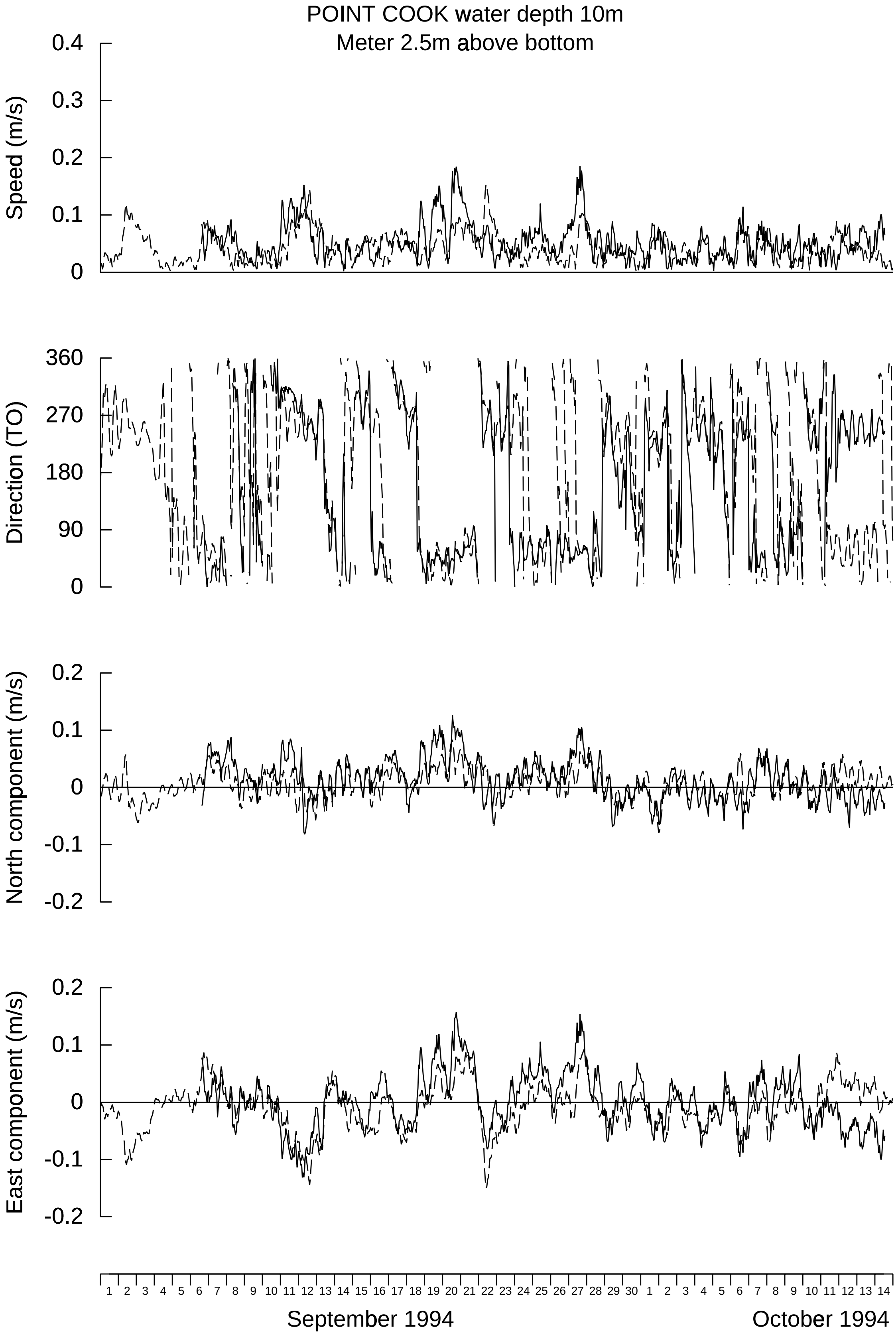

Figure 69: Measured (solid) and modelled (dashed) currents at the Point Cook site, lower meter, September-October 1994.

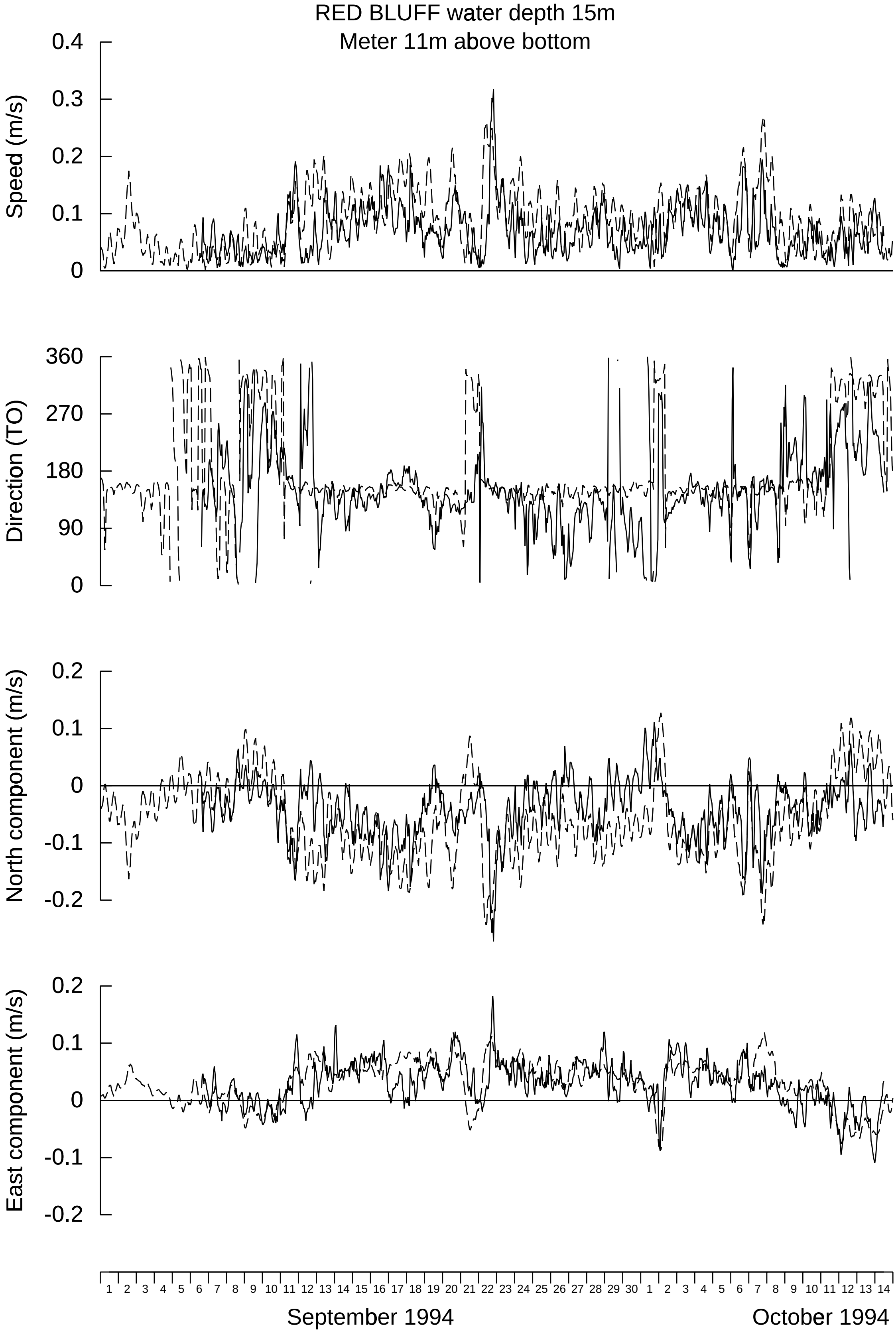

Figure 70: Measured (solid) and modelled (dashed) currents at the Red Bluff site, upper meter, September-October 1994.

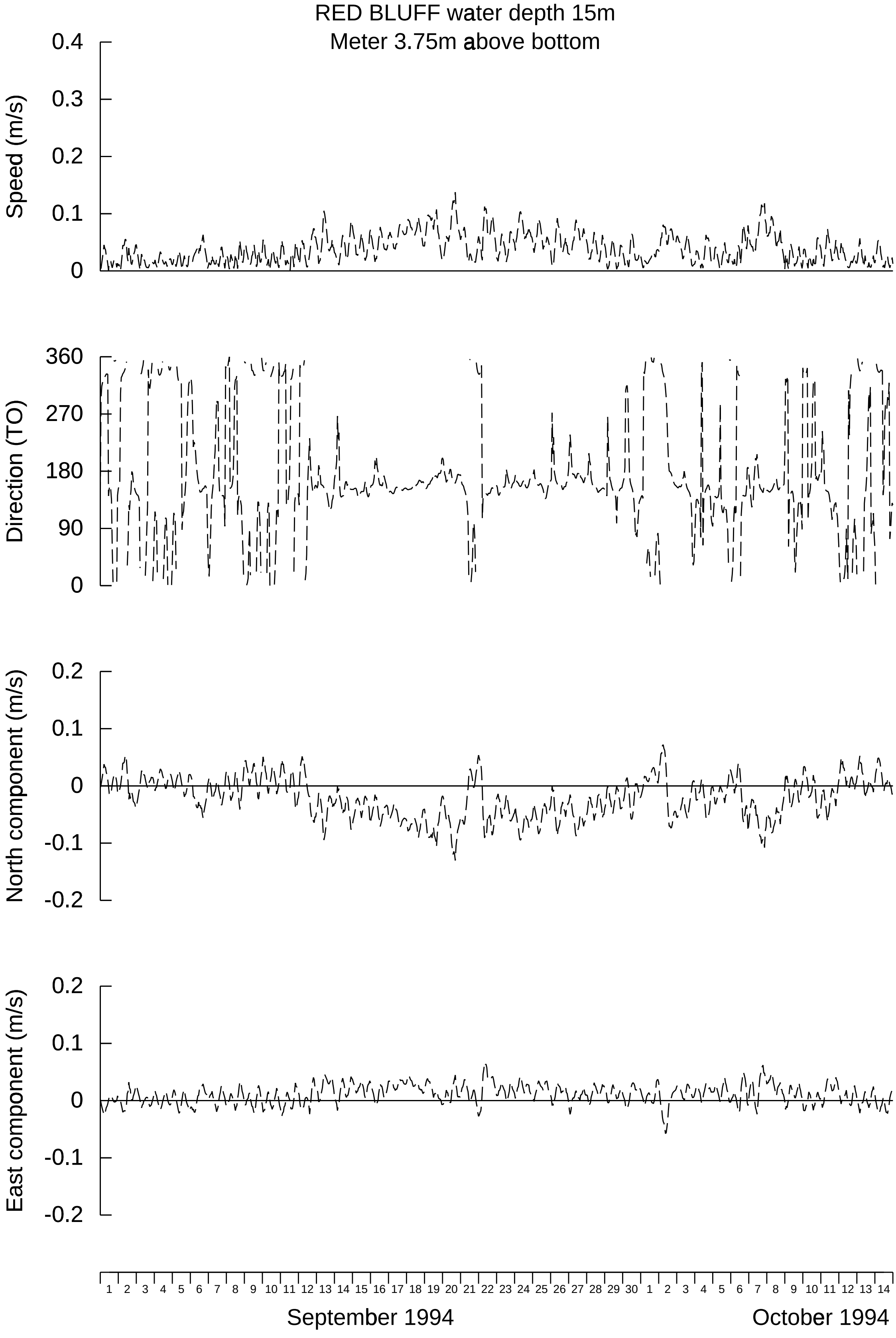

Figure 71: Modelled currents at the Red Bluff site, lower meter, September-October 1994. No data was recovered from the meter at this site.

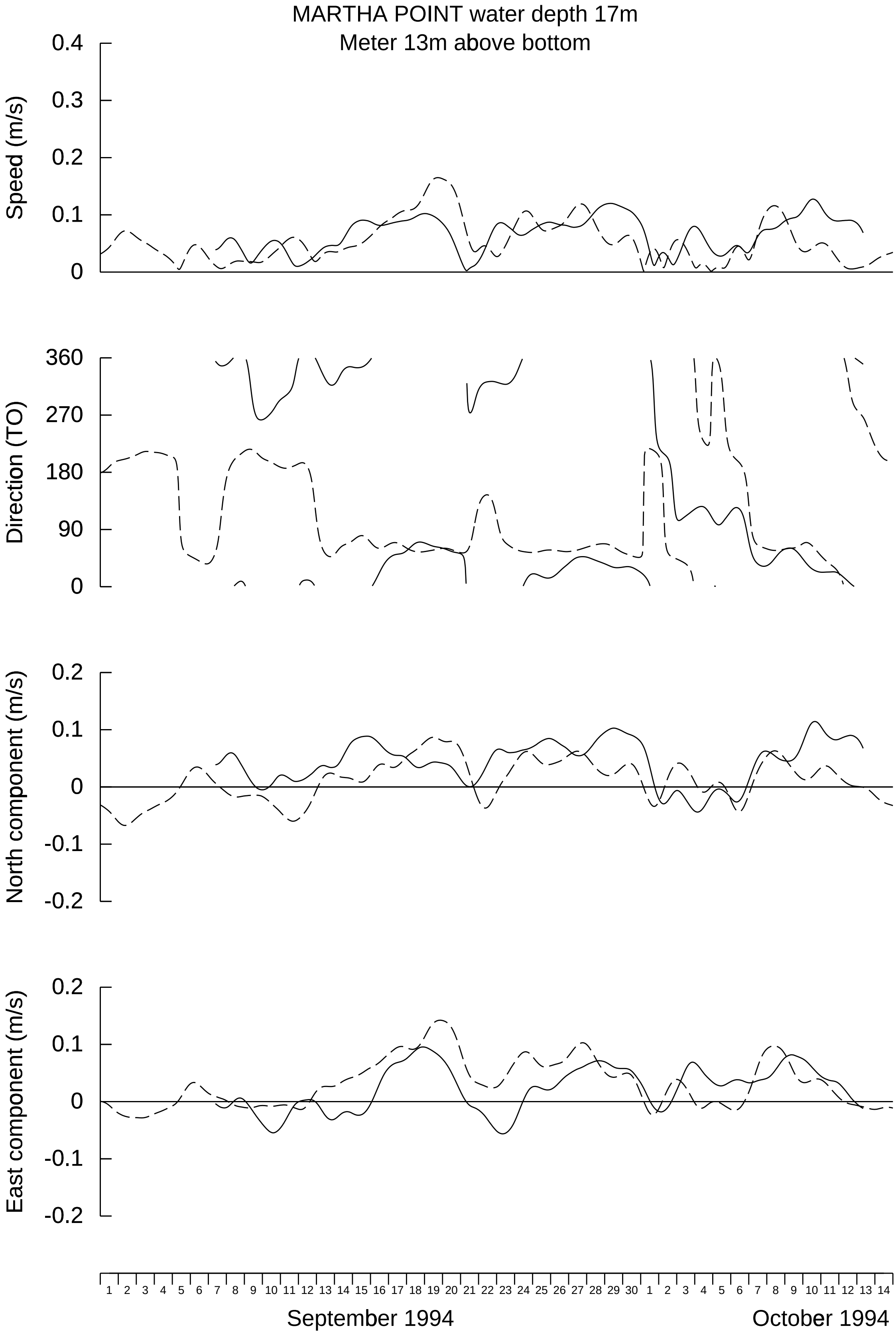

Figure 72: Measured (solid) and modelled (dashed) low pass filtered currents at the Martha Point site, upper meter, September-October 1994.

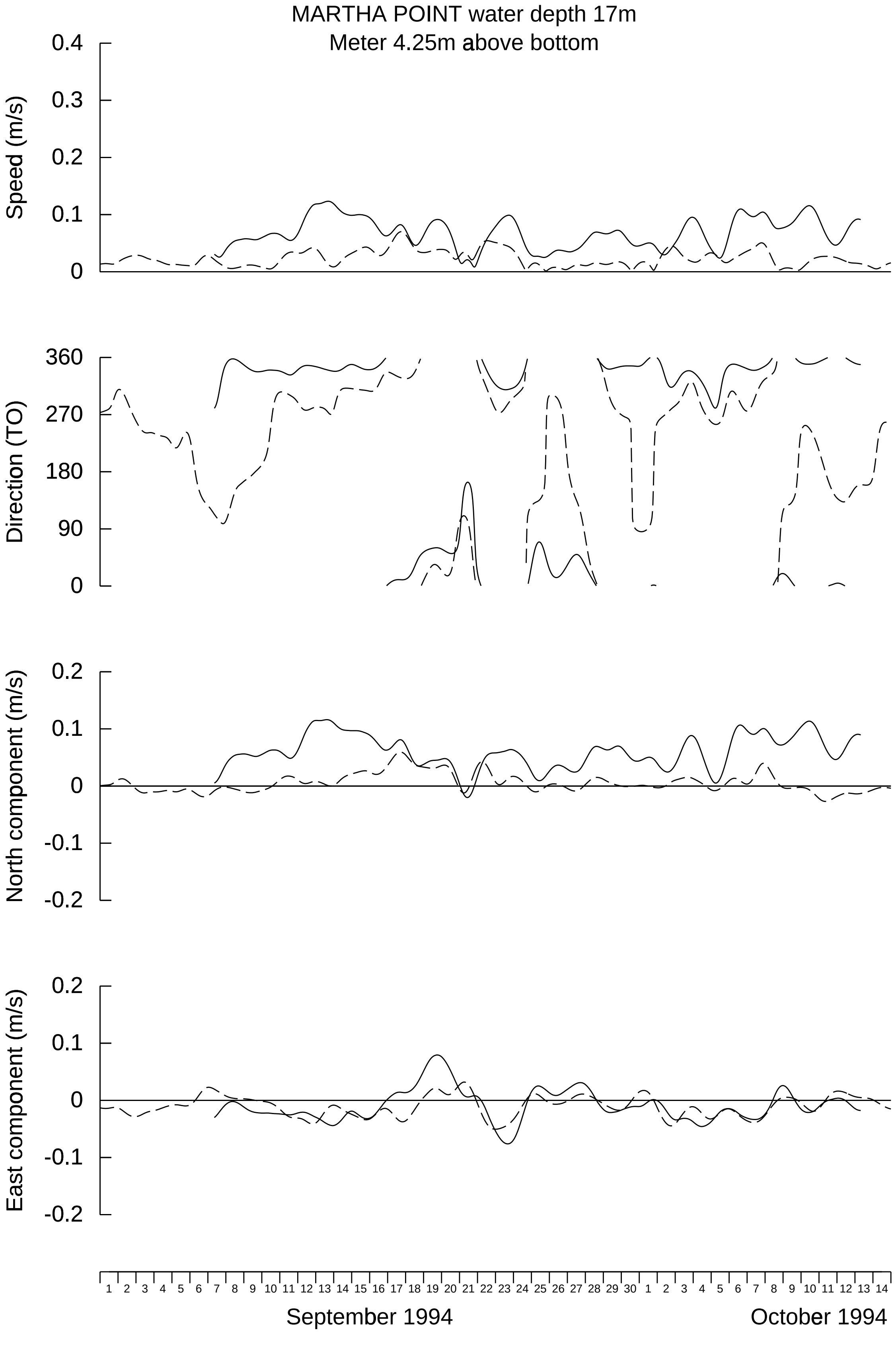

Figure 73: Measured (solid) and modelled (dashed) low pass filtered currents at the Martha Point site, lower meter, September-October 1994.

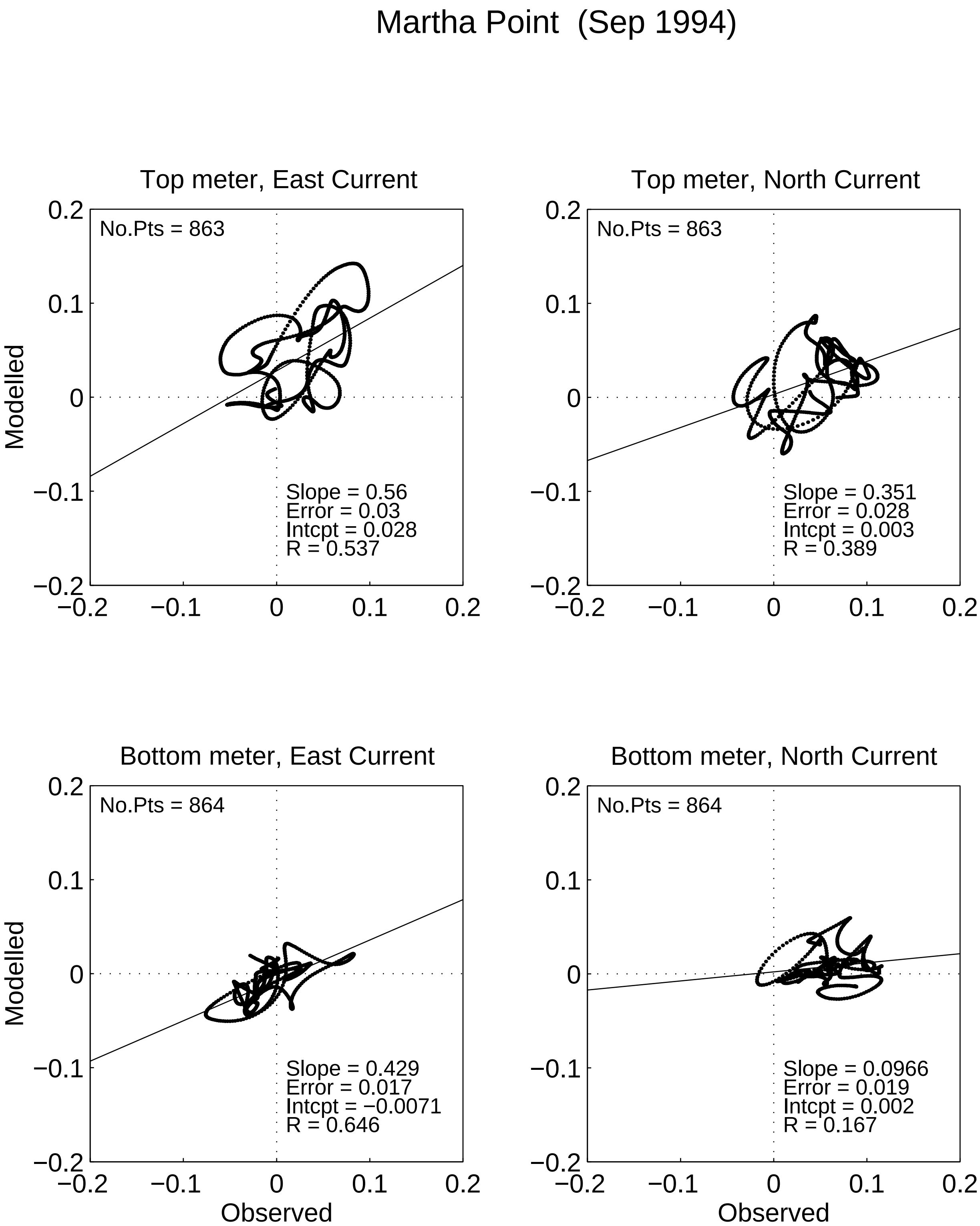

Figure 74: Observed (x-axis) versus modelled (y-axis) low pass filtered current components for the Martha Point mooring, September-October 1994.

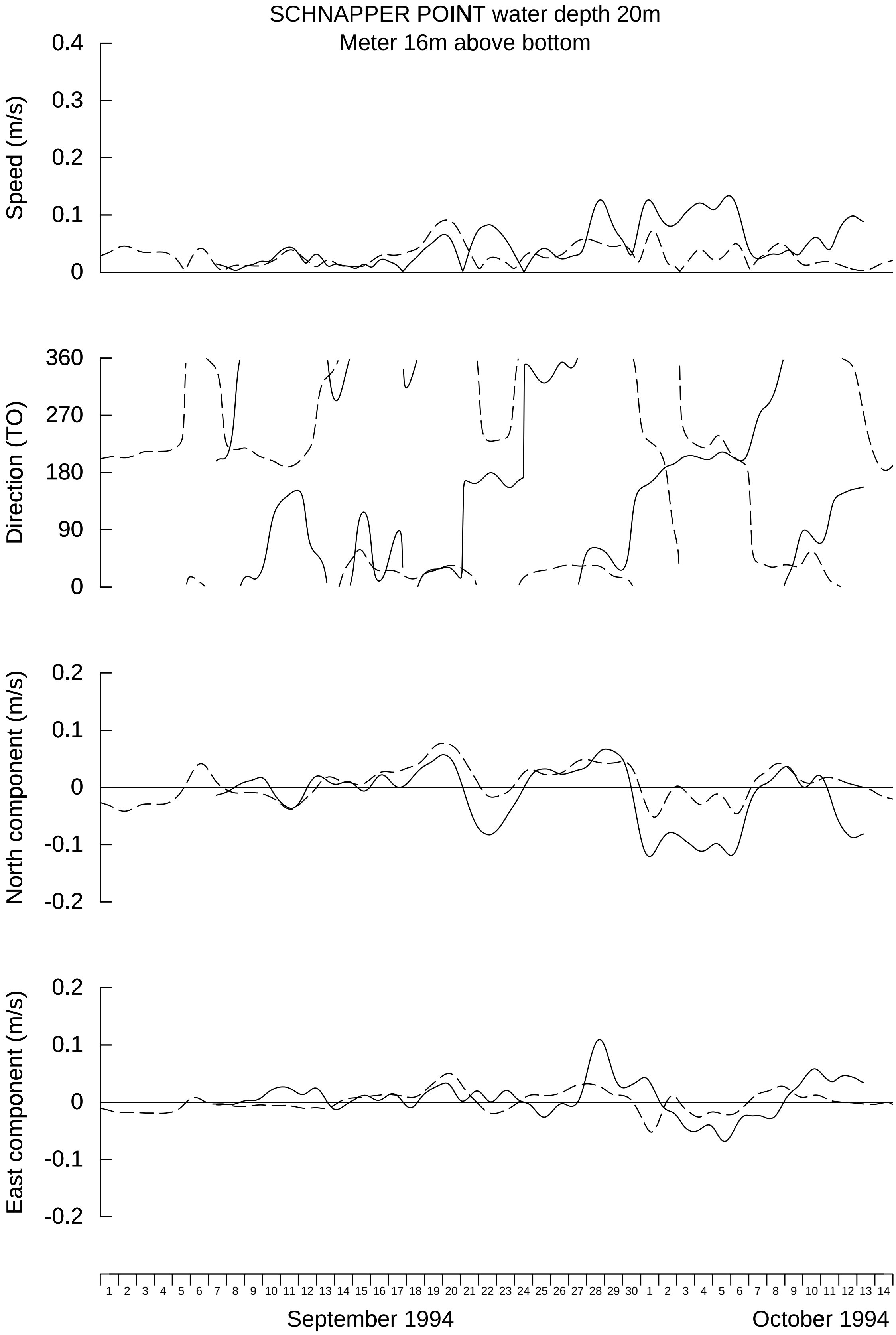

Figure 75: Measured (solid) and modelled (dashed) low pass filtered currents at the Great Sands site, upper meter, September-October 1994.

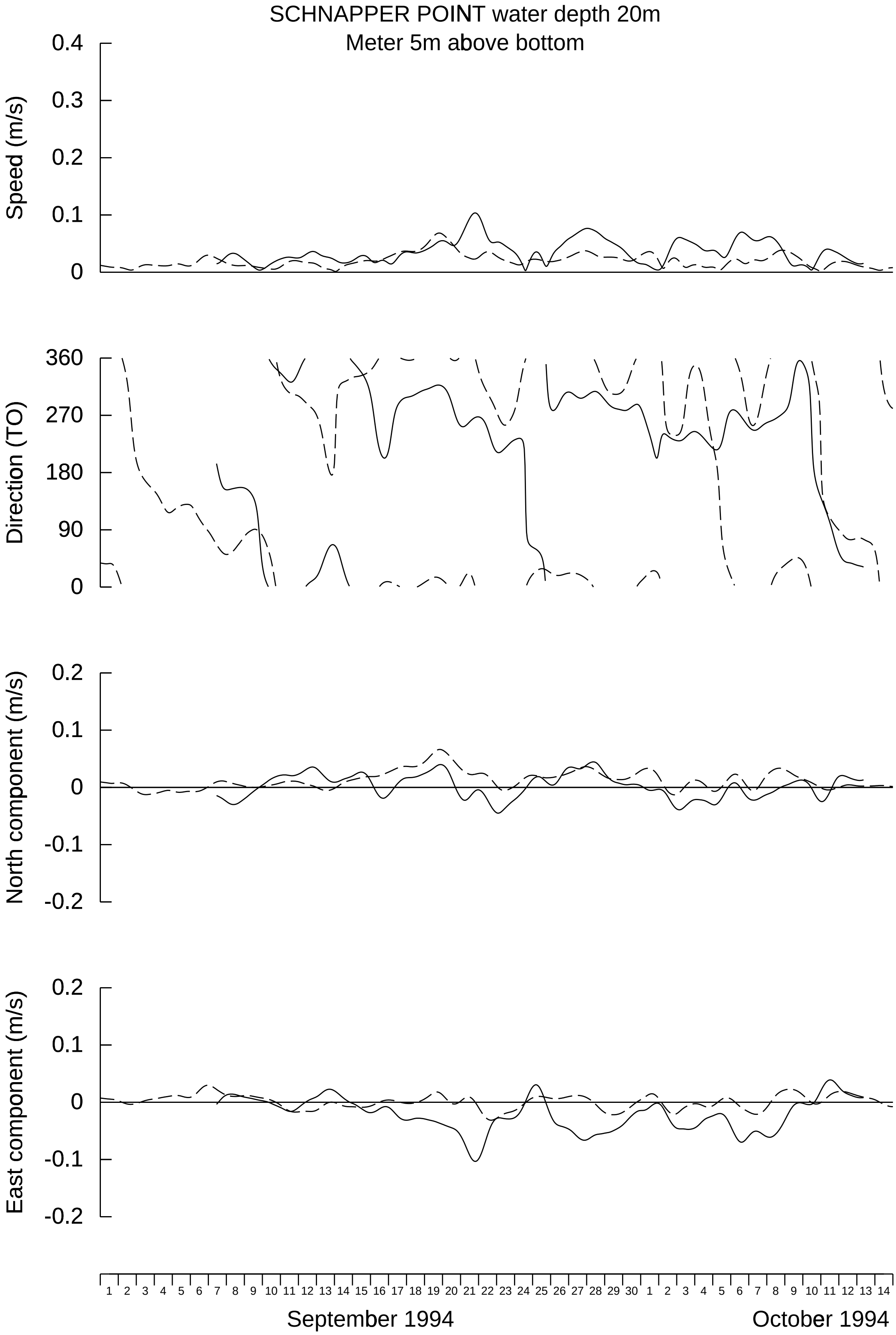

Figure 76: Measured (solid) and modelled (dashed) low pass filtered currents at the Great Sands site, lower meter, September-October 1994.

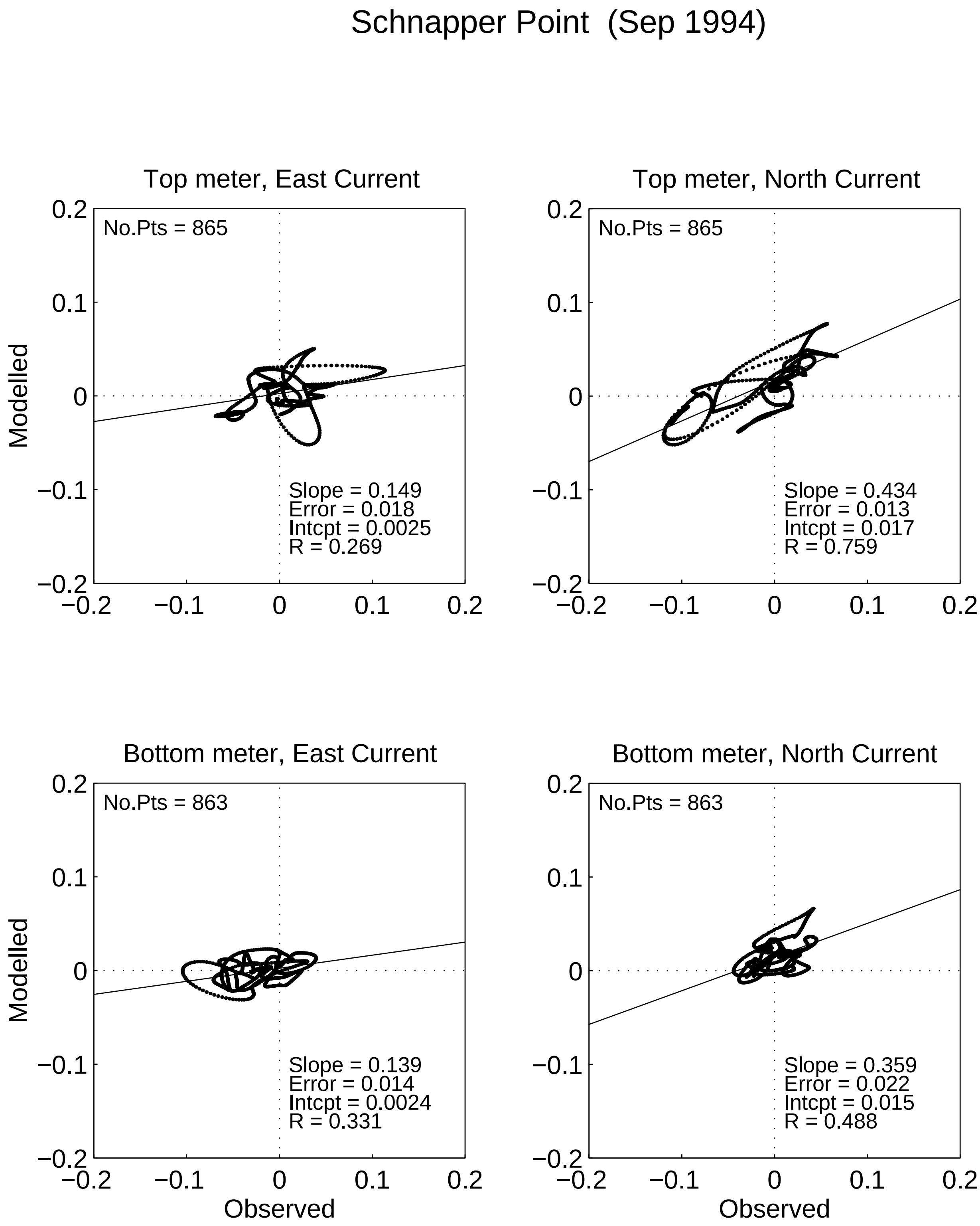

Figure 77: Observed (x-axis) versus modelled (y-axis) low pass filtered current components for the Schnapper Point mooring, September-October 1994.

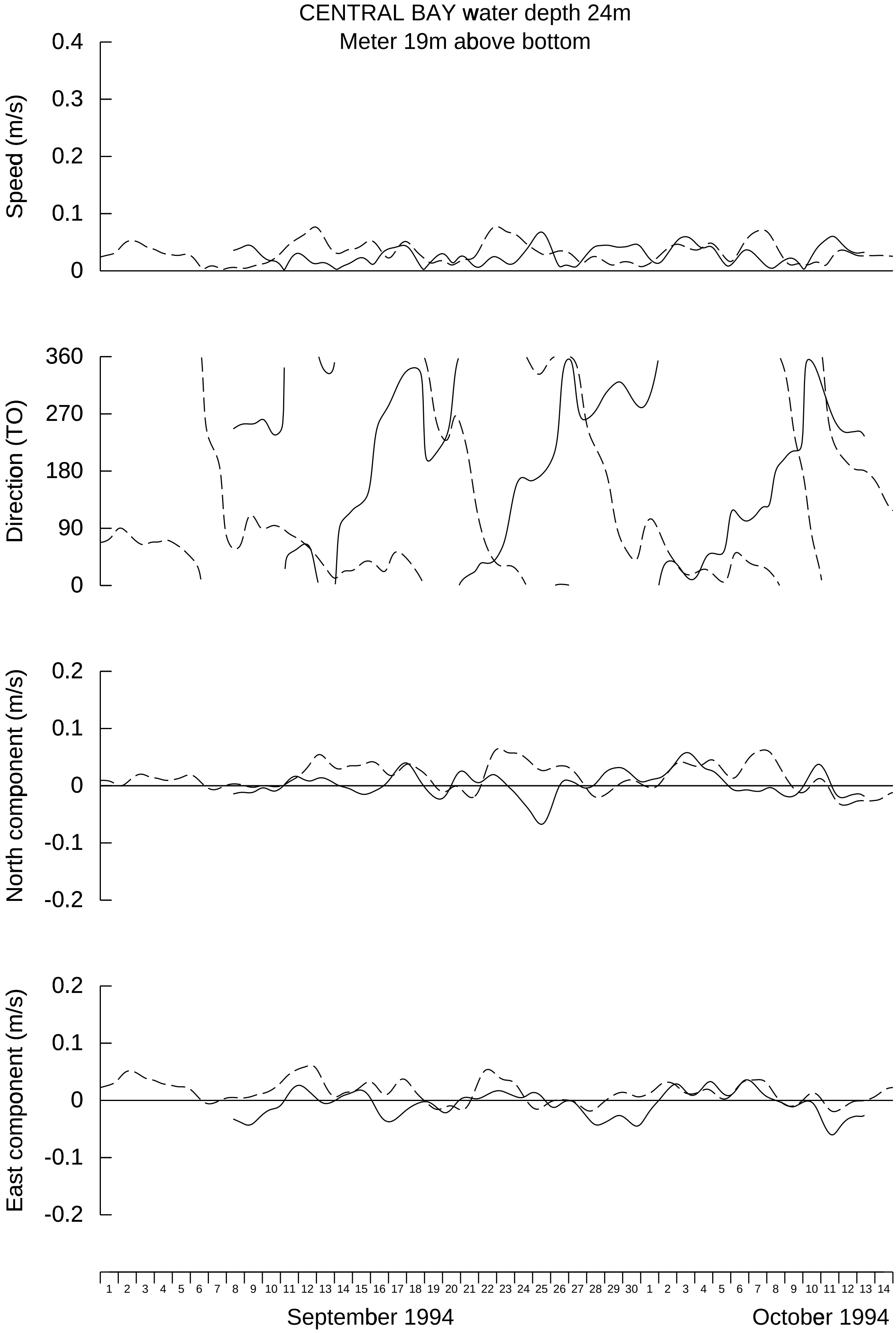

Figure 78: Measured (solid) and modelled (dashed) low pass filtered currents at the Central Bay site, upper meter, September-October 1994.

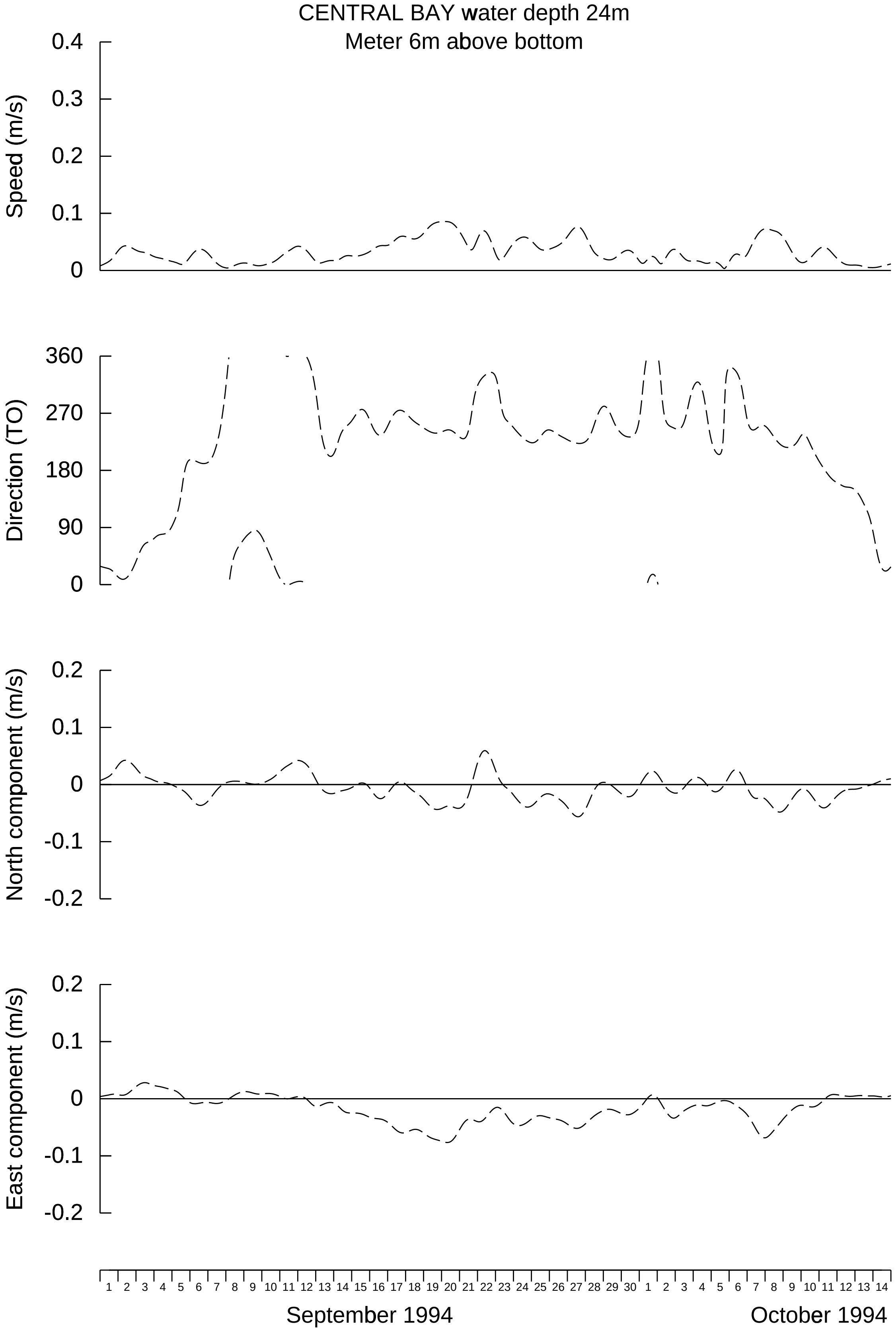

Figure 79: Modelled low pass filtered currents at the Central Bay site, lower meter, September-October 1994. No data was recovered from the meter at this site.

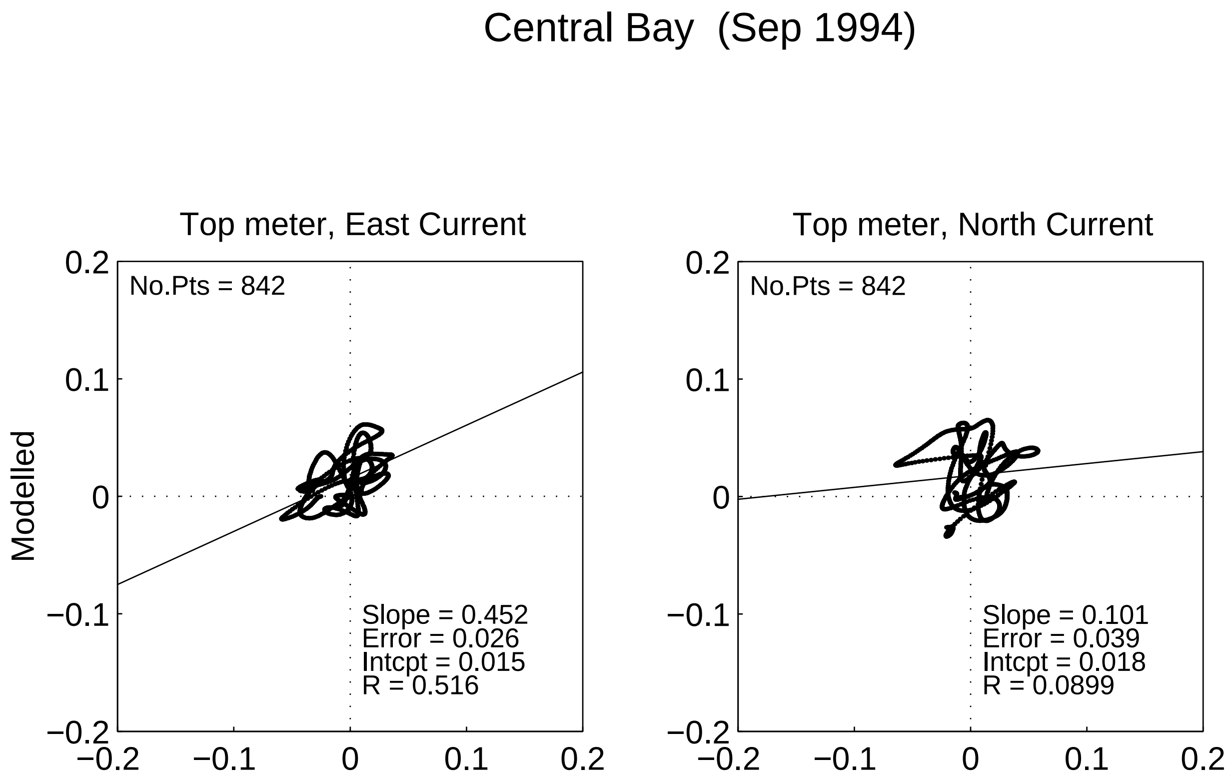

Figure 80: Observed (x-axis) versus modelled (y-axis) low pass filtered current components for the Central Bay mooring, September-October 1994.

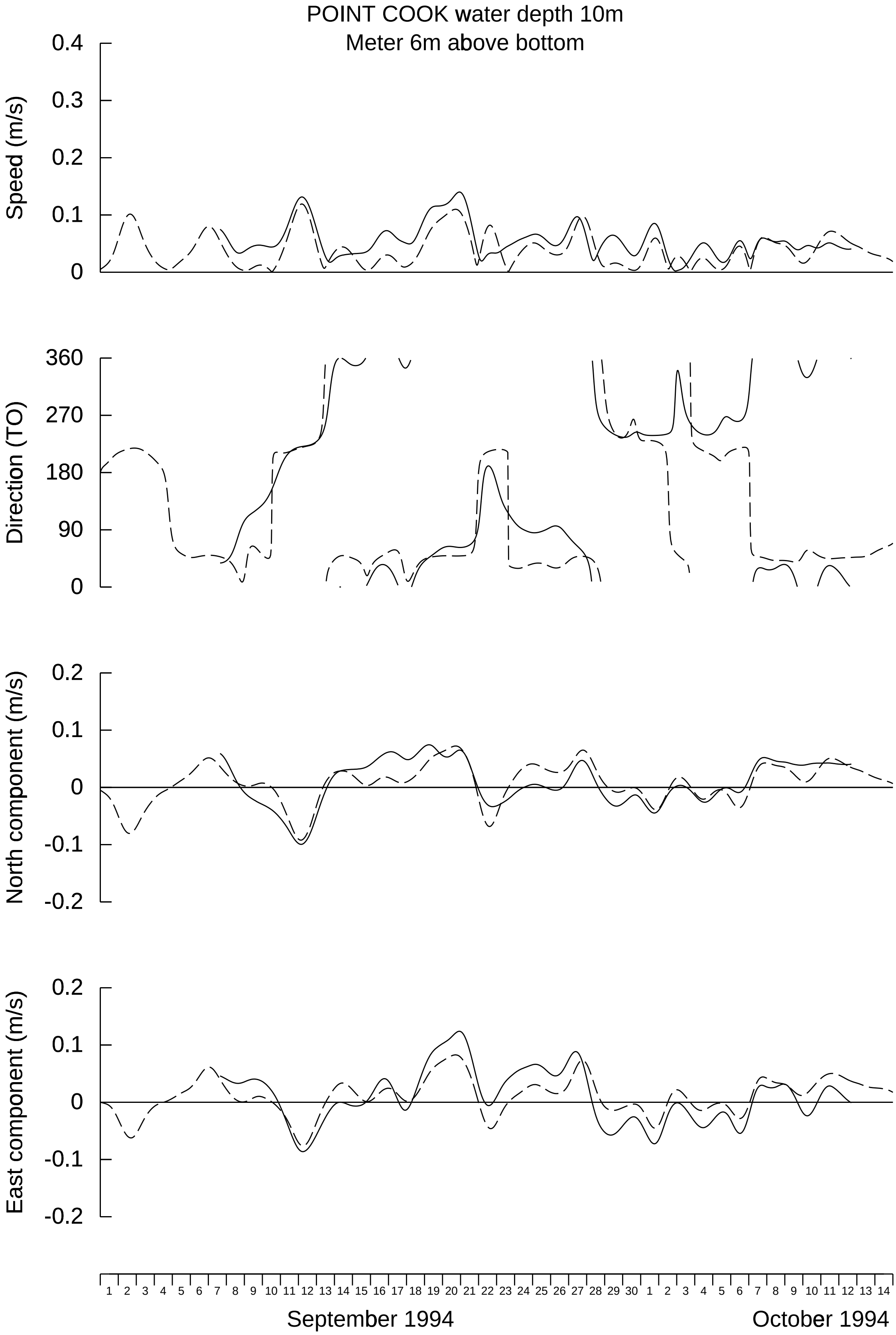

Figure 81: Measured (solid) and modelled (dashed) low pass filtered currents at the Point Cook site, upper meter, September-October 1994.

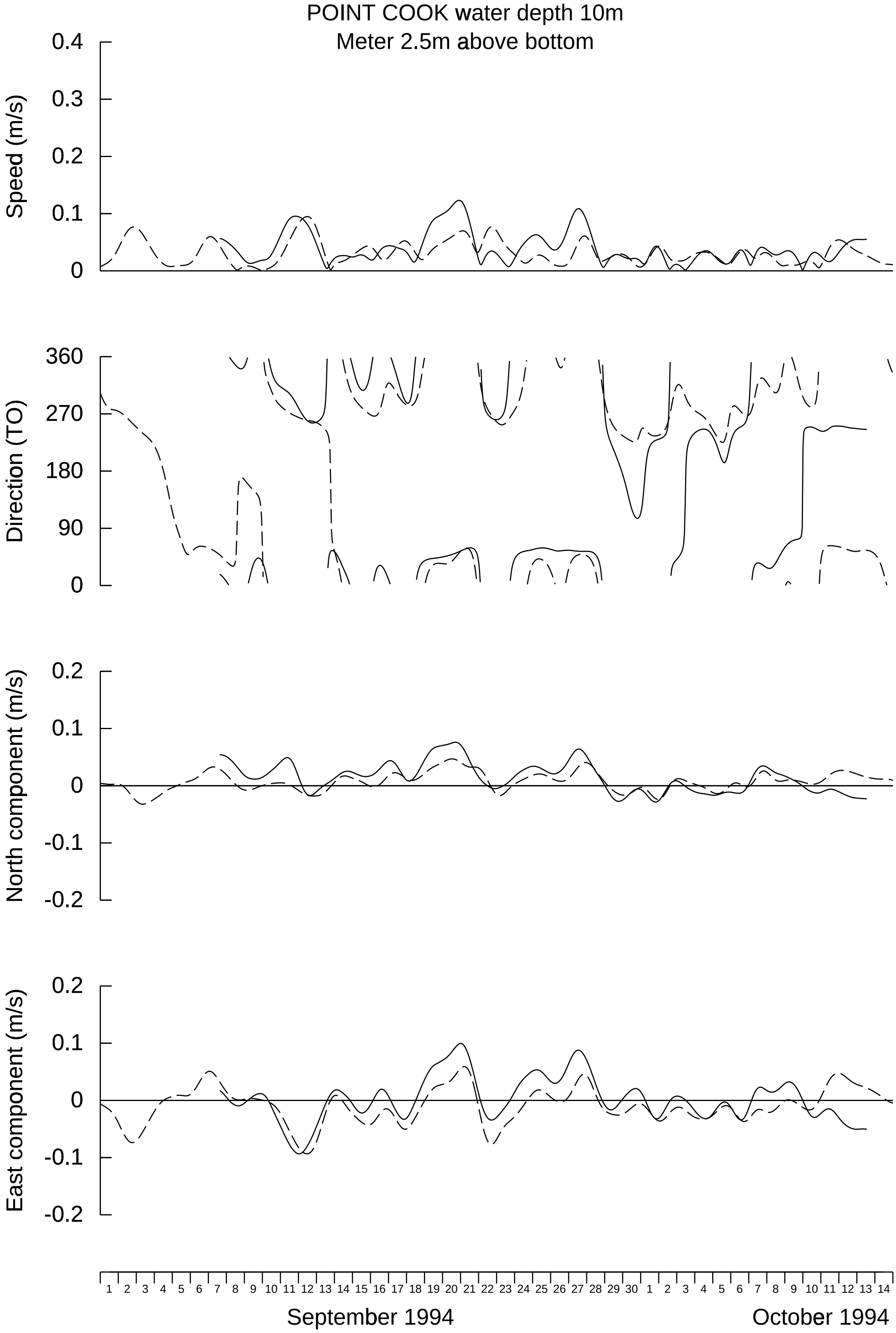

Figure 82: Measured (solid) and modelled (dashed) low pass filtered currents at the Point Cook site, lower meter, September-October 1994.

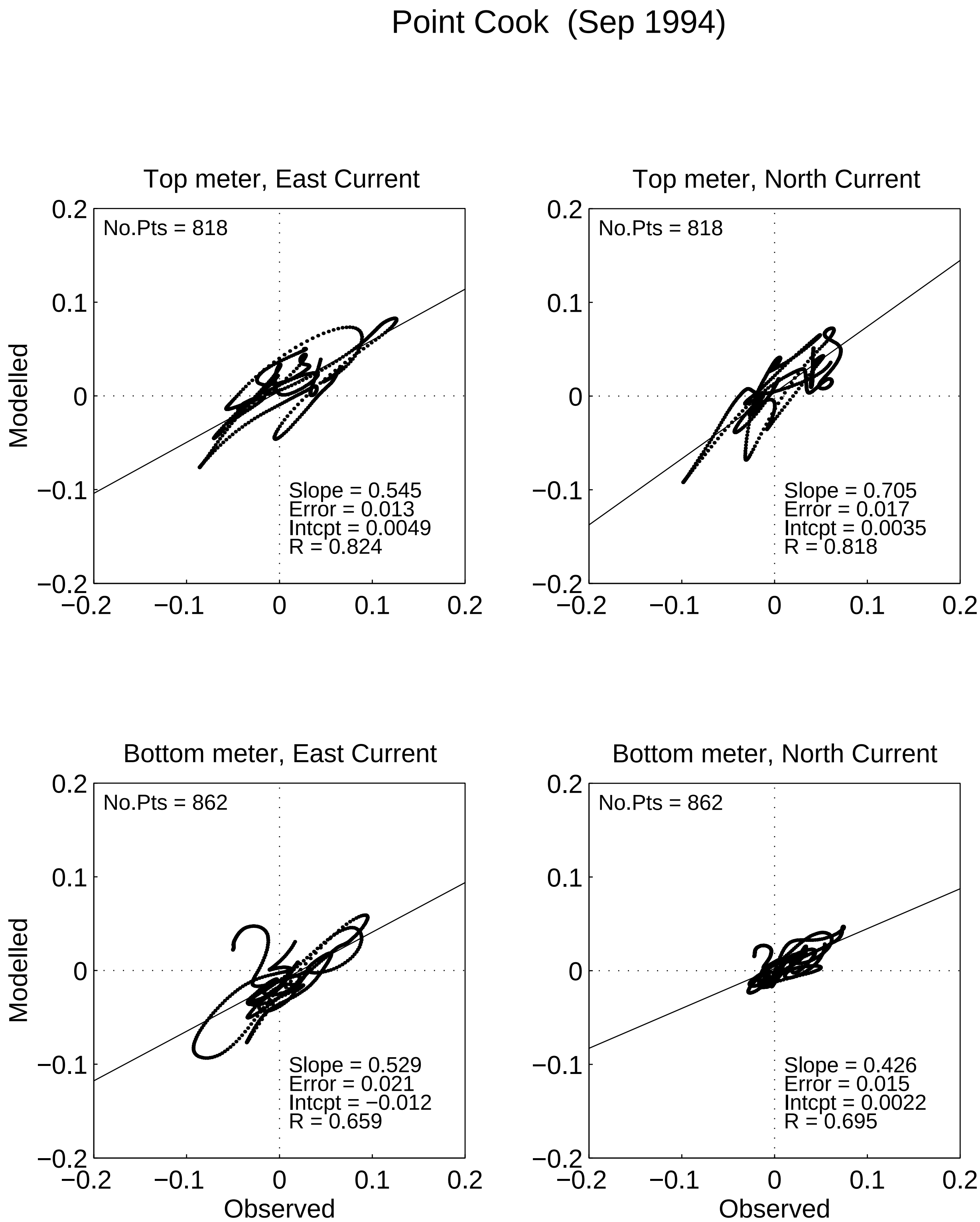

Figure 83: Observed (x-axis) versus modelled (y-axis) low pass filtered current components for the Point Cook mooring, September-October 1994.

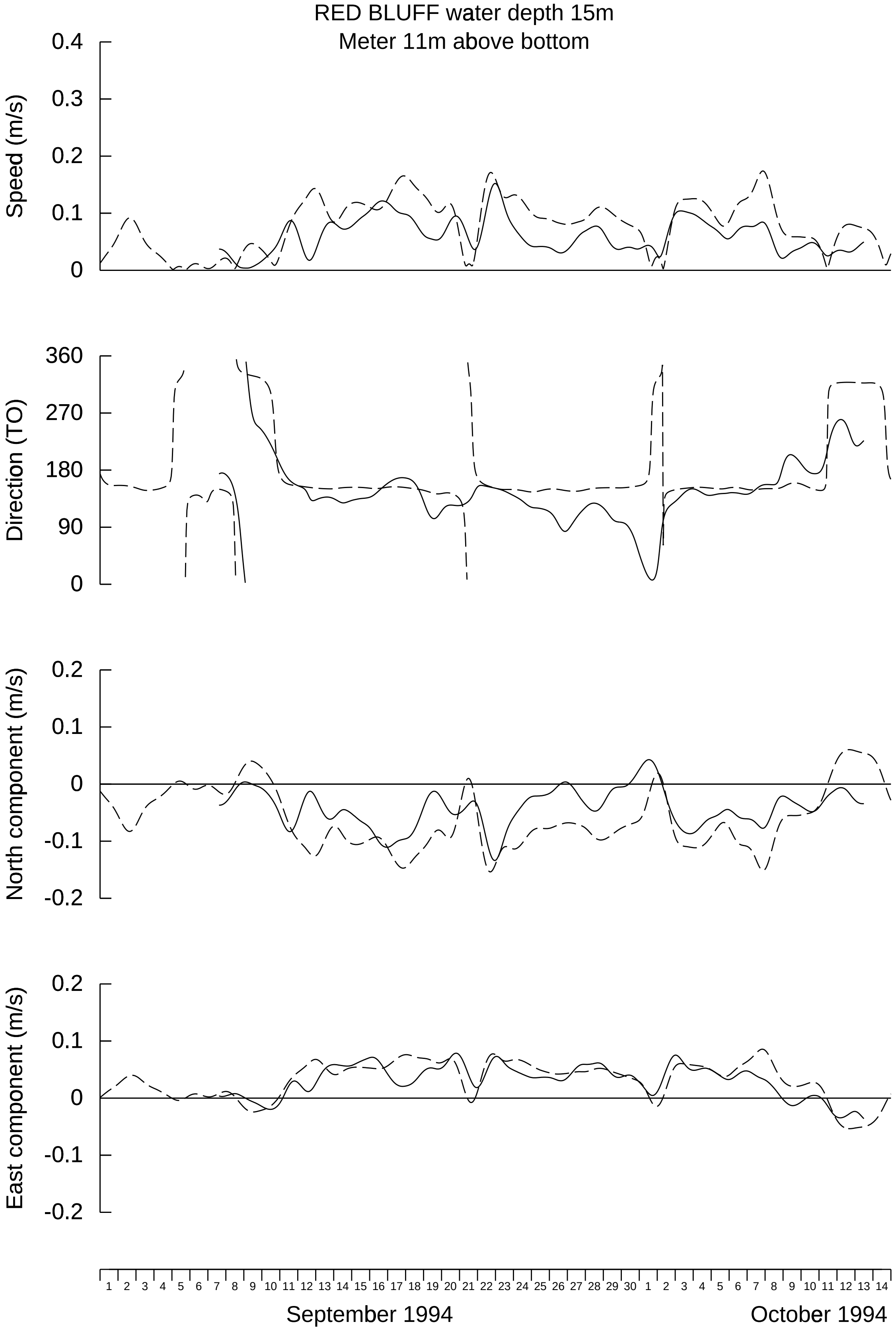

Figure 84: Measured (solid) and modelled (dashed) low pass filtered currents at the Red Bluff site, upper meter, September-October 1994.

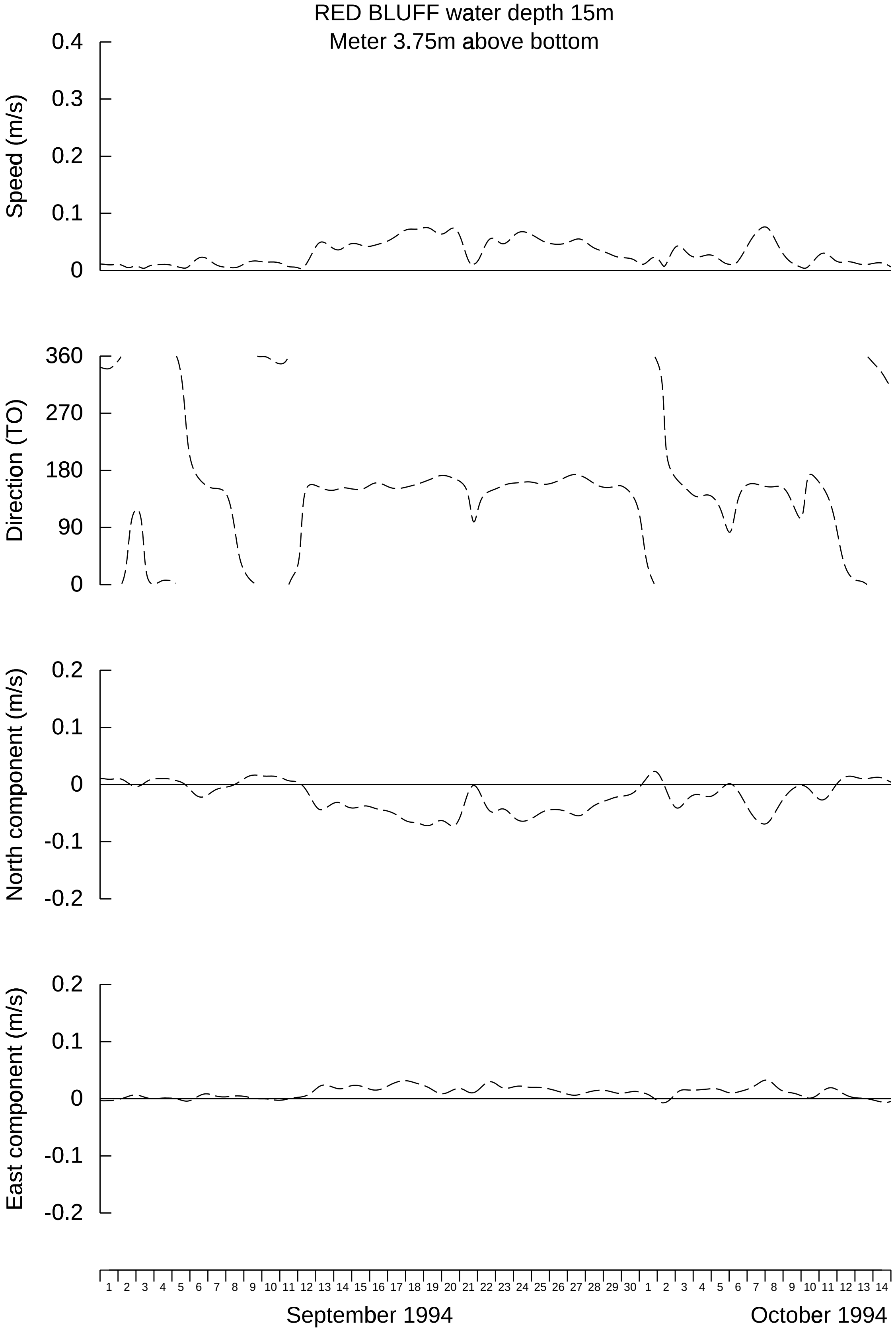

Figure 85: Modelled low pass filtered currents at the Red Bluff site, lower meter, September-October 1994. No data was recovered from the meter at this site.

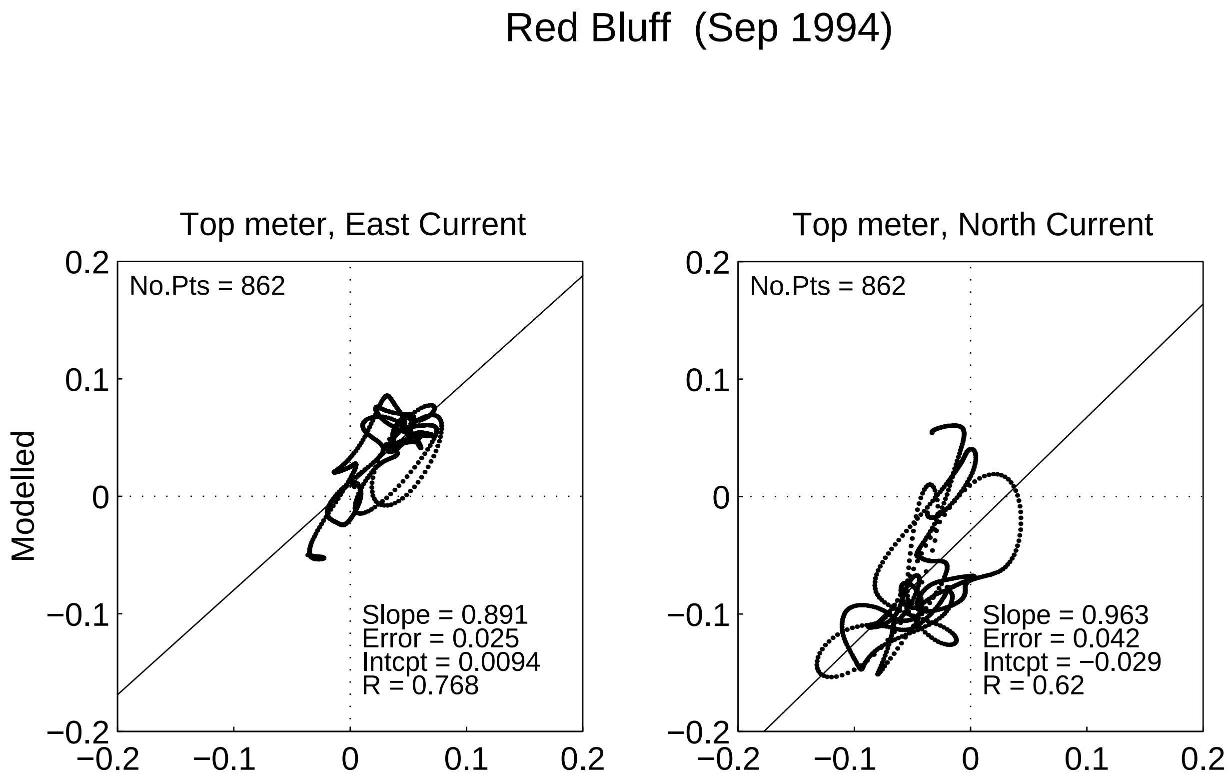

Figure 86: Observed (x-axis) versus modelled (y-axis) low pass filtered current components for the Red Bluff mooring, September-October 1994.

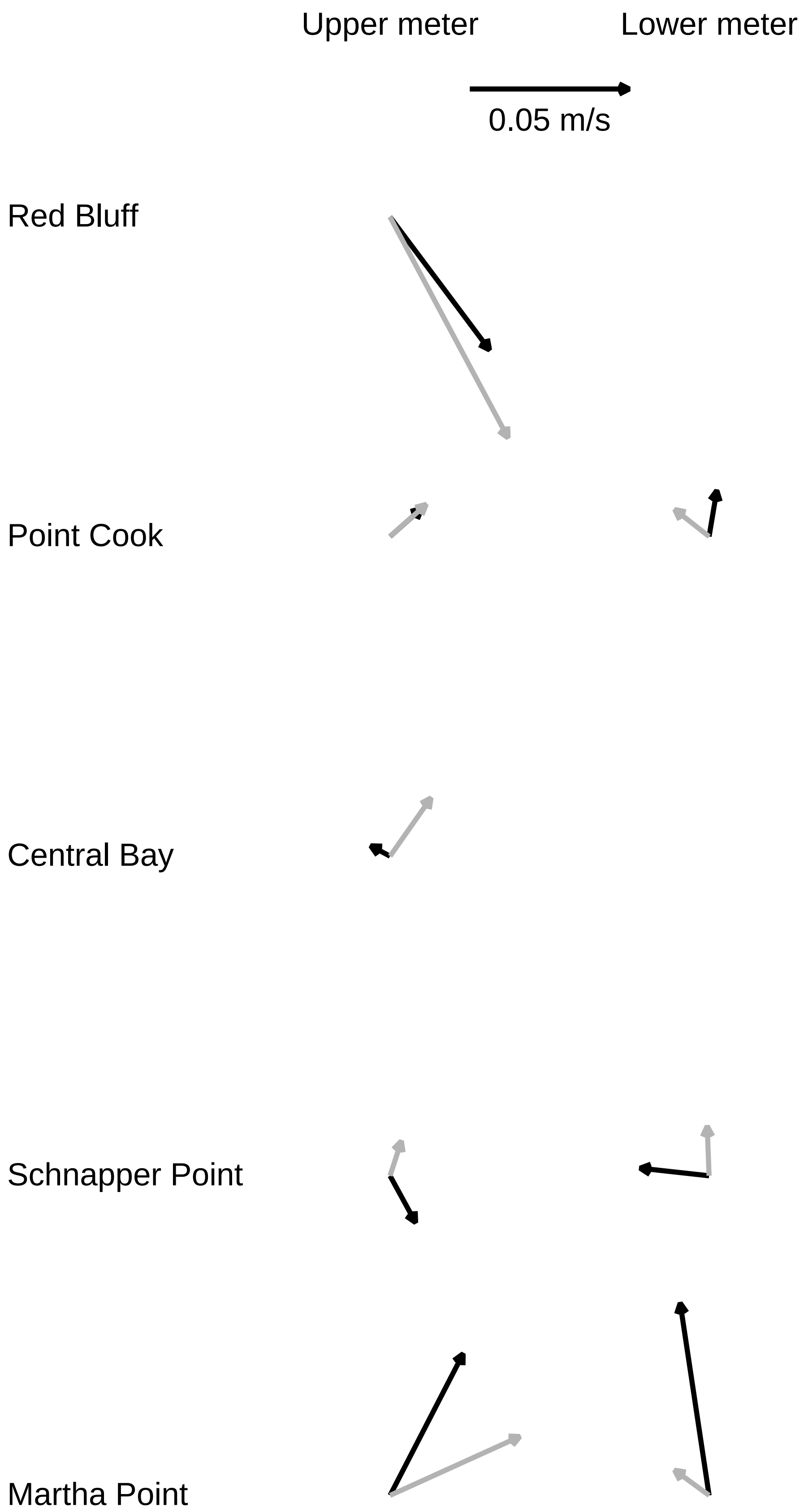

Figure 87: Vector mean currents for the entire September-October 1994 current meter deployment period. Measured data are shown as black arrows, model results are shown as grey arrows. The arrow at the top of the figure indicates a magnitude of 0.05 m/s. North is towards the top of the page.

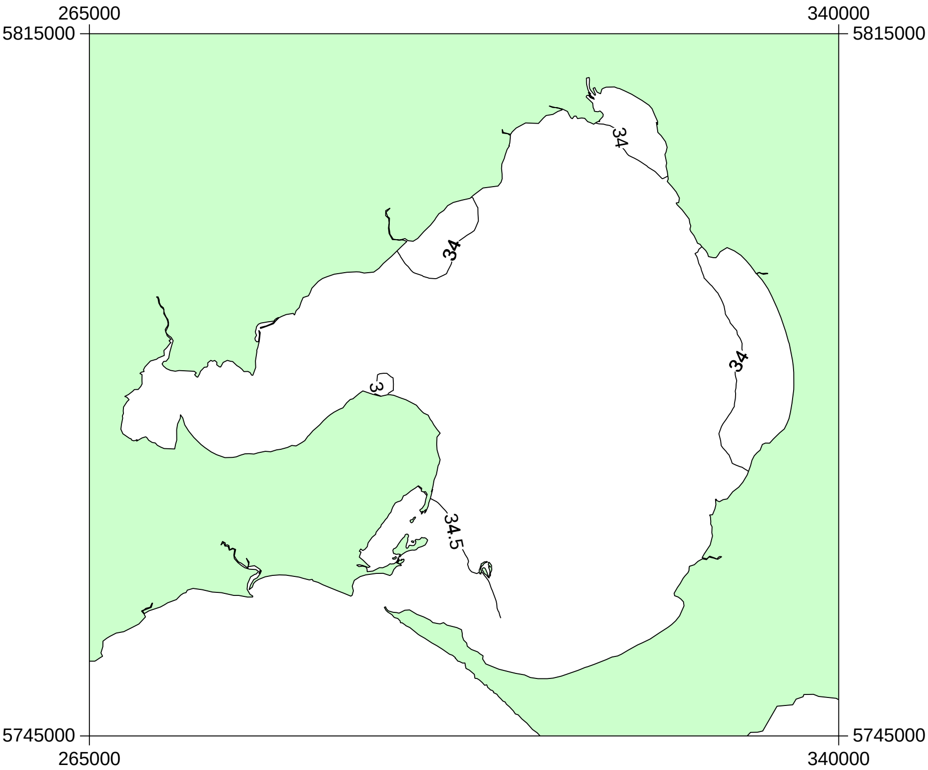

Figure 88: Surface (0-2m) salinity measured by CTD, 14-15 September 1994.

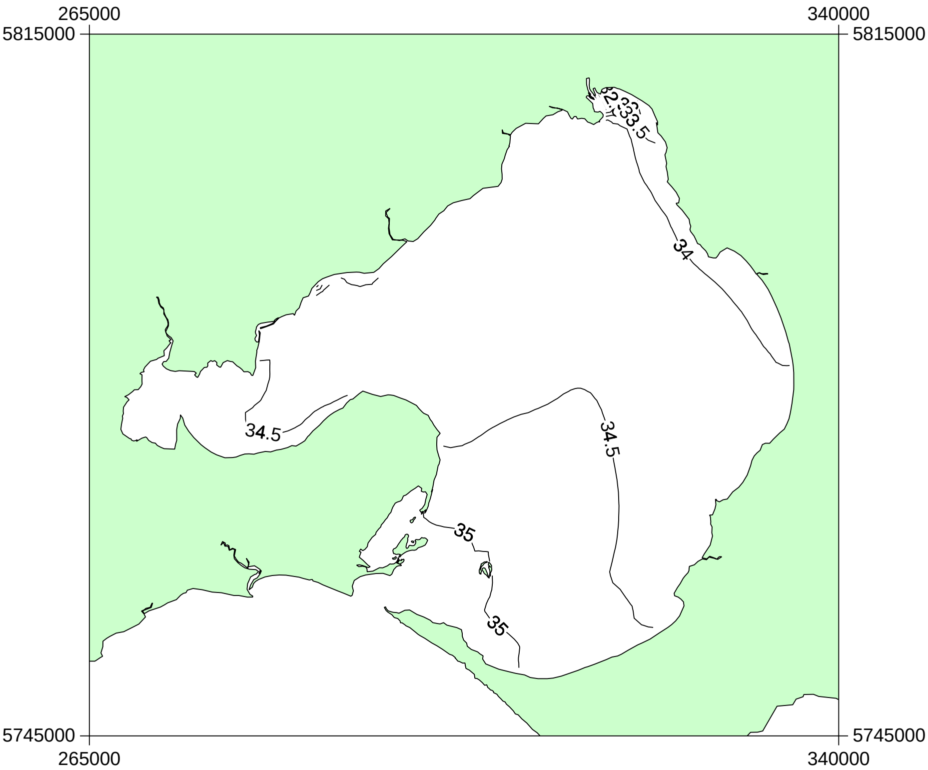

Figure 89: Surface (0-2m) salinity from model, 00:00 15 September 1994.

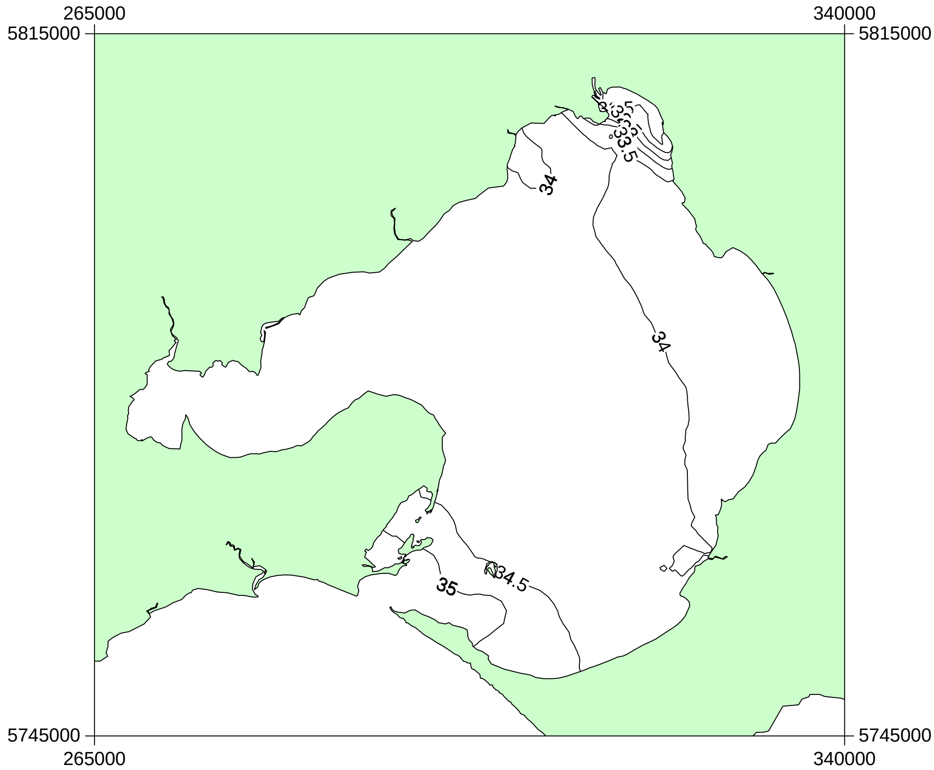

Figure 90: Surface (0-2m) salinity measured by CTD, 29 September - 3 October 1994.

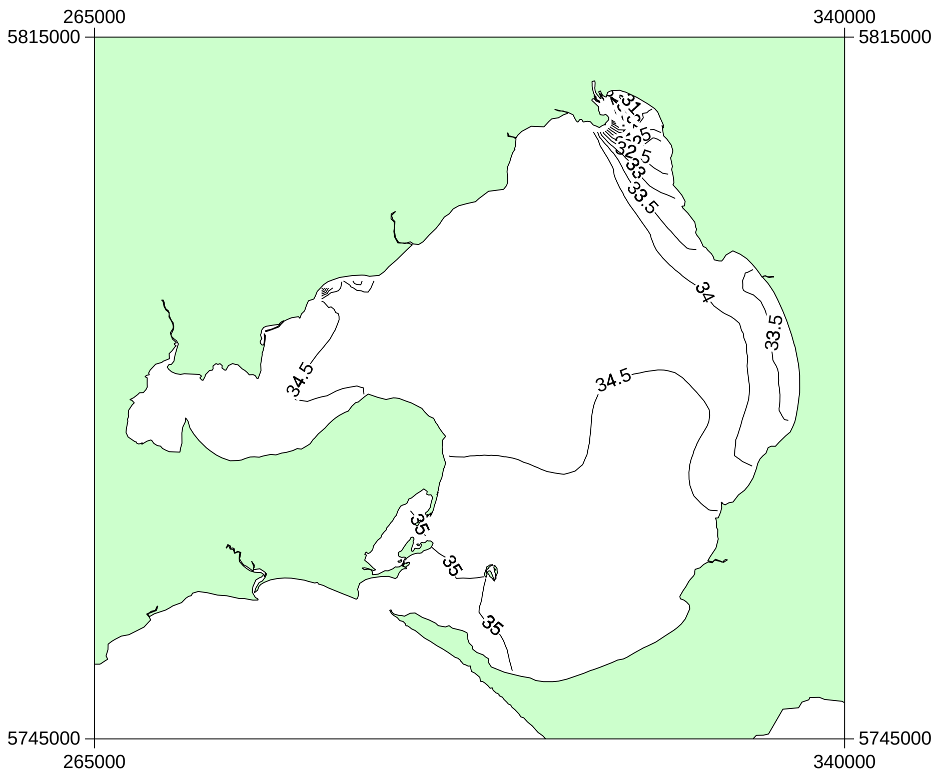

Figure 91: Surface (0-2m) salinity from model, 00:00 1 October 1994.

.

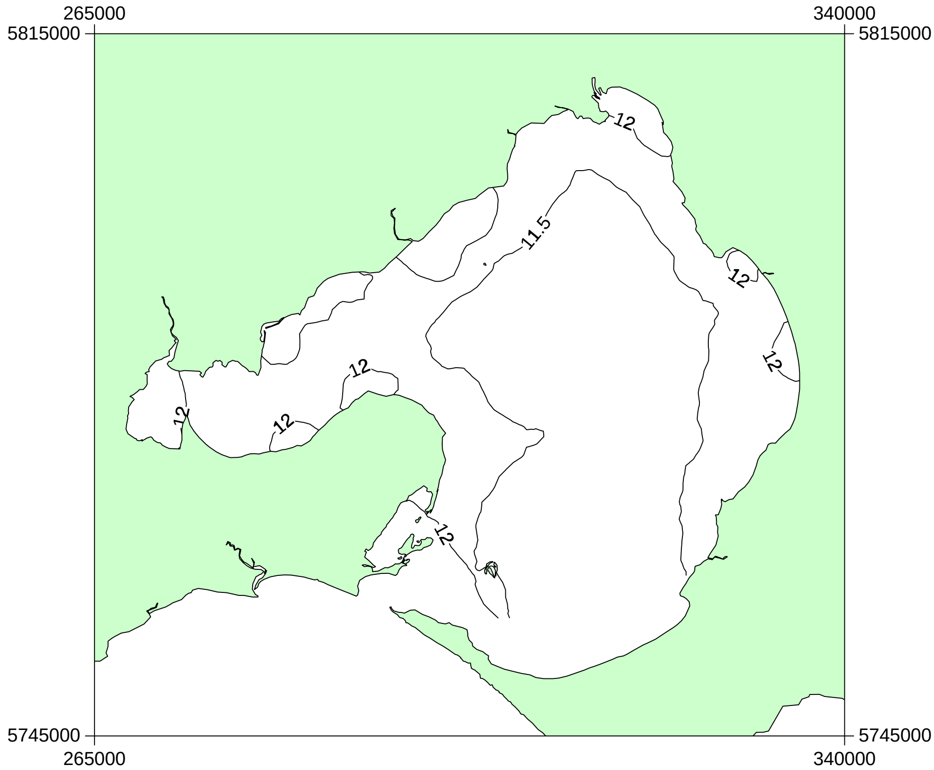

Figure 92: Surface (0-2m) temperature measured by CTD, 14-15 September 1994.

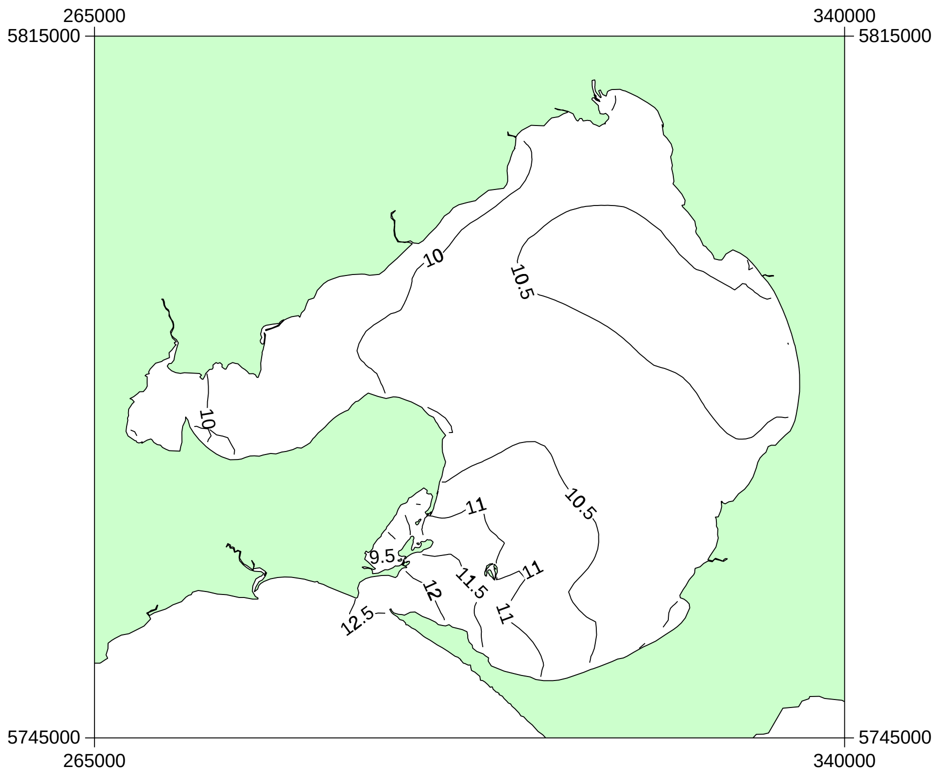

Figure 93: Surface (0-2m) temperature from model, 00:00 15 September 1994.

.

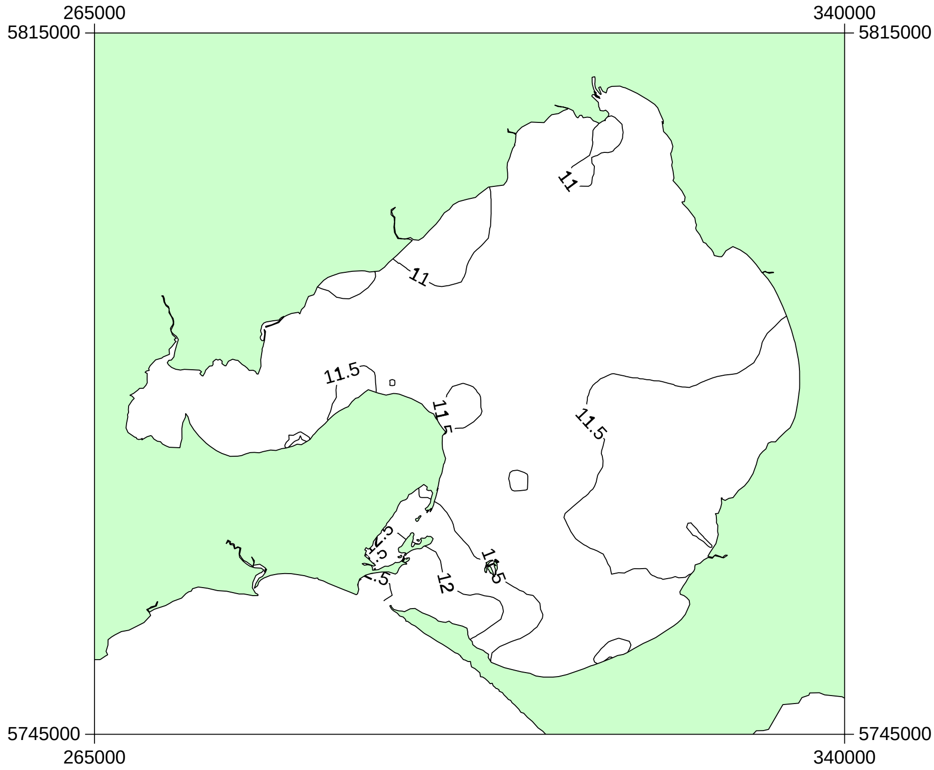

Figure 94: Surface (0-2m) temperature measured by CTD, 29 September - 3 October 1994.

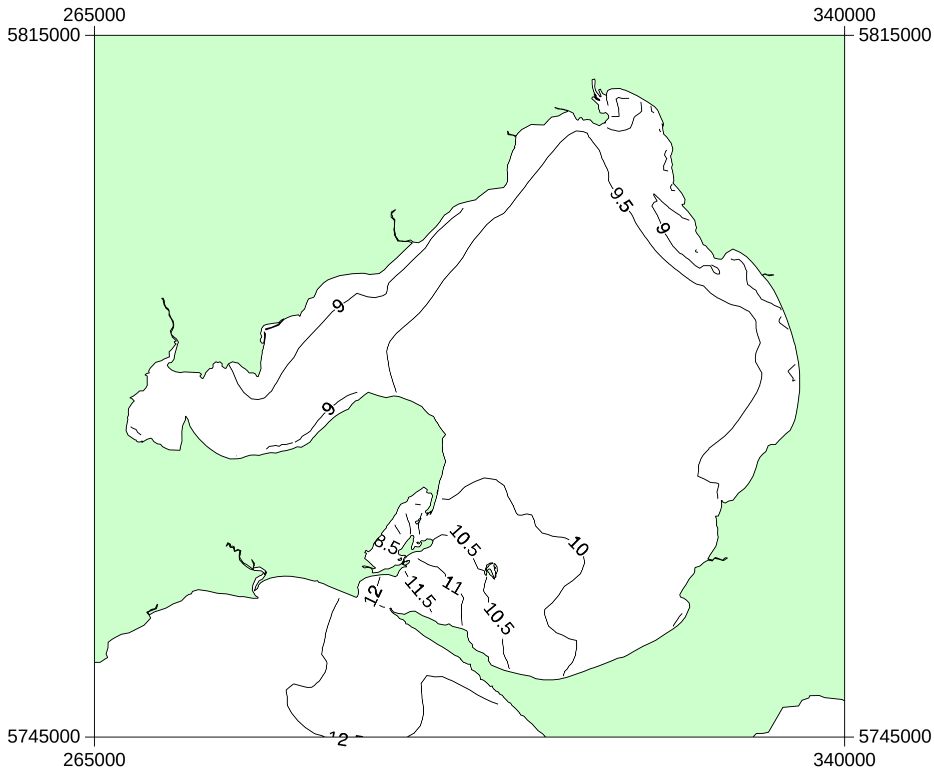

Figure 95: Surface (0-2m) temperature from model, 00:00 1 October 1994.

.

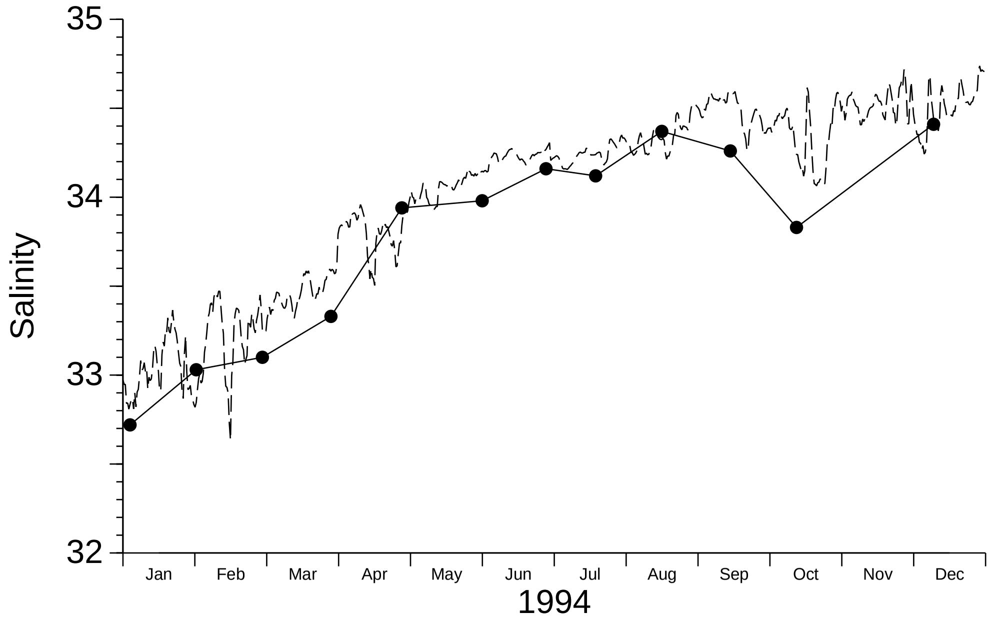

Figure 96: Surface salinity in the main body of the Bay throughout 1994. Observations were obtained approximately monthly from the VFRI site (MW2) near the centre of the Bay, and are shown as dots, connected by solid lines. Model values (dashed) are from the Central Bay site.

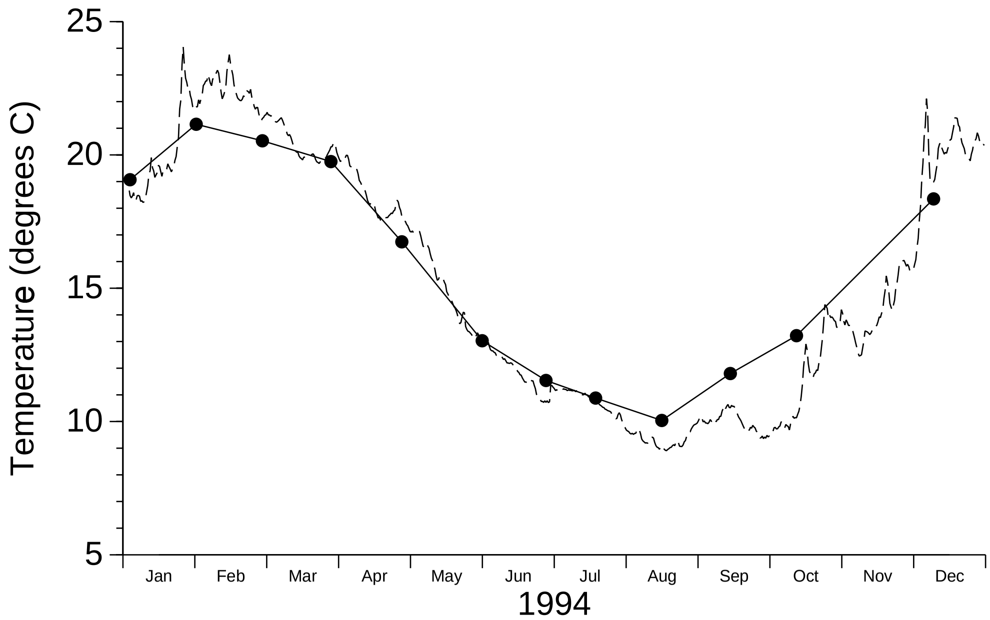

Figure 97: Surface temperature in the main body of the Bay throughout 1994. Observations were obtained approximately monthly from the VFRI site (MW2) near the centre of the Bay, and are shown as dots, connected by solid lines. Model values (dashed) are from the Central Bay site.